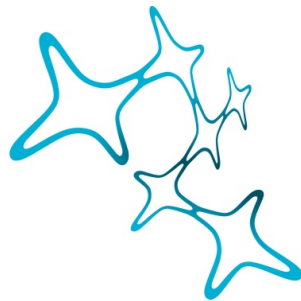


---

# The Relevance Of Posterior Thalamo-Cortical Connectivity For Visual Short-Term Memory Capacity: Evidence From Aging And Preterm Birth

---



Graduate School of  
Systemic Neurosciences  
LMU Munich



Aurore Menegaux

Dissertation der  
Graduate School of Systemic Neurosciences  
Der Ludwig-Maximilians-Universität München

November 14<sup>th</sup> 2018

Supervisor

PD Dr. Kathrin Finke

Hans Berger Department of Neurology,  
Jena University Hospital, Jena, Germany

First Reviewer: PD Dr. Kathrin Finke (Universitätsklinikum Jena)

Second Reviewer: PD Dr. Christian Sorg (TUM München)

External Reviewer Prof. Dr. Stefan Teipel (DZNE Rostock)

Date of Submission: November 14<sup>th</sup> 2018

Date of Defense : April 11<sup>th</sup> 2019



To my father, Dr. Sylvain Menegaux

To my grandfather



# ABSTRACT

Visual short-term memory (vSTM) capacity represents the maximum number of visual items that can be perceived and stored into vSTM. One way to measure it is by using simple psycho-physical experiments together with the theory of visual attention (TVA) computational framework in which visual processing is conceived as a race between objects to be consciously perceived and stored into vSTM. The neural theory of visual attention (NTVA), which gives an interpretation of the TVA at both the cellular and systemic level, suggests that recurrent loops between posterior thalamus and visual cortices are relevant for vSTM capacity. Nevertheless, no clear evidence for the role of posterior thalamus and its connection to visual cortices in vSTM capacity has been found thus far. This thesis investigated the role of posterior thalamo-cortical connectivity in vSTM capacity in healthy young individuals as well as in two populations that have shown to exhibit both vSTM capacity impairments and posterior cortical and subcortical white matter damages: healthy aging and premature birth. We found that vSTM capacity in healthy young adults was significantly associated with the tracts connecting posterior thalamus to occipital cortices and their microstructure. However, this association was modified in elderly individuals and in young adults born prematurely, in which the recruitment of additional, cortico-cortical, tracts, takes place. Together, these findings bring the first structural evidence for the NTVA model with respect to the relevance of posterior thalamo-cortical tracts for vSTM capacity and show how alterations of these tracts affect vSTM capacity.



# OVERVIEW

Every day, our visual system is confronted with more stimuli that it can process due to its limited resources. Indeed, the number of visual items that can be stored into visual short-term memory (vSTM) or vSTM capacity – and be consciously perceived - is limited to a few items, usually around four. The theory of visual attention computational framework (TVA, Bundesen et al., 1990) allows for parametric quantification of such vSTM capacity independently of other attentional sub-functions. According to the neural interpretation of the TVA or NTVA (Bundesen et al., 2005), recurrent loops between the thalamus and parieto-occipital cortices subserve vSTM capacity. However, there is no clear evidence for the relevance of posterior thalamo-cortical connectivity for vSTM capacity. Therefore, as suggested by NTVA, we first investigated whether posterior thalamo-cortical structural connectivity was associated with vSTM capacity in a group of healthy young adults aged 21 to 53 years.

Using the TVA framework, it has been shown that aging was associated with a reduced attentional capacity i.e lower processing speed and reduced visual short term memory storage capacity (McAvinue et al., 2012, Wiegand et al., 2014a). Similarly, it has been shown that early life adversity such as premature birth was also associated with long lasting impairments in vSTM capacity (D’Onofrio et al., 2013, Finke et al., 2015). Nevertheless, the structural underpinnings of this impairment in both populations remain unclear. Interestingly, it has been shown that both aging and premature birth lead to alterations in posterior white matter microstructure and connectivity (Vernooij et al., 2008, de Groot et al., 2015; Ball et al., 2012; Counsell et al., 2007; Meng et al., 2015). Thus, we investigated the relevance of posterior thalamo-cortical connectivity for vSTM capacity in healthy individuals aged 20 to 77 years and in young adults born prematurely.

In the introduction I will describe the TVA model and its neural interpretation (NTVA), the experimental methods to obtain a vSTM capacity measure and the different ways to study thalamo-cortical connections. Since the first study investigated vSTM capacity together with attentional selection, the method to assess attentional selection parameters will be presented as well. Lastly, I will introduce two models of vSTM capacity deficits and posterior white matter alterations, healthy aging and premature birth. Finally, the three guiding hypotheses of the thesis are presented: (i) Based on the NTVA model and macaque studies of attentional selection, we hypothesized that vSTM capacity and top down control are associated with the structural connectivity of posterior thalamus to occipital cortex, (ii) Since it has been shown that vSTM capacity and posterior white matter microstructure were impaired in elderly individuals, we investigated whether the association between vSTM capacity and the structural connectivity of posterior thalamus to occipital cortex (PT-OC) might be affected by aging (iii) Finally, based on changes in thalamo-cortical connectivity in preterm-born infants and on the emergence of compensatory activity pattern in posterior cortices associated with vSTM capacity in preterm born adults, we hypothesized that the association between vSTM capacity and the posterior thalamo-cortical tracts microstructure changes following preterm birth. The three studies addressing these hypotheses respectively are then presented.

In brief, all three studies provided evidence for the three stated hypotheses i.e., we provide strong empirical evidence for the critical role of the structural connectivity of posterior thalamus to occipital cortices for vSTM capacity.

In the end I will discuss the three studies main findings in detail i.e. the association between vSTM capacity and the structural connectivity and integrity of posterior thalamus to visual cortices in healthy individuals and individuals with early and late life disturbances. This thesis is based on three papers: Structural connectivity between posterior thalamus and occipital cortices underpins visual short-term memory capacity and attentional weighting in humans (under review in *NeuroImage*); Aging modulates the association between vSTM capacity and the structural connectivity of posterior thalamus to occipital cortices (in prep.); Impaired visual short-term memory capacity is distinctively associated with structural connectivity of the posterior thalamic radiation and the splenium of the corpus callosum in preterm-born adults (published in *NeuroImage* in 2017).

# LIST OF ABBREVIATIONS

AD: Axial Diffusivity

DTI: Diffusion tensor imaging

DWI: Diffusion weighted imaging

EEG: Electroencephalography

FA: Fractional Anisotropy

fMRI: Functional magnetic resonance imaging

FT: Full-term

HARDI: High angular resolution diffusion imaging

MD: Mean Diffusivity

MNI: Montreal Neurological institute

MRI: Magnetic resonance imaging

NODDI: Neurite orientation

NTVA: Neural theory of visual attention

PT-OC: Posterior thalamus to occipital cortex

PT: Preterm

PTR: Posterior Thalamic Radiations

RD: Radial Diffusivity

SC: Structural connectivity

TVA: Theory of visual attention

vSTM: Visual short-term memory



# TABLE OF CONTENTS

|   |             |
|---|-------------|
| <b>ABSTRACT</b> .....   | <b>ii</b>   |
| <b>OVERVIEW</b> .....   | <b>vi</b>   |
| <b>List of Abbreviations</b> .....  | <b>viii</b> |
| <b>TABLE OF CONTENTS</b> .....  | <b>x</b>    |
| <b>1 INTRODUCTION</b> .....   | <b>2</b>    |
| <b>1.1 Visual attentional capacity and the Theory of Visual attention framework</b> .....   | <b>2</b>    |
| 1.1.1 Biased Competition, attentional selection and capacity.....   | 2           |
| 1.1.2 Modeling visual attention in TVA.....   | 3           |
| 1.1.3 TVA and the brain: NTVA and the particular relevance of thalamo-cortical connections.....   | 4           |
| <b>1.2 Experiments: psychophysical assessment of attention functions</b> .....  | <b>7</b>    |
| 1.2.1 Assessment of attentional capacity: The whole report paradigm.....  | 8           |
| 1.2.2 Assessment of attentional selection: The partial report paradigm.....   | 9           |
| <b>1.3 Investigating thalamo-cortical connections with Diffusion Tensor Imaging (DTI)</b> .....   | <b>11</b>   |
| 1.3.1 Basic principles of DTI.....  | 11          |
| 1.3.2 Investigating white matter microstructure with Tract-Based Spatial Statistics.....  | 14          |
| 1.3.3 Studying thalamo-cortical structural connectivity with probabilistic tractography.....  | 14          |
| <b>1.4 Examples of vSTM capacity- and white matter alterations along development</b> .....  | <b>15</b>   |
| 1.4.1 Example of late life disturbances: Effect of aging.....   | 16          |
| 1.4.2 Example of early life disturbances: Long term outcomes of preterm birth.....  | 18          |
| <b>1.5 Aims of the thesis: three hypotheses</b> .....   | <b>19</b>   |
| <b>2 STUDY I:</b> .....   | <b>22</b>   |
| <b><i>Structural connectivity between posterior thalamus and occipital cortices underpins visual short-term memory capacity and attentional weighting in humans</i></b> ..... | <b>22</b>   |
| <b>2.1 Abstract</b> .....   | <b>24</b>   |
| <b>2.2 Introduction</b> .....   | <b>25</b>   |
| <b>2.3 Material and methods</b> .....   | <b>29</b>   |
| 2.3.1 Participants.....   | 29          |
| 2.3.2 TVA-based behavioural assessment of vSTM capacity and top-down control.....   | 30          |
| 2.3.3 Imaging data acquisition.....   | 34          |
| 2.3.4 Quality check.....  | 34          |
| 2.3.5 Preprocessing.....  | 34          |
| 2.3.6 Probabilistic tractography and seed and target masks creation.....  | 35          |
| 2.3.7 Estimation of total intracranial volume (TIV).....  | 36          |
| 2.3.8 Statistical analyses.....   | 37          |
| 2.3.9 Control analyses.....   | 37          |
| <b>2.4 Results</b> .....  | <b>38</b>   |
| 2.4.1 Behavioural data.....   | 38          |
| 2.4.2 Posterior thalamus-occipital cortex (PT-OC) structural connectivity and vSTM capacity.....  | 38          |
| 2.4.3 Posterior thalamus-occipital cortex structural connectivity and attentional selection.....  | 38          |
| 2.4.4 Control analyses.....   | 40          |

|            |  |                  |
|------------|--|------------------|
| <b>2.5</b> | <b>Discussion.....</b>   | <b>41</b>        |
| 2.5.1      | Top down control is associated with posterior thalamus – occipital cortex structural connectivity<br>41  |                  |
| 2.5.2      | vSTM capacity is associated with posterior thalamus – occipital cortex structural connectivity....   | 42               |
| 2.5.3      | Limitations.....   | 43               |
| <b>2.6</b> | <b>Conclusion.....</b>   | <b>44</b>        |
| <b>2.8</b> | <b>Supplementary material.....</b>   | <b>50</b>        |
| <b>3</b>   | <b>STUDY II:.....</b>  | <b>52</b>        |
|            | <b><i>Aging modulates the association between vSTM capacity and the structural connectivity of posterior thalamus to occipital cortices.....</i></b>   | <b><i>52</i></b> |
| <b>3.1</b> | <b>Abstract.....</b>   | <b>54</b>        |
| <b>3.2</b> | <b>Introduction .....</b>  | <b>55</b>        |
| <b>3.3</b> | <b>Material and methods.....</b>   | <b>58</b>        |
| 3.3.1      | Participants.....  | 58               |
| 3.3.2      | TVA-based behavioural assessment of vSTM capacity.....   | 59               |
| 3.3.3      | Imaging data acquisition and preprocessing .....   | 62               |
| 3.3.4      | Extraction of FA, MD, AD, and RD maps from path probability maps.....  | 65               |
| 3.3.5      | Estimation of tissue type and total intracranial volumes .....   | 65               |
| 3.3.6      | Statistical analysis .....   | 65               |
| 3.3.7      | Sliding Window Analysis.....   | 66               |
| <b>3.4</b> | <b>Results.....</b>  | <b>67</b>        |
| 3.4.1      | Aging modulates the association between PT-OC structural connectivity and vSTM capacity .....  | 67               |
| 3.4.2      | The age effect on the association between left PT-OC structural connectivity and vSTM capacity:<br>Shift and alteration of microstructure .....  | 68               |
| <b>3.5</b> | <b>Discussion.....</b>   | <b>71</b>        |
| 3.5.1      | Aging modulates the association between PT-OC structural connectivity and vSTM capacity .....  | 71               |
| 3.5.2      | The association between vSTM capacity and left PT-OC structural connectivity is continuously<br>inversed with age: Potentially relevant microstructural alterations. ....  | 72               |
| 3.5.3      | Limitations.....   | 74               |
| <b>3.6</b> | <b>Conclusion.....</b>   | <b>74</b>        |
| <b>3.7</b> | <b>Supplementary material.....</b>   | <b>84</b>        |
| <b>4</b>   | <b>STUDY III:.....</b>   | <b>86</b>        |
|            | <b><i>Impaired visual short-term memory capacity is distinctively associated with structural connectivity of the posterior thalamic radiation and the splenium of the corpus callosum in preterm-born adults .....</i></b> | <b><i>86</i></b> |
| <b>4.1</b> | <b>Abstract.....</b>   | <b>87</b>        |
| <b>4.2</b> | <b>Introduction .....</b>  | <b>87</b>        |
| <b>4.3</b> | <b>Material and Methods.....</b>   | <b>89</b>        |
| 4.3.1      | Participants.....  | 89               |
| 4.3.2      | Theoretical TVA framework and TVA-based behavioral assessment of cSTM capacity .....   | 89               |
| 4.3.3      | Statistical analysis .....   | 90               |
| 4.3.4      | Diffusion imaging and data analysis.....   | 90               |
| <b>4.4</b> | <b>Results.....</b>  | <b>91</b>        |
| 4.4.1      | vSTM capacity is reduced in preterm-born adults .....  | 91               |
| 4.4.2      | Preterm birth modulates the relationship between vSTM capacity and FA in posterior thalamic<br>radiation.....  | 91               |

|            |   |            |
|------------|---|------------|
| 4.4.3      | Preterm birth modulates the relationship between vSTM capacity and FA in the splenium of the corpus callosum.....                   | 91         |
| <b>4.5</b> | <b>Discussion.....</b>  | <b>91</b>  |
| 4.5.1      | Prematurity modulates the relationship between vSTM capacity and posterior thalamic radiation microstructure.....                   | 91         |
| 4.5.2      | Prematurity modulates the relationship between vSTM capacity and the splenium of the corpus callosum microstructure.....            | 93         |
| 4.5.3      | Methodological issues and limitations.....  | 94         |
| <b>4.6</b> | <b>Conclusion.....</b>  | <b>94</b>  |
| <b>4.7</b> | <b>Supplementary Material.....</b>  | <b>96</b>  |
| <b>5</b>   | <b>GENERAL DISCUSSION.....</b>  | <b>100</b> |
| <b>5.1</b> | <b>Key Findings.....</b>  | <b>100</b> |
| 5.1.1      | First structural evidence supporting the NTVA assumptions of a thalamo-cortical system for vSTM processes.....                      | 100        |
| 5.1.2      | The association between vSTM capacity and posterior thalamo-cortical connections is changed when these connections are altered..... | 102        |
| 5.1.3      | The association between vSTM capacity and the microstructure of posterior thalamo-cortical connections is complex.....              | 104        |
| 5.1.4      | Integrating our findings with current views.....  | 105        |
| <b>5.2</b> | <b>Limitations.....</b>   | <b>107</b> |
| <b>5.3</b> | <b>Future directions.....</b>   | <b>108</b> |
| <b>5.4</b> | <b>Conclusion.....</b>  | <b>109</b> |
|            | <b>REFERENCES.....</b>  | <b>110</b> |
|            | <b>ACKNOWLEDGMENTS.....</b>   | <b>124</b> |
|            | <b>LIST OF PUBLICATIONS.....</b>  | <b>128</b> |
|            | <b>CURRICULUM VITAE.....</b>  | <b>130</b> |
|            | <b>EIDESSTATTLICHE VERSICHERUNG/AFFIDAVIT.....</b>  | <b>134</b> |
|            | <b>DECLARATION OF AUTHOR CONTRIBUTIONS.....</b>   | <b>136</b> |



# 1 INTRODUCTION

## 1.1 VISUAL ATTENTIONAL CAPACITY AND THE THEORY OF VISUAL ATTENTION FRAMEWORK

Our environment is composed of more stimuli than our visual system can process. Thus, it is necessary to filter out relevant information from irrelevant one. This function is called visual attention. Considering the limited processing resources of the visual system, objects of the environment compete to be selected i.e. encoded into visual short term memory (vSTM). This competition can be biased by attention so that the most important objects are favored. This constitutes the basis of the biased competition model by Desimone and Duncan (1995) and a core principle of the Theory of visual attention mathematical model formulated by Bundesen in 1990.

### 1.1.1 BIASED COMPETITION, ATTENTIONAL SELECTION AND CAPACITY

The biased competition model by Desimone and Duncan (1995) has profoundly influenced the domain of cognitive psychology and neuroscience. It describes the mechanisms underlying selective visual attention. According to this model, objects represented in the visual field compete for access to the limited processing resources of the brain. Biased competition elucidates this competition so that the more important objects are given more processing resources. Indeed, both target- and non-target stimuli compete for attention which is resolved by bottom up and top down processes. For example, if a red apple, which is the target, is located in the middle of a box of yellow apples, bottom up processes take place based on the saliency of the visual object (red apple) whereas top down processes represent goal oriented processes such as aiming to find the blue target and then the green one. Both bottom up and top down processes will influence which objects are represented and stored into visual short term memory (vSTM). Objects that are stored into vSTM are done so in an accessible form to interact with the changing environment.

At the cellular level, the biased competition model is based on the assumption that the amount of competition is affected by the size of the receptive fields in visual areas, with large receptive fields leading to increased competition. The size of the receptive fields increases from the primary visual cortex toward the inferotemporal cortex. In the biased competition model, information about any stimulus decreases as more objects enter the receptive field. When several objects enter a cell's receptive field, they supposedly compete for the limited processing resources. Evidence for this mechanism has been found in single cells recordings in higher visual areas such as V2 and V4, but not primary visual areas. (Luck et al., 1997; Reynolds, Chelazzi & Desimone, 1999). At the system level, frontoparietal networks, posterior parietal and occipital cortices as well as posterior thalamic nuclei

including the pulvinar are supposed to be the regions relevant for biased competition. To sum up, the biased competition model suggests that the need for attentional selection arises from the competition between objects in the visual field and is influenced by both the properties of the objects and the goal of the task.

### 1.1.2 MODELING VISUAL ATTENTION IN TVA

Similarly, visual processing in TVA is conceived as a parallel race between objects of the visual display to be represented in the vSTM store (Bundesen 1990). According to the TVA, an object can be consciously recognized only if one or several properties of this object can be encoded into vSTM. Using different colored shapes in a visual array, Luck and Vogel (1997) directly assessed the capacity of vSTM and showed that it was around 4 items, it did not vary when increasing display duration. This constitutes the capacity of vSTM or parameter  $K$  in TVA. The TVA model also specifies that although all objects in the visual field are processed independently and in parallel, they are not processed equally fast. If the vSTM store is filled, no further objects can be encoded. If the store is not fully filled, the probability of an object encoding will be determined by the processing rate which reflects the amount of total processing capacity allocated to the object (its attentional weight). This mechanism is described by the rate equation of TVA:

$$v(x, i) = \eta(x, i) \beta_i \frac{w_x}{\sum_{z \in S} w_z}$$

Where  $v(x, i)$  represents the processing rate at which a visual categorization “ $x$  belongs to  $i$ ” is encoded into vSTM,  $\eta(x, i)$  is the strength of the sensory evidence that  $x$  belongs to category  $i$ ,  $\beta_i$  is the perceptual bias associated with category  $i$  with  $0 < \beta_i < 1$  and  $\frac{w_x}{\sum_{z \in S} w_z}$  represents the relative attentional weight of object  $x$ . More specifically,  $w_x$  is the weight of object  $x$  and  $\sum_{z \in S} w_z$  represents the sum of weights across all objects in the visual field  $S$ .

The sum of the processing rates for all objects in the visual environment constitutes the total processing speed of the visual system or parameter  $C$ . Together, vSTM capacity  $K$  and visual processing speed  $C$  parameters constitute attentional capacity.

The attentional weight of an object  $x$  is determined by bottom up and top down generated bias signals. It is described by the weight equation of TVA:

$$w_x = \sum_{j \in R} \eta(x, j) \pi_j$$

Attentional weights are derived from pertinence values  $\pi_j$ . Every visual category  $j$  has a pertinence,  $\pi_j$ , which is a nonnegative real number representing the temporary importance of attending to objects that belong to category  $j$ . In this equation,  $R$  is the set of all visual categories and  $\eta(x, j)$  the strength of sensory evidence that object  $x$  belongs to category  $j$ . Thus, the weight equation of TVA is a weighted sum of pertinence values.

The computation of attentional weights as described by the equation above allows for comparison of weights between different objects and thus provides the basis of two additional parameters: the efficiency of top down control of attention or parameter  $\alpha$  which reflects the task related differences in weights for targets  $w_T$  and distractors  $w_D$  and is defined by the ratio  $\frac{w_D}{w_T}$ , and the spatial attentional bias (parameter  $w_{lat}$ ) which describes the spatial distribution of attentional weights across the left and right visual hemifields and is defined by the ratio  $\frac{w_{Left}}{w_{Left} + w_{Right}}$ . Accordingly, a value of  $w_{lat} = 0.5$  indicates balance weighting across hemifields. The TVA model contains a 5<sup>th</sup> parameter called perceptual threshold or  $t_0$  which is a measure of the lower threshold for visual perception i.e it is the time at which the processing race starts and objects in the visual field start to have a probability above 0 of being recognized.

### 1.1.3 TVA AND THE BRAIN: NTVA AND THE PARTICULAR RELEVANCE OF THALAMO-CORTICAL CONNECTIONS

#### CELLULAR INTERPRETATION

The Neural Theory of Visual Attention (NTVA) is based on event related potentials and single-cell recordings in monkeys and provides an interpretation at the cellular level of the rate and weight equations. Together, those equations describe two mechanisms of selection, one for the selection of objects called filtering and another for selection of features called pigeonholing. Filtering and pigeonholing are terms used in reference to Broadbent (1971). Filtering changes the number of neurons representing an object so that the number of neurons increases with the behavioral importance of the object, while pigeonholing influences the level of activation of neurons coding for a specific feature. Based on these two mechanisms, behaviorally relevant features and objects will dominate and become encoded into vSTM. Thus, the total activation representing a visual categorization “object  $x$  has feature  $i$ ” described by the rate equation is proportional to the number of neurons representing the visual categorization, as regulated by filtering, and the level of activation of the individual neurons representing the categorization as regulated by pigeonholing. According to NTVA, a neuron in the visual system is assumed to represent one single feature which can be a simple physical feature or a micro feature in a wide representation. This neuron can also respond to the properties of solely one object at any given time. Moreover, the activation of a neuron corresponds to the increase in firing rate

above a baseline rate which represents the undriven activity of this neuron. A neuron gets activated by the appearance of an object in its receptive field. If the baseline is zero, then activation corresponds to the firing rate. Such activation can be calibrated independently of filtering, i.e., independently of the number of neurons coding for an object. This calibration of firing rates corresponds to  $\beta_i$  values in the rate equation.

As mentioned previously, filtering influences the number of neurons coding for an object with a higher number of neurons corresponding to higher behavioral importance of the object, so that important objects are represented in many cells. Considering that the attribution of processing resources depends on the attentional weight of objects, the computation of the weights must precede such attribution of resources. Thus visual processing is divided into two processing waves, the first unselective and the second selective. In the first wave, processing resources are distributed randomly (unselectively) across the visual field resulting in the computation of one attentional weight per object of the visual field which is stored into a priority map. In the second wave, the reallocation of visual processing capacity based on the attentional weights takes place through dynamic remapping of the receptive fields of cortical neurons. As a result, the higher the attentional weight of an object, the higher the number of neurons allocated to this object. Thus, the dynamic remapping of receptive fields corresponds to the filtering mechanism. The second wave of processing is said to be selective since the number of neurons coding for the object (processing resources) varies with the attentional weight of the object. Given that more processing resources are allocated to more important objects than less important ones, important objects are more prone to be encoded into vSTM. The vSTM system can be considered as a feedback mechanism sustaining the activity of the neurons that have won the competition. Such feedback mechanism follows the notion formulated by Hebb (1949) that short-term memory relies on the activity of neurons coding for the selected information which is sustained in a positive feedback loop. This notion has since gained wide acceptance in neuroscience. A main candidate for this feedback mechanism is thalamo-cortical interaction which is also suggested in the NTVA model.

## SYSTEMS-LEVEL INTERPRETATION

Indeed, the NTVA does not depend on any specific brain localization of the neural computations it describes. Nevertheless, it is important to consider how the computations are distributed across the brain and one possibility is the thalamic model of NTVA (figure 1). According to this model, visual inputs from the retina enter the lateral geniculate nucleus (LGN) of the thalamus and are then transmitted to the striate and extrastriate visual cortices. There, individual perceptual values of the objects  $\eta$  are computed and multiplied with their pertinence values  $\pi$  before entering the pulvinar nucleus of the thalamus where the saliency map of objects is assumed to be located. In the pulvinar,

products are summed up as attentional weights. This constitutes the first and unselective wave of processing (Fig1).

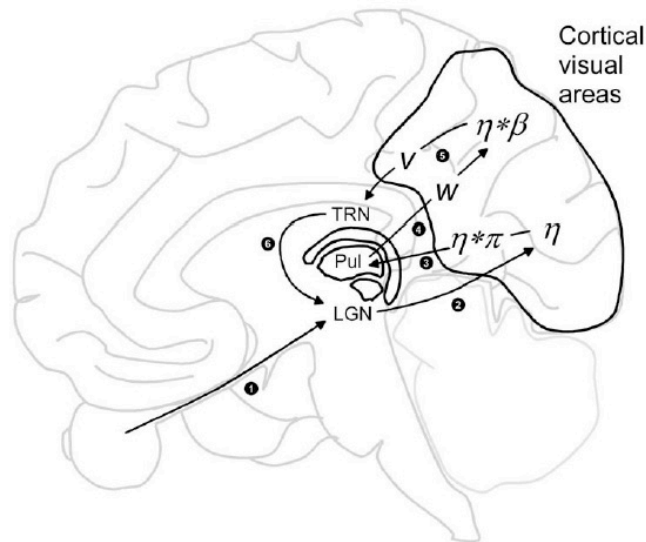


**Figure 1: NTVA thalamic model of visual processing.** Reproduced with permission from Bundesen et al., 2005

During the second and selective wave, weighted information  $w$  is processed from the pulvinar to higher level visual cortical areas so that objects with higher attentional weights are processed by many neurons. The resulting perceptual values  $\eta$  are multiplied by bias values  $\beta$  and their products are transmitted from the cortex to a vSTM storage capacity map of locations localized in the thalamic reticular nucleus (TRN). This topographically organized map does not represent (per se) the characteristics of the selected objects, but rather operates as an indication of their location. Thus, neurons representing the characteristics or features of objects in the visual cortex are kept active once the sensory stimulation has disappeared by reciprocal connections to the corresponding areas in the vSTM map of locations of the TRN. This feedback interaction between sensory neurons and the vSTM map of locations allows visual representation to remain despite the sensory stimulation disappearing.

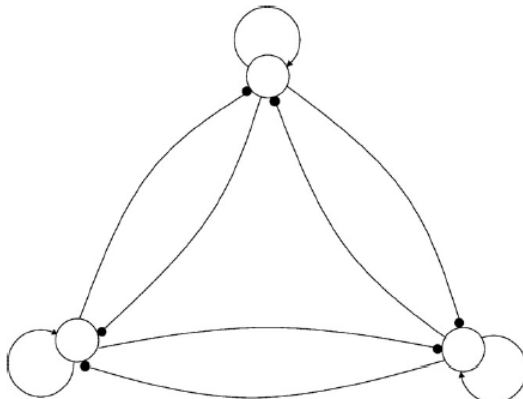


**Figure 2:** Winner-take-all network. Arrows represent excitatory connections and lines ending in solid circles represent inhibitory connections. Reproduced with permission from Bundesen et al., 2005.

Finally, encoding information into vSTM starts every time the map is cleared of the previous activity (initialized). The process of selection operates in a winner-take-all manner, i.e., the first representations of objects in the vSTM map prevent further representation of objects from entering (figure 2). This winner-take-all network functions in the following manner: When externally triggered, all nodes in the network excite themselves while inhibiting each other. In more detail: once a node is externally triggered, its activity will sustain itself while inhibiting the other nodes so they can no longer be activated by external stimulation. Thus, when fewer than  $K$  units are active, an external stimulation can still overcome the inhibition. However, when  $K$  objects are active, an external stimulation corresponding to a new object cannot activate a new object node anymore. This  $K$ -winner-take-all network also explains the limitation of storage capacity of vSTM to only  $K$  active objects at the same time.

## 1.2 EXPERIMENTS: PSYCHOPHYSICAL ASSESSMENT OF ATTENTION FUNCTIONS

In the TVA framework, measures of attentional capacity (vSTM capacity  $K$ , processing speed  $C$ , and perceptual threshold  $t0$ ) and attentional selection (top down control  $\alpha$ , spatial bias  $w_{lat}$ ) can be obtained using a whole and partial report paradigm, respectively. Both paradigms are composed of briefly presented letter arrays appearing on a black screen and preceded by a fixation point. The letters' exposure duration is determined for each participant individually in a pretest session. In both tasks, the presented letters are randomly chosen from a predefined set and appear only once in a given trial. Following stimulus presentation, participants are asked in the whole report task to verbally report to the experimenter every letter they are fairly certain to have seen while only reporting the target letters for the partial report task. The verbal report of individual letters is performed in arbitrary order and without speed constraint. In order to avoid too liberal or too conservative responses, participants receive after each trial a visual performance feedback displaying the correctness of the letters actually reported and allowing them to adjust their performance, e.g. guess less, when the accuracy is below 70% or to try to report more letters when it reaches 90%. During both whole and partial report tasks, the experimenter is sitting behind the participant and manually enters the letters reported by the participants on a keyboard. The applied neuropsychological study that aimed at assessing parameters  $K$ ,  $C$ ,  $\alpha$  and  $w_{lat}$  in patients was implemented by Duncan and colleagues (Duncan et al., 1999).

### 1.2.1 ASSESSMENT OF ATTENTIONAL CAPACITY: THE WHOLE REPORT PARADIGM

The original whole report paradigm designed by Duncan and colleagues (1999) displayed five letters in a column either on the left or on the right side of the screen. Letters were flashed during a well-defined presentation time, or exposure duration, and followed by pattern masks in half of the trials in order to erase the visual afterimage and thus control exactly the time the stimuli are available for processing. Five exposure duration times set during a pre-test session are used in such a version of the whole report task. It is advised to precede the testing by a short practice session of 30 to 40 trials so the participant can get used to the task. A reliability study by Finke and colleagues (2005) has shown that 192 trials were sufficient to get reliable measures of vSTM capacity  $K$  and visual processing speed  $C$ . Following a sufficient number of trials with exposure times avoiding floor and ceiling effects, the number of correct letters reported is estimated as a function of exposure duration (see figure 3). Parameter  $t_0$  (in ms) represents the visual perception threshold below which no letters can be reported. The number of correct letters reported increases as the exposure duration  $t$  increases above  $t_0$ . The slope of the curve for  $t = t_0$  represents the visual processing speed parameter  $C$  while the maximum storage capacity of vSTM, parameter  $K$  corresponds to the asymptote curve where the number of corrected reported letters is stable while exposure duration continues to increase. For more details on the fitting procedure see Kyllingsbaek and colleagues (2006).

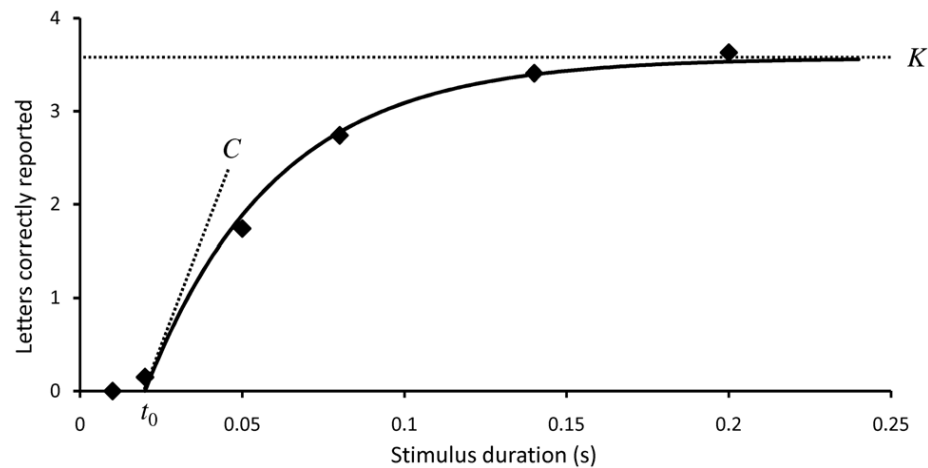


**Figure 3:** Typical performance curve of a whole report paradigm. Reproduced with permission from Habekost et al., 2005.

The original whole report paradigm described above was used in the third study of this thesis while a modified version was used in our first and second studies due to event-related electroencephalography

(EEG) assessment (See figure 4). In this modified version of the task, letters are briefly presented on an imaginary semi-circle rather than in a column. Moreover, for event related components (ERP) assessment with EEG, it is necessary to ensure balanced visual stimulation in both hemifields. Thus, symbols were presented in the visual hemifield opposite to the target stimuli. Furthermore, due to the special requirements of ERP assessment; some of the experimental trials in the whole and partial report tasks were repeated more often than others. These specific manipulations, however, should not affect the TVA parameters derived from fitting report accuracy in the different conditions. For details about fitting procedure see Dyrholm et al., 2011.

## Whole Report Task

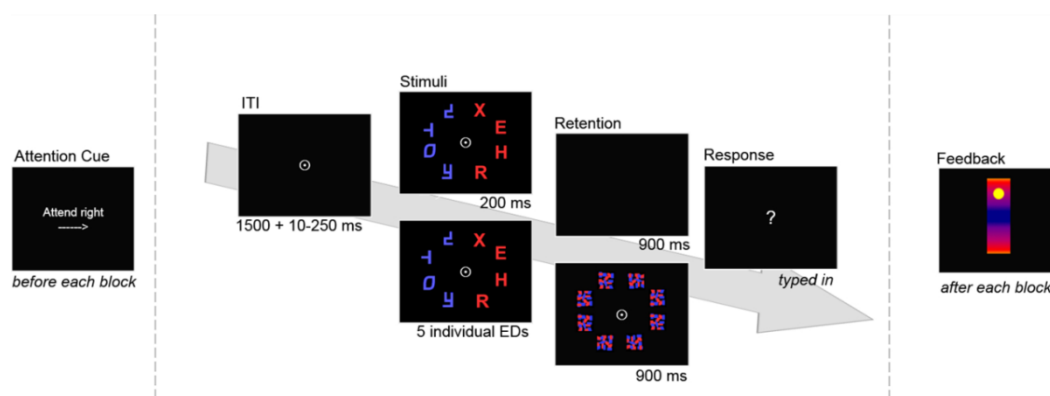


**Figure 4:** Example of the EEG-adapted whole report paradigm used in our first and second studies.

### 1.2.2 ASSESSMENT OF ATTENTIONAL SELECTION: THE PARTIAL REPORT PARADIGM

In the partial report task, two types of stimuli are flashed on the screen, target letters and distractor ones. The aim of the task is to report only the target letters and ignore the distractors. There are three different combinations of stimuli that can be presented, one single target letter, two target letters or one target letter and one distractor. When both a target and a distractor are presented, performance, i.e. report of the target, will be reduced compared to when only one target is presented. The report of the target will suffer even more when it is presented together with a second target of equal relevance. The relative performance in the target plus distractor condition might be either more equal to that of the single target condition (reflecting efficient selection) or might be more equal to that of the dual target condition (indicating less efficient selection). This allows the measure of top down selectivity efficiency (or top-down control), parameter  $\alpha$ . As described previously,  $\alpha$  reflects the task related

differences in weights for targets  $w_T$  and distractors  $w_D$  and is defined by the ratio  $\frac{w_D}{w_T}$ . Thus, an  $\alpha$  value of 1 indicates no selectivity between targets in distractor while perfect selection would correspond to an  $\alpha$  value of 0. Since in reality selection is not perfect, the lower the  $\alpha$  value of an individual, the better his top down control. As both targets and distractors can be displayed on the left and right visual hemifield, a measure of the spatial distribution of attentional weights across the left  $w_{left}$  and right  $w_{right}$  visual hemifield can be obtained. This represents the spatial distribution of attentional weights parameter  $w_{lat}$ . A  $w_{lat}$  value of 0 indicates balanced weighting across hemifields whereas a value of  $w_{lat} > 0,5$  indicates a leftward spatial bias and a value of  $w_{lat} < 0,5$  indicates a rightward bias.

## Partial Report Task

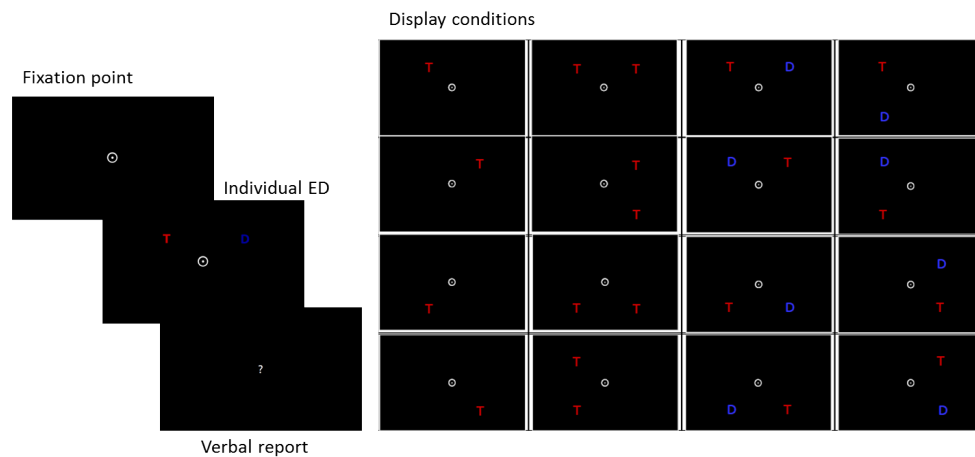


**Figure 5:** example of a partial report task

The psychometric properties of TVA-based assessment, such as the reliability of the tests, have been investigated in several studies. Using bootstrap methods, Habekost and Bundesen (2003) and Habekost and Rostrup (2006) have shown that the measurement error related to each of the TVA parameters was very low, especially for the  $K$  parameter. Bootstrap statistics was also used by Finke and colleagues (2005) to compare parameters estimates based on full or subsets of datasets. They demonstrated that after just 192 trials,  $K$  and  $C$  parameters were highly stable, thus implying that a minimum of 30 min testing is necessary to obtain reliable results. In a more general study, Habekost and colleagues (Habekost et al., 2014) found that TVA-based assessments provided more reliable results than the attentional network test (ANT; Fan et al., 2002). Another strength of TVA-based assessment is its specificity, with five different aspects of attention being measures separately. With the exception of  $K$  and  $C$  being moderately correlated with each other ( $r = 0,3$  to  $0,4$ ), TVA parameters are not correlated with each other. Moreover, as neither the whole nor the partial report tasks involve reaction time measures, the influence of motor processes on performance is removed. Finally, TVA-

based assessment is very sensitive. Indeed, it has been used successfully to assess attention deficits in a wide range of disorders and diseases such as neglect (Duncan et al., 1999; Habekost and Bundesen 2003), simultagnosia (Duncan et al., 2003), alexia (Starrfelt et al., 2009; Starrfelt et al., 2010), stroke (Habekost and Rostrup 2006; Habekost and Rostrup 2007), mild cognitive impairment (Bublak et al., 2006; Bublak et al., 2011; Redel et al., 2012), Alzheimer's disease (Sorg et al., 2012), Huntington's disease (Finke et al., 2006; Finke et al., 2007) or ADHD (Finke et al., 2011; McAvinue et al., 2012). Given such advantages, TVA based assessment constitutes the appropriate tool to investigate attention in healthy individuals and in people with brain alterations such as older individuals or individuals born prematurely.

## 1.3 INVESTIGATING THALAMO-CORTICAL CONNECTIONS WITH DIFFUSION TENSOR IMAGING (DTI)

As previously presented, the NTVA suggests interactions between thalamus and visual cortices to subservise vSTM capacity. Thus, it seems highly relevant to focus our investigation on the white matter tracts connecting those regions and their properties. In order to assess the structural characteristics of thalamo-cortical connections, two types of analysis can be done: investigation of thalamo-cortical tracts' microstructure and reconstruction of pathways via fiber tracking. Both analyses are performed on diffusion weighted imaging data.

### 1.3.1 BASIC PRINCIPLES OF DTI

Diffusion Tensor imaging is an MRI technique providing in vivo non-invasive mapping of white matter tracts at a millimeter resolution (Le Bihan et al., 1988; Le Bihan 1990; Basser et al., 1994). It measures the displacement of water molecules at the scale of tens of microns and is extremely sensitive to changes in tissue microstructure. It is based on the principle that at non-zero temperature, water molecules are in constant motion, which is also known as Brownian motion. In free water, molecules can diffuse equally in all directions, a phenomenon which is called isotropic diffusion. However, in biological tissues, the diffusion of such water molecules will be restricted by cell membranes and organelles, thus resulting in anisotropic diffusion. This is particularly the case in axons where water molecules will diffuse primarily according to the main orientation of the axons whereas diffusion will occur almost equally in all directions in grey matter or cerebro-spinal fluid. Based on such differential diffusion patterns, it is possible to distinguish white matter and delineate tract pathways. By applying magnetic gradients in different directions it is possible to estimate the diffusion of water molecules in the entire brain. The direction of maximum diffusivity has been shown

---

to coincide with the white matter fiber tract orientation (Moseley ME et al., 1990; Pierpaoli and Basser, 1996). The diffusion information can be modeled in 3D space using a tensor. A tensor is a 3x3 matrix subjects to diagonalization and resulting in a set of three eigenvectors. A tensor can be visualized as an ellipsoid where the three eigenvectors represent the major, medium and minor axis of the ellipsoid and the corresponding three eigenvalues ( $\lambda_1$   $\lambda_2$   $\lambda_3$ ) represent the apparent diffusivities along these axes (see figure 6 A and B). From the tensor, one can determine the direction of maximum diffusivity or estimate the diffusivity in any arbitrary direction (Jellison et al., 2004). A typical diffusion MRI sequence is composed of a non-diffusion weighted image called b0 as well as a number of direction-related gradient images (minimum 6 directions and in clinical use, usually around 32). Several measures can be derived from the tensor, each supposedly reflecting different properties of white matter. Fractional anisotropy (FA) describes how directional diffusion is (Basser and Pierpaoli, 1996) with  $0 < FA < 1$ . A FA value close to 1 indicates that water molecules diffuse along one main direction while a value close to 0 suggests no preferential direction of diffusion. In parallel fiber bundles, FA values will typically be very high while in case of degeneration or demyelination, FA values will be lower (see figure 6D). Thus, FA as well as mean diffusivity, (MD) which represents the average diffusion along the 3 axis of the ellipsoid, radial diffusivity (RD), which represents the diffusivity perpendicular to axonal fibers, and axial diffusivity (AD), representing the diffusion parallel to the axon fibers, reflect the microstructure of white matter (see figure 6C). A change in any of these values is indicative of changes in white matter microstructure, often referred to as white matter integrity. Those measures are derived in both animal and human studies. The results of these studies suggest compatibility between species which makes these measures highly relevant for the study of abnormal developments or diseases.

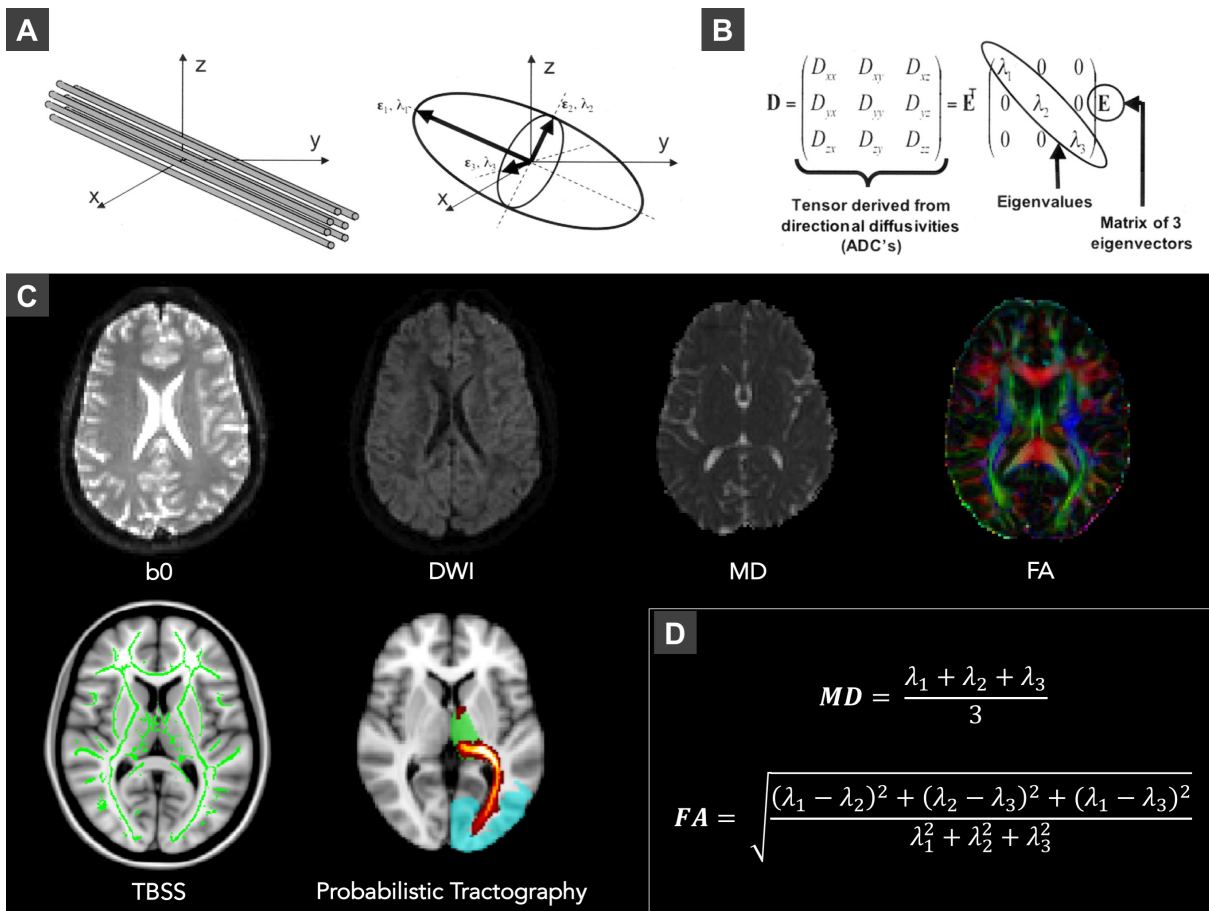


**Figure 6:** Principles of Diffusion tensor imaging and main output measures (adapted with permission from Jellison et al., 2004). **A:** Fiber tracts have an arbitrary orientation with respect to scanner geometry (x, y, z axes) and impose directional dependence (anisotropy) on diffusion measurements. The three-dimensional diffusivity is modeled as an ellipsoid whose orientation is characterized by three eigenvectors ( $\epsilon_1, \epsilon_2, \epsilon_3$ ) and whose shape is characterized by three eigenvalues ( $\lambda_1, \lambda_2, \lambda_3$ ). **B:** This ellipsoid model is fitted to a set of at least six non collinear diffusion measurements by solving a set of matrix equations involving the diffusivities and requiring a procedure known as matrix diagonalization. **C:** Example of b0, DWI, MD images of a subject. On the right side, an example of an FA image modulated by the main eigenvector V1 is shown (red represent a left-right orientation, green antero-posterior and blue up and down orientation). On the bottom left, an example of FA skeleton obtained by TBSS is shown as well as an example of probabilistic tractography between left occipital cortex (in blue) and left thalamus (green). The color gradient from red to yellow represent the number of streamlines generated from the seed region that reach the target region with yellow representing a higher number of streamlines. **D:** MD and FA formulas.

### 1.3.2 INVESTIGATING WHITE MATTER MICROSTRUCTURE WITH TRACT-BASED SPATIAL STATISTICS

When investigating white matter microstructure in healthy or diseased populations, studies commonly used voxelwise analysis of FA images. However such investigations are compromised by the use of standard registration algorithms, which do not account well for differences in brain structure, caused, e.g., by age or neurodegenerative diseases, and, thus, potentially lead to false discoveries. Another issue with voxelwise analysis comes from the fact that no satisfactory solutions regarding the alignment of FA have been found and that there is no universal agreement on the issue of spatial smoothing.

Tract-Based Spatial Statistics (TBSS; Smith et al., 2004; Smith et al., 2006) aims at overcoming such difficulties via the use of non-linear registration and projection onto an alignment-invariant tract representation, the mean FA skeleton. Globally, after being obtained via tensor modeling, FA images are aligned to a template, usually from the Montreal Neurological Institute (MNI) via non-linear registration, thus enabling FA group comparisons. All standardized FA images are then merged together to create a mean FA image and ran into a skeletonization program to obtain the mean FA skeleton image. The skeleton provides the location of the center of white matter tracts and is thresholded to  $FA > 0.2$  in order to keep the main tracts. A distance map from the skeleton mask is then created so that each subject's FA image can be projected onto the mean FA skeleton (see figure 6C). The file containing all subjects' skeletonized FA images is then used for voxelwise statistics using permutation testing, for example to examine which FA voxels are significantly different between term and preterm born adults or between young and old adults. Although a whole brain approach using the mean FA skeleton is often used, it is also possible to use regions of interest (ROIs), such as the splenium of the corpus callosum, obtained from an atlas. Combining ROIs created from an atlas with the TBSS skeleton can allow us to investigate the anisotropy of white matter tract such as posterior thalamic radiations or splenium of the corpus callosum without doing tractography or tracing-based tract estimation and without worrying about the extent of spatial smoothing that should be used. Such advantages make TBSS a widely used and reliable method to analyze changes in white matter properties.

### 1.3.3 STUDYING THALAMO-CORTICAL STRUCTURAL CONNECTIVITY WITH PROBABILISTIC TRACTOGRAPHY

Measures such as FA and MD are based on the principal direction of water diffusion, and thus indirectly reflect the microstructure of white matter tracts. Nevertheless, they do not provide information about the pathway connecting two regions, such as, for example, the thalamus and the occipital cortex. The optimum standard in measuring connections has been neuroanatomical tracing

which consists in injecting a compound in a specific location of the brain. The localization of the compound in locations distant from the original injection site provides strong evidence for a connection between the two regions (Schuz, 2002). Unfortunately, it is not possible to use such methods to study connections in vivo. Thanks to the fast improvements of MRI in the 1980s and 1990s effective methods to measure function and structure non-invasively were developed. Diffusion MRI tractography is currently the only available tool to estimate in vivo the trajectories of white matter in the brain. Tractography integrates voxelwise fiber orientations into a pathway connecting brain regions. The two main types of tractography are deterministic (Mori et al., 1999) and probabilistic tractography (Behrens et al., 2003). In deterministic tractography, each streamline generated follows the main direction of diffusion of each voxel step by step, until a too wide curvature angle or a low signal stops it. The pathway reconstructed is very sensitive to noise and based on one main direction of diffusion and, thus, on one fiber model per voxel. Probabilistic tractography however takes into account the uncertainty of the main direction of diffusion and estimates a distribution of possible orientations. The widely used method from Behrens and colleagues (Behrens et al., 2007), which was also employed in this thesis, uses a Bayesian method to estimate the appropriate number of fiber orientations at each voxel, thus leading to more reliable pathways than deterministic tractography, particularly in regions of crossing fibers. Streamlines are generated following each of these possible orientations. The value in each voxel represents the number of streamlines generated from the seed region (for example the thalamus) that reaches the target region (for example the occipital cortex; see figure 6C). Larger numbers of streamlines in a voxel represent a higher probability for a pathway to be located in this voxel, while fewer numbers of streamlines represent a lower probability for a pathway to be located in a voxel. The reconstructed pathway connecting two regions and its properties are often referred to as structural connectivity between two regions. Although tractography allows the reconstruction of pathways between two regions such as the thalamus and occipital cortex for example, it is not possible to differentiate whether the reconstructed paths reflect connections from thalamus to occipital cortex or the other way around. Overall, probabilistic tractography enables whole brain measurements of long-range connections and together with white matter integrity measures such as FA constitutes the appropriate tool to investigate posterior thalamo-cortical connections.

## 1.4 EXAMPLES OF VSTM CAPACITY- AND WHITE MATTER ALTERATIONS ALONG DEVELOPMENT

As previously described, white matter tracts can be analyzed by investigating either their microstructure using TBSS or pathways connecting two regions, for example via probabilistic tractography. Those two methods have been employed to investigate alterations in white matter in a

wide range of developmental disorders and diseases. In this thesis, we were particularly interested in posterior white matter alterations due to healthy aging and premature birth, as it has previously been shown that both conditions lead to impairment in vSTM capacity (McAvinue et al., 2012; Finke et al., 2015).

#### 1.4.1 EXAMPLE OF LATE LIFE DISTURBANCES: EFFECT OF AGING

Aging has been shown to be associated with a decline in both brain structure and cognitive functions (Sullivan et al., 2001). Among cognitive functions, attention and more particularly vSTM capacity has been shown to be decreased in older individuals (Verhaegen et al., 1993; Jost et al., 2011; Sander et al., 2011), particularly when using the theory of visual attention modeling. Indeed using the whole report paradigm, several studies found reduced vSTM capacity and processing speed in older individuals compared to young adults (McAvinue et al., 2012; Wiegand et al., 2014a; Wiegand et al., 2018).

It is well known that aging is associated with multiple changes in brain structure, such as reduction of grey matter volume and increase of cerebro-spinal fluid (CSF) volume starting in early adulthood (Courchesne et al., 2000; Ge et al., 2002; Raz and Rodrigue, 2006; Walhovd et al., 2011). Nevertheless, the evolution of white matter volume with increasing age seems more complex. Indeed, several studies have found an increase in white matter volume until the fourth or fifth decade of life, interpreted as ongoing myelination, (Courchesne et al., 2000; Ge et al., 2002; Bartzokis et al., 2004) and, following this, a decrease in white matter volume which is accelerated in late adulthood (Courchesnes et al., 2000; Raz et al., 2005). Volumetric studies, despite being informative, do not provide information regarding the mechanisms responsible for those age-related white matter changes. Using diffusion weighted imaging, however, several studies have found changes in white matter microstructure with aging (Pfefferbaum and Sullivan 2003, Pfefferbaum et al., 2000, Sullivan et al., 2001; Wozniak and Lim 2006; Malloy et al., 2007; Madden et al., 2009a; Gunning Dixon et al., 2009; Bennett et al., 2010; for review see Sullivan and Pfefferbaum 2006 and Bennett and Madden 2014). Pfefferbaum, Sullivan and colleagues were the first to show that FA was reduced in older individuals in frontal regions compared to younger individuals (Pfefferbaum and Sullivan 2003, Pfefferbaum et al., 2000, Sullivan et al., 2001). This pattern of reduced FA has since been replicated and found in combination with increased MD in various tracts such as in fronto-occipital fasciculus, sagittal stratum or posterior thalamic radiations (Malloy et al., 2007; Hugenschmidt et al., 2008; Vernooij et al., 2008; Westlye et al., 2010, Bennett, I.J., et al., 2010; for review Fama et al., 2015). Those findings suggest an age-related decline in composition and integrity of white matter with aging. They have been confirmed by longitudinal studies (Barrick et al., 2010; Teipel et al., 2010). Age-related changes in RD and AD were also found, which seem to be more prominent in RD than AD (Baghat and Beaulieu, 2004; Zhang et al., 2010; Madden et al., 2009b). Higher RD was found in older adults than younger

ones, whereas both patterns of increased and decreased AD were found in older participants (Zahr et al., 2009; Bennett et al., 2010; Sullivan et al., 2010; Burgmans et al., 2011). Interestingly, age-related changes in RD and AD were particularly documented in posterior thalamic areas (Kumar et al., 2013) and alterations in thalamo-cortical projections' volume have been reported as well (Hughes et al., 2012). The changes in white matter integrity with aging reported using DTI are consistent with post-mortem histological studies. Indeed, histological studies have shown that, in healthy aging, axonal and myelin degeneration take place along with other changes in the cellular environment such as accumulation of cellular debris and formation of glial scars (Meier-Ruge et al., 1992; Aboitiz et al., 1996; Peters et al., 2002).

These alterations in white matter integrity are at the basis of the cortical disconnection concept in which a disruption of the communication between neural networks underlying cognitive functions is supposed to lead to cognitive dysfunction (O'Sullivan et al. 2001, Bartzokis 2004; Andrews-Hanna et al., 2007; Salat et al., 2011). As reported in several studies compiled by Madden and colleagues (Madden et al., 2009b and Madden et al., 2012) significant links between white matter tracts and cognitive performance in multiple domains have been found. Several studies have shown that higher integrity was associated with better cognitive performance across groups of younger and older adults (Schulze et al., 2011; Coxon et al., 2012) and within groups of older adults (Charlton et al., 2009; Sexton et al., 2010; Ystad et al., 2011; Lockhart et al., 2012; Jacobs et al., 2013 for review see Bennett & Madden 2014). For example Ystad and colleagues (2011) found that FA in tracts connecting the thalamus and inferior putamen to the frontal component of the default mode network, as well as FA in tracts connecting the inferior putamen to the dorsal attention network were significantly positively associated with executive functions. These data are consistent with the idea that age-related decreases in white matter integrity are linked to impaired cognition in older adults. Other studies reported that white matter integrity mediated the relationships between age and cognitive functions (Madden et al., 2009a; Brickman et al., 2012; Borghesani et al., 2013) and between age and processing speed (Salami et al., 2012). Taken together, these findings are consistent with the notion that white matter integrity contributes to age-related impairments in cognitive functions. In our second study, we investigated whether and how alterations in posterior thalamo-cortical connections contribute to impairments in vSTM capacity in older individuals.

### 1.4.2 EXAMPLE OF EARLY LIFE DISTURBANCES: LONG TERM OUTCOMES OF PRETERM BIRTH

Preterm birth is defined by birth before the completion of 37 weeks of gestation. Due to medical improvements primarily, the global prevalence of preterm birth is above 10% (i.e., about 15 million preterm newborns per year) and increasing (Blencowe et al., 2012). Thus, studying the long term neuronal and behavioral changes of preterm born individuals seems highly relevant to our society. Preterm birth is associated with an increased risk for long-term impairments in brain structure and cognitive functions (Baron and Rey Casserly 2010, D’Onofrio 2013). Among cognitive functions, visual attention is particularly affected, (Anderson & Doyle, 2003; Atkinson & Braddick, 2007; Shum et al., 2008; Strang-Karlsson et al., 2010). The long-term stability of attention deficits has been established through, for example, changed eye-movements at infancy (van de Weijer-Bergsma et al., 2008; Atkinson & Braddick 2012), impairments in neuropsychological tests at school age (Anderson & Doyle, 2003; Atkinson & Braddick, 2007; Shum et al., 2008) and slower reaction times in early adulthood (Strang-Karlsson et al., 2010). More recently, using the TVA framework, Finke and colleagues (Finke et al., 2015) found that vSTM capacity  $K$  was reduced in preterm compared to full-term born adults while other attention parameters such as processing speed or top down control remained unchanged. When investigating the neural mechanisms associated with such impairment, Finke and colleagues found that the more the functional connectivity of bilateral posterior brain networks in the preterm group differed from the one of the term group, the higher their vSTM capacity, suggesting a compensatory mechanism (Finke et al., 2015). Interestingly, it has been shown that functional connectivity depends not only on local activity but also on underlying structural connectivity (Honey et al., 2009; Hagmann et al., 2008; Kringelbach et al., 2014) Thus it seems relevant to investigate the structural underpinnings of potential compensatory mechanisms subserving vSTM capacity.

Preterm birth has been associated with widespread impairments in white matter integrity and connectivity. With respect to white matter integrity, it has been shown that preterm born adults exhibited reduced FA and increased MD in widespread tracts including posterior thalamic radiations, corpus callosum and superior longitudinal fasciculi (Meng et al., 2015). At the microstructural level, preterm birth disrupts brain maturation by impairing the maturation of GABAergic interneurons and subplate neurons as well as by aberrant development of oligodendrocytes and astrocytes (Dean et al., 2013; Komitova et al., 2013; for review see Deng 2010; Salmaso et al., 2014). Premyelinating oligodendrocytes affected by hypoxia or ischemia cause a loss or maturation delay of their cellular targets which results in hypomyelination or axonal damage (Ment et al., 2009). Accordingly, a reorganization of cortico-cortical and cortico-thalamic tracts of the thalamocortical system takes place after preterm delivery (Ball et al., 2012; Ball et al., 2013a and Ball et al., 2013b). Indeed, using probabilistic tractography, Ball and colleagues (Ball et al. 2012, Ball et al. 2013, Ball et al. 2014) have

shown that preterm born infants had reduced thalamo-cortical structural connectivity and locally increased cortico-cortical connectivity (Ball et al. 2014).

Considering such structural connectivity patterns and changes in functional connectivity associated with vSTM capacity  $K$  in preterm born adults, we focused on posterior thalamic radiations and splenium corpus callosum and investigated whether and how FA of these tracts was associated with vSTM capacity  $K$  in preterm and full-term born adults.

## 1.5 AIMS OF THE THESIS: THREE HYPOTHESES

The purpose of this thesis is to investigate the association between vSTM capacity  $K$ , and the structural connectivity of posterior thalamus to visual cortices in healthy individuals based on the NTVA framework and thus to potentially bring first structural evidence supporting the NTVA thalamic model in humans. The second and third studies composing this thesis aim at exploring the effects of alterations of the tracts connecting posterior thalamus to occipital cortices resulting from aging or preterm birth on vSTM capacity.

In detail:

- 1) The neural interpretation of the TVA suggests recurrent loops between thalamus and visual cortices to subserve vSTM capacity. So far, only posterior cortical white matter has been proven to be relevant for vSTM capacity. Thus we hypothesized that the structural connectivity of posterior thalamus to occipital cortex would subserve vSTM capacity in healthy adults. Similarly, previous work in humans and monkeys suggest a role for pulvinar nuclei and visual cortices in attentional selection. Therefore, we hypothesized that attentional selection might be associated with the structural connectivity of posterior thalamus to occipital cortices.
- 2) It has been shown that increasing age is associated with a linear decline in vSTM capacity and widespread reduction in white matter microstructure, including in the thalamus. Thus we investigated whether the association between vSTM capacity and the structural connectivity of posterior thalamus to visual cortices found in young participants in the first study remains the same throughout the lifespan or whether aging affects it.
- 3) Finally, it is known that infants born prematurely have impaired cortico-thalamic structural connectivity while local cortico-cortical connectivity is increased. Previous work also shows that vSTM capacity was reduced in preterm born adults. Interestingly, preterm-born adults

with better vSTM storage capacity showed more pronounced changes in intrinsic functional connectivity in bilateral posterior brain networks, compared to term-born individuals suggesting some compensatory mechanism. Given the fact that functional connectivity depends on structural connectivity and considering the previously described complex pattern of brain reorganization, we hypothesized that the association between thalamo-cortical structural connectivity and vSTM capacity might be changed in preterm born adults compared to term-born ones..



## 2 STUDY I:

### STRUCTURAL CONNECTIVITY BETWEEN POSTERIOR THALAMUS AND OCCIPITAL CORTICES UNDERPINS VISUAL SHORT-TERM MEMORY CAPACITY AND ATTENTIONAL WEIGHTING IN HUMANS

This chapter contains a manuscript entitled “Structural connectivity between posterior thalamus and occipital cortices underpins visual short-term memory capacity and attentional weighting in humans.” It is currently under review in NeuroImage.

Authors: Aurore Menegaux, Natan Napiorkowski, Julia Neitzel , Adriana L. Ruiz-Rizzo, Anders Petersen , Hermann J. Müller , Christian Sorg , Kathrin Finke

#### **Contributions**

The author of this thesis is the first author of this manuscript. **A.M.**, K.F. and C.S. designed this study, **A.M.**, J.N. and A.R.R. acquired imaging data and N.N behavioral data, **A.M.** analyzed data and drafted the manuscript and. **A.M.**, A.P., H.J.M., K.F. and C.S. wrote and revised the manuscript before submission.

## TITLE PAGE

**Title:** Structural connectivity between posterior thalamus and occipital cortices underpins visual short-term memory capacity and attentional weighting in humans

### Authors and Affiliations

Aurore Menegaux<sup>1,2,3</sup>, Natan Napiorkowski<sup>1,2</sup>, Julia Neitzel<sup>1,5</sup>, Adriana L. Ruiz-Rizzo<sup>1</sup>, Anders Petersen<sup>6</sup>, Hermann J Müller<sup>1,2</sup>, Christian Sorg<sup>3,4\*</sup>, Kathrin Finke<sup>1,2,7\*</sup>

<sup>1</sup>Department of Psychology, General and Experimental Psychology, Ludwig-Maximilians-Universität München, Leopoldstrasse 13, 80802 Munich, Germany; <sup>2</sup>Graduate School of Systemic Neurosciences GSN, Ludwig-Maximilians-Universität, Großhaderner Strasse 2, 82152 Planegg, Germany; Departments of <sup>3</sup>Neuroradiology, <sup>4</sup>Psychiatry of the Klinikum rechts der Isar, Technische Universität München TUM, Ismaninger Strasse 22, 81675 Munich, Germany; <sup>5</sup>Institute of Stroke and Dementia Research, Klinikum der Universität München, Feodor-Lynen-Straße 17, 81377Munich, Germany; <sup>6</sup>Center for Visual Cognition, University of Copenhagen, Øster Farimagsgade 2A, Copenhagen, Denmark; <sup>7</sup>Hans Berger Department of Neurology, Jena University Hospital, Erlanger Allee 101, 07747 Jena, Germany.

\* These authors contributed equally

### Corresponding author

Aurore Menegaux, Department of Psychology, General and Experimental Psychology, Ludwig-Maximilians-Universität München, Leopoldstrasse 13, 80802 Munich, Germany.

E-mail: aurore.menegaux@psy.lmu.de, phone: +49 89 2180 72567

### Counts

Number of words: Abstract 218; Textbody 7520

Number of figures: 2

Number of tables: 2

Number of Supplementary material: 3

## 2.1 ABSTRACT

In the theory of visual attention (TVA), it is suggested that objects in a visual scene compete for representation in a visual short-term memory (vSTM) store. The race towards the store is assumed to be biased by top-down controlled weighting of the objects according to their task relevance. Only objects that reach the store before its capacity limitation is reached are represented consciously in a given instant. TVA-based computational modelling of participants' performance in whole- and partial-report tasks permits independent parameters of individual efficiency of top-down control  $\alpha$  and vSTM storage capacity  $K$  to be extracted. The neural interpretation of the TVA proposes recurrent loops between the posterior thalamus and posterior visual cortices to be relevant for generating attentional weights for competing objects and for maintaining selected objects in vSTM. Accordingly, we tested whether structural connectivity between posterior thalamus and occipital cortices (PT-OC) is associated with estimates of top-down control and vSTM capacity. We applied whole- and partial-report tasks and probabilistic tractography in a sample of 37 healthy adults. We found vSTM capacity  $K$  to be associated with left PT-OC structural connectivity and a trend-wise relation between top-down control  $\alpha$  and right PT-OC structural connectivity. These findings support the assumption of the relevance of thalamic structures and their connections to visual cortex for top-down control and vSTM capacity.

**Keywords:** Diffusion tensor imaging, probabilistic tractography, neural theory of visual attention, visual short-term memory capacity, posterior thalamus

**Abbreviations:** vSTM, visual short-term memory; TVA, theory of visual attention; NTVA, neural theory of visual attention; DTI, diffusion tensor imaging; PT-OC, Posterior thalamus-occipital cortex; ROI, region of interest; IQ, intelligence quotient

## 2.2 INTRODUCTION

As our visual system is constantly confronted with more objects and features than it can process simultaneously, selection is mandatory. To that end, the visual attention system distributes the limited resources in a way that allows preferential processing of relevant and filtering-out of irrelevant information (Desimone & Duncan, 1995). According to the ‘theory of visual attention’ (TVA; Bundesen 1990), visual processing is conceived as a parallel race between objects in a visual scene for representation in a visual short-term memory (vSTM) store that has a limited storage capacity (Bundenen, 1990). Only those objects that are selected into vSTM are consciously accessible, thus, available for voluntary, task-appropriate actions such as, e.g., verbal report. In line with the ‘biased competition’ account of attention (Desimone & Duncan, 1995), the competition for vSTM representation is assumed to be biased. According to TVA, the probability of a given object  $x$  to become represented in vSTM before its capacity limit is reached is proportional to the relative amount of attentional weight allocated to that object  $w_x$  compared to weight of all other objects in the visual field. Besides bottom-up factors such as stimulus salience, the distribution of attentional weights across objects is influenced by top-down-controlled biases reflecting the objects’ relevance to the current task.

Based on two simple psychophysical tasks involving verbal report of briefly presented letter arrays and TVA-based modelling, individual estimates of a given participant’s efficiency of top-down controlled selection, parameter  $\alpha$ , and vSTM capacity, parameter  $K$ , can be quantified. The individual efficiency of top-down control is derived from TVA-based fitting of performance in a ‘partial-report task’, in which participants have to name target letters (e.g., letters possessing a particular color) only while ignoring distractor letters (in a different color). Based on differences in report accuracy between conditions with and without distractors, separate attentional weights are estimated for target and distractor objects. The efficiency of top-down control, parameter  $\alpha$ , is then derived as the weight allocated to distractors divided by the weight allocated to targets,  $w_D/w_T$ . The capacity of vSTM is derived from a ‘whole-report task’, more precisely, TVA-based fitting of the number of accurately reported letters from a letter array as a function of the (varying) effective exposure duration of array (all letters are of the same color, so no selection is necessary in this task); formally, parameter  $K$  is estimated as the asymptotic value of the growth function relating report accuracy to exposure time. Typical estimates of vSTM storage capacity  $K$  in TVA-based paradigms are around 3-4 items (e.g., Finke et al., 2005; Wiegand et al., 2014a; Wiegand et al., 2014b) which fits well with estimates obtained from other vSTM paradigms (Luck & Vogel 1997; Cowan, 2001; Vogel & Machizawa, 2004).

With respect to the underlying systems in the human brain, the neural interpretation of TVA (NTVA) suggests that ‘visual’ cortical regions, thalamic areas, and white-matter tracts interconnecting these regions are of particular relevance for top-down controlled attentional weighting processes and vSTM

storage (Bundesen et al., 2005). In particular, it is assumed that, following a first, unselective wave of processing, attentional weights are computed for the displayed objects by a priority map in the pulvinar nucleus of the thalamus. In the subsequent, selective wave of processing, attentional weight signals from the pulvinar mediate biased processing of objects in visual brain areas, so that objects with higher attentional weights are processed, or represented by more neurons. The winners of the race are thought to be categorized in a vSTM map of locations assumed to be localized in the posterior thalamic reticular nucleus (see Figure 1). The reticular nucleus then gates activation in positive feedback loops that sustain the activity in neurons representing these winner objects. Thus, the NTVA model – in line with several authors suggesting a critical role of visual thalamic areas in the coordination of attentional selection and vSTM (Danziger et al., 2001; Danzinger et al., 2004; Saalman et al., 2012; Shipp et al., 2003; Shipp et al., 2004; Strumpf et al., 2013; Wurtz et al., 2011) – would predict that the structural connectivity between posterior thalamus and visual cortex is of relevance for both vSTM capacity and top-down controlled weighting processes (Bundesen et al., 2005).

TVA-based studies provided some empirical evidence for the relevance of thalamic structures and posterior white-matter connections for voluntary attentional selection and vSTM storage. The assumed role of the pulvinar in the computation of attentional weights of the objects in the display array was supported by findings of spatial attentional weighting biases towards the ipsilesional field in patients with unilateral pulvinar lesions (Habekost & Rostrup, 2007; Kraft et al., 2015). Of note, such findings in TVA-based paradigms are in line with spatial and task-based attentional selection deficits in the contralesional field following unilateral pulvinar deactivation in monkeys (Petersen et al., 1987; Desimone et al., 1990; Wilke et al., 2010; Wilke et al., 2013; Zhou, Schafer & Desimone, 2016) and damage in humans (Zihl & von Cramon, 1979; Rafal & Posner, 1987; Arend et al., 2008, Snow et al., 2009; Karnath, Himmelbach & Rorden, 2002). Evidence for a critical role of white-matter connections for vSTM storage comes from studies of Habekost and colleagues (2006), who documented deficits in vSTM capacity in patients with lesions to posterior tracts, and of Chechlacz and colleagues (2015), who found inter-individual differences in vSTM capacity in healthy individuals to be related to differences in the microstructure of fronto-occipital tracts. The first more specific analysis of the presumed importance of especially the thalamo-cortical tracts for vSTM capacity revealed that in healthy young adults at the age of 26 years, better microstructure in the posterior thalamic radiation (as reflected by higher fractional anisotropy) was associated with higher vSTM capacity (Menegaux et al., 2017). This was in line with prior findings from Golestani and colleagues (Golestani et al., 2014), who reported an association between a vSTM span task and white-matter microstructure of the optic radiations and the posterior thalamus. Nevertheless, no evidence for the association between the structural connectivity of posterior thalamus to visual cortices and vSTM capacity or attentional weighting has been brought thus far.

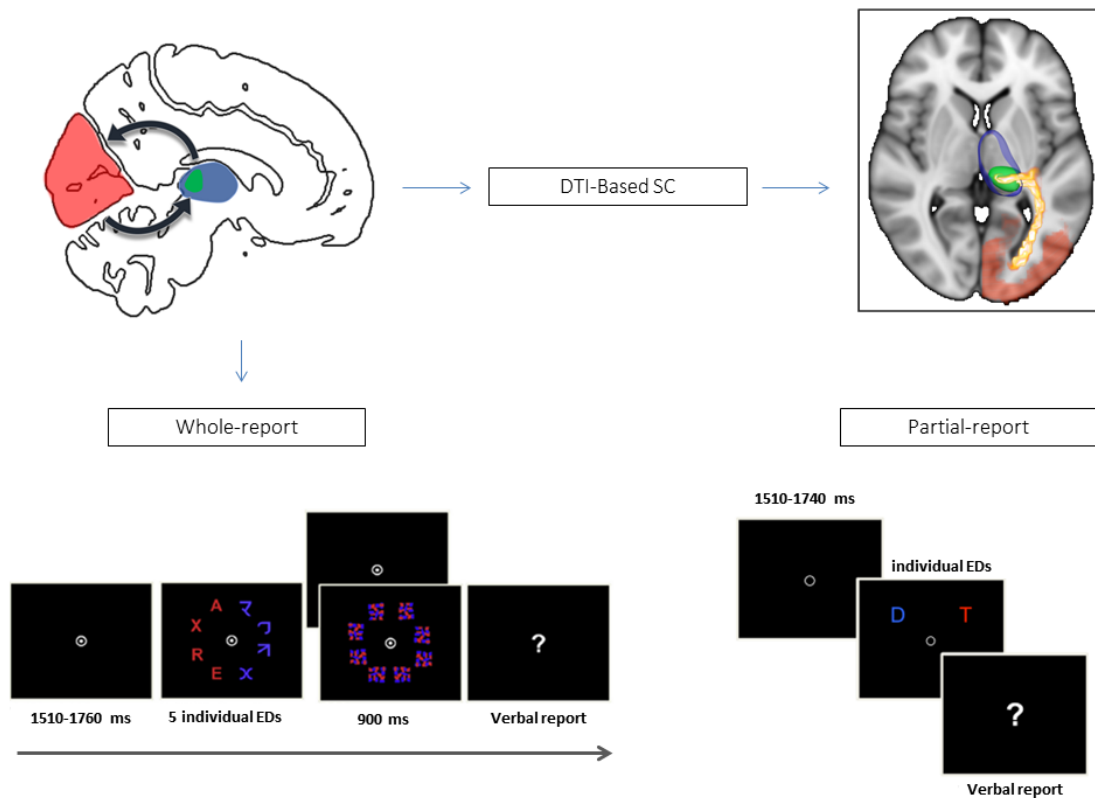


**Figure 1: Presentation of the NTVA model, regions of interest (ROIs) and tasks used in this study.** On the top left corner, the regions of interest derived from the NTVA model of Bundesen are shown with red representing the occipital cortex, blue the whole thalamus and green the posterior thalamus. On the top right corner an example of probabilistic tractography for one subject is represented; on the bottom left and right corner, representations of the whole and partial report tasks respectively are shown.

Given the suggested importance of the posterior thalamus and of thalamo-cortical communication for attentional weighting and vSTM capacity in NTVA (Bundesen et al., 2005) and the prior evidence from TVA-based studies supporting this relevance (Habekost & Rostrup, 2006; Kraft et al., 2015, Menegaux et al., 2017), we hypothesized that individual differences in structural connectivity of the posterior thalamus to occipital cortices would be reflected in the efficiency of top-down control of attention as well as in vSTM capacity. In order to obtain an in-vivo measure of structural connectivity, we performed probabilistic tractography between posterior thalamus and occipital cortices, separately for each hemisphere. The number of streamlines generated between two regions by probabilistic tractography provides the spatial probability distribution of pathways. Voxels with the largest number of streamlines represent the highest probability of a pathway to be located in these voxels (Jones, 2010; Jones et al., 2013; Jbabdi & Johansen Berg 2011). Of note, this number of streamlines does not inform about the strength or quality of connections between those two regions. In other words,

---

probabilistic tractography can only be used to test whether thalamo-cortical connectivity is, in principle, associated with vSTM capacity  $K$  or top-down control  $\alpha$ . However, it is difficult to make predictions concerning the direction of potential relationships (i.e., whether higher or lower connectivity would be related to better attentional performance). Probabilistic tractography was based on diffusion-weighted imaging data obtained from healthy individuals. The same subjects were assessed with TVA-based whole- and partial-report paradigms, in order to derive their individual vSTM capacity  $K$  and top down control  $\alpha$  parameters, respectively. The association of these parameters with posterior thalamus to occipital cortex connection probability was analyzed via partial correlation analysis, controlling for age, gender, crystallized IQ, and total intracranial volume (TIV). Control analyses were carried out to ensure both cognitive and cortical specificity of our findings using other TVA parameters as well as motor cortex, respectively.

## 2.3 MATERIAL AND METHODS

### 2.3.1 PARTICIPANTS

Thirty-seven participants, aged 21 to 53 years were included in the present study. All participants were fluent in German and had normal or corrected-to-normal vision. 32 participants were right-handed, 4 were left-handed, and 1 was ambidextrous according to the Edinburgh Handedness Inventory (Oldfield 1971). All the participants were highly educated, with years of school education ranging from 10 to 13 years (see Table 1) ( $M = 12.4$   $SD = 0.9$ ). The German version of the multiple-choice vocabulary test MWT-B (Lehr, 1977) was used to measure crystallized IQ, and the Beck Depression Inventory test (BDI; Beck et al. 1996) was used to rule out depression.

| Variable           | N = 66 |       |              |
|--------------------|--------|-------|--------------|
|                    | M      | SD    | Range        |
| Gender (F/M)       | 32/34  |       |              |
| Handedness (R/L/B) | 60/4/2 |       |              |
| Education (years)  | 12.1   | 1.65  | 8.50-14      |
| Age (years)        | 48.8   | 19.56 | 20 - 77      |
| <i>K</i>           | 3.22   | 0.39  | 2.29 – 3.83  |
| <i>C</i>           | 23.26  | 8.41  | 9.71 – 47.01 |
| <i>t0</i>          | 12.82  | 13.93 | 0.00 – 67.13 |
| Crystallized IQ    | 102.07 | 16.58 | 72.5 – 140.0 |

**Table 1:** Sample characteristics

Exclusion criteria included alcohol intake at the day of testing, chronic eye diseases (e.g., colour blindness, glaucoma), history of neurological (e.g., brain injury, stroke) or psychiatric (e.g., anxiety disorder, schizophrenia) diseases, any occurrence of epileptic seizure, intake of medication affecting cognitive performance, claustrophobia, and current symptoms of depression (BDI score > 18). 50 participants were recruited for this study. In total, thirteen participants had to be excluded: three because of high BDI scores, four because they did not follow the task instructions of the behavioral tasks adequately (three in the whole-report and one in the partial-report task), five due to bad quality of and one due to incomplete diffusion-weighted imaging data. Our final cohort of participants consisted of 37 individuals. The study was approved by the ethics committees of the Department of Psychology of the Ludwig-Maximilians-Universität (LMU) Munich and the Medical Department of the Technische Universität München (TUM), and all participants gave prior informed consent in

writing. Cognitive testing was performed at the LMU Department of Psychology, brain imaging at the TUM Department of Neuroradiology.

### 2.3.2 TVA-BASED BEHAVIOURAL ASSESSMENT OF VSTM CAPACITY AND TOP-DOWN CONTROL

#### GENERAL ASSESSMENT PROCEDURE

Whole- and partial-report tasks were conducted in a dimly-lit sound-attenuated chamber (Industrial Acoustics Company) with simultaneous EEG recordings<sup>1</sup>. Stimuli were presented to participants on a 24" LED screen (800 x 600 pixel resolution, 100-Hz refresh rate) at a viewing distance of 65cm.

Each participant completed two sessions of 1.5 to 2 hours each on different days: in one session, the whole-report was conducted and in another session the partial report task. Each session included EEG preparation, presentation of written instructions and stimuli used in the experiment, a procedure for adjustment of the individual exposure durations, and approximately 45 minutes of testing proper.

At the beginning of each trial, a fixation point (a white circle, 0.9° of visual angle in diameter, with a white dot in the centre) was presented in the centre of the display for a duration drawn randomly from 10 to 240 ms. Participants were instructed to fixate this marker throughout the blocks of trials administered. Following the fixation marker, red and/or blue letters were briefly presented on a black background. Letters' exposure durations were determined individually for each participant in a short pre-experimental practice session in order to ensure a comparable level of task difficulty across participants. The letters were randomly chosen from the following set {A, B, D, E, F, G, H, J, K, L, M, N, O, P, R, S, T, V, X, Z} and appeared only once in a given trial display. After stimulus presentation, a white question mark appeared in the centre of the screen, indicating the start of a verbal letter report. The participant could perform the report in any, arbitrary order, without speed constraint. In order to avoid too much guessing, participants were instructed to report only letters they were fairly certain they had seen. Following each block, participants received feedback related to the accuracy of the letters they actually reported (note that this feedback was independent from the overall performance

---

<sup>1</sup>EEG recording was used for the assessment of event-related components (ERPs) during task performance, which are not the focus of the current study. Due to the special requirements of ERP investigation, some of the experimental trials in the whole- and partial-report tasks were repeated more often than others. Furthermore, for the ERP assessment, it was also necessary to ensure balanced visual stimulation in both hemifields in the whole-report task. This is why task-irrelevant (non-letter) symbols were presented in the visual hemifield opposite to the target stimuli. These specific manipulations, however, would not affect the TVA parameters derived from fitting report accuracy in the different conditions.

level reached). A visual feedback bar indicated whether the report accuracy of the actually reported letters ranged between 70 and 90%. If accuracy fell below 70%, the participant was told by the experimenter to try to refrain from guessing and report only the letters relatively sure to have seen. If it was above 90%, the participant was encouraged to be less anxious and report more letters, even if not absolutely sure that they are correct. During the administration of both (the whole- and partial-report) tasks, the experimenter was seated behind the participant and entered the letters orally reported by the participant on a keyboard and then manually started the next trial by a key press action.

### WHOLE-REPORT TASK

On each trial, four letters were briefly presented along an imaginary semi-circle, of a radius of  $5.27^\circ$  of visual angle, either to the left or the right of the fixation point. Participants were instructed to report orally as many of the letters as possible. Four blue symbols (composed of random letter parts; see Figure 1) of the same luminance were displayed on the symmetrical semicircle on the other side of fixation. Letter and symbol stimuli subtended  $1.3^\circ$  of visual angle. At the beginning of each trial block, a white arrow in the center pointed towards the side on which the target (i.e., letter) stimuli would appear throughout the upcoming block. The target side in the first block was counterbalanced across participants and then alternated throughout the experiment. Seven timing conditions were used. In five conditions, the stimulus array was followed by post-display masks (see Figure 1) that consisted of eight red-blue scattered squares (also subtending  $1.3^\circ$  of visual angle) which were presented at each (letter and symbol) stimulus location for a duration of 900 ms. These arrays were presented for five different, individually adjusted exposure durations. In two additional conditions, the stimuli were presented unmasked, i.e., they were followed by a blank screen also presented for 900 ms. In one of these conditions, the exposure time was the second shortest duration (of the total five individually adjusted durations); in the other condition, the exposure time was fixed at 200 ms for all participants. In these unmasked conditions, the exposure durations are effectively prolonged compared to the masked conditions, due to the uninterrupted visual persistence of the stimuli (Sperling, 1960). Thus, the five masked and the two unmasked conditions resulted in seven different effective exposure durations. The various experimental conditions were equally distributed across blocks of trials, and were displayed in randomized order within each block.

The exposure time adjustment phase consisted of 48 trials, divided into 4 blocks of 12 triples of trials. Each triple consisted of two trials that were not used for adjustment, but were simply presented for allowing the participant to become familiar with the task. These were either unmasked trials with an exposure duration of 200 ms or masked trials with an exposure duration of 250 ms. The critical trial display in each triple that was used for the exposure duration adjustment was masked and initially presented for 80 ms. Each time the participant reported at least one correct letter on this trial, exposure duration was decreased by 10 ms. When an exposure duration was reached at which the participant

was no longer able to name a single letter correctly, this was set as lowest exposure duration used in the subsequent whole-report experiment proper. Based on this value, a set of 4 longer exposure durations was chosen from predefined sets.

The testing phase consisted of 10 experimental blocks, each of 40 trials. For each exposure duration, 30 trials were presented; the only exception was the condition with unmasked trials presented for 200 ms, for which 220 trials were presented (these were the critical trials for ERP analysis).

### PARTIAL-REPORT TASK

On each trial, either a single (red) target letter, two target letters, or a target accompanied by a (blue) distractor were presented on a black background (see Figure 1). Red and blue letters were of the same luminance and had a size of  $0.9^\circ$  of visual angle. They appeared at the corners of an imaginary square, centred on the midpoint of the screen, with an edge length of  $12.3^\circ$  of visual angle. In displays containing two letters, these were presented either both vertically or both horizontally, but never diagonally.

Initially, 16 practice trials were presented with an exposure duration of 80 ms. Next, the procedure to adjust the individual exposure duration was applied, which consisted of 24 trials (4 single-target, 12 dual-target, and 8 target-distractor trials, in pseudorandomized order), with an initial exposure duration of 80 ms. Note that only the dual-target trials were used for exposure duration adjustment; the single-target and target-distractor trials were included simply to allow participants to become familiar with all conditions of task. In the dual-target condition, if the participant reported both letters correctly, the exposure duration was decreased by 10 ms; if only one of the two letters was reported correctly, the exposure duration remained unchanged; and if none of the letters were reported correctly, the exposure duration was increased by 10 ms. Following this adjustment procedure, a performance check block with 24 trials (8 single-target, 8 dual-target, and 8 target-distractor-trials) was presented for the previously determined exposure duration. Accuracy for the single-target and the dual-target condition was displayed on the screen. The proper partial-report experiment was started by the experimenter when the accuracy achieved was within a range of 70 to 90% correct in the single-target condition and above 50% in the dual-target condition (i.e., if, on average, more than one letter was reported correctly in the dual-target condition). If performance was too high or too low, the exposure duration was manually adjusted by the experimenter, who also repeated the performance check procedure until an appropriate exposure duration was found. In total, 112 single-target, 112 dual-target, and 280 target-distractor trials were presented. Overall, there were 504 trials divided into 14 blocks. The experimental conditions were equally distributed across blocks, and were displayed in randomized order within the blocks.

## ESTIMATION OF TOP DOWN CONTROL AND VISUAL SHORT TERM MEMORY CAPACITY

Modeling of participants' top-down control and vSTM capacity parameters utilized the TVA computational model implemented in the *libTVA* toolbox for Matlab (Mads Dyrholm, [www.machlea.com/mads/libtva.html](http://www.machlea.com/mads/libtva.html)). Detailed descriptions of the fitting procedure can be found in Dyrholm et al., 2011. In brief, top-down control was derived by modeling individual performance accuracy across the different partial-report conditions. This fitting procedure provided estimates of the attentional weights  $w_i$  assigned to both targets and distractors displayed at each location in the partial report experiment. Based on these values, the top-down control parameter ( $\alpha$ ), which reflects the difference in the weights assigned to targets  $w_T$  and distractors  $w_D$ , was estimated. As  $\alpha$  is defined by the ratio  $w_D/w_T$ , (lower)  $\alpha$  values approaching 0 indicate highly efficient top-down control, whereas values approaching 1 indicate rather non-selective processing. The spatial bias parameter  $w_{lat}$ , an indicator of the spatial distribution of attentional weights across the left ( $w_{left}$ ) and right ( $w_{right}$ ) visual hemifields, was also obtained from this fitting procedure. It is defined as the ratio  $w_{left} / (w_{left} + w_{right})$ . Thus, a value of  $w_{lat} = 0.5$  indicates balanced weighting, a value of  $w_{lat} < 0.5$  indicates a rightward spatial bias, and a value of  $w_{lat} > 0.5$  indicates a leftward bias. The spatial bias parameter  $w_{lat}$  was not of primary interest in our study, but was used to assess the cognitive specificity of our results<sup>2</sup>.

Furthermore, vSTM capacity was derived by a TVA-based whole-report fitting procedure that models the probability of correct letter report in whole-report as an exponential growth function with increasing (effective) exposure duration. The exposure time variation (7 durations) generated a broad range of performance which specified the whole probability distribution of the number of correctly reported elements as a function of the effective exposure duration. Parameter  $K$  is the asymptote of the fitted function, representing vSTM capacity in terms of the maximum number of items that can be simultaneously represented in visual short-term memory (VSTM)<sup>3</sup>. The slope of the function at its origin represents visual processing speed (parameter  $C$ ) which is defined as the rate of visual information uptake (in elements per second). Similarly to the spatial bias parameter  $w_{lat}$  in the partial-report task, the processing speed parameter  $C$  was drawn upon to ensure the cognitive specificity of our results. Two additional parameters which are of little or no interest for the questions at issue in the present study were also estimated: the perceptual threshold (parameter  $t_0$ ), the longest ineffective exposure duration (in ms) below which information uptake is effectively zero; and parameter  $\mu$ , representing the prolongation of the effective exposure duration (in ms) on unmasked trials. For

---

<sup>2</sup> Finally, sensory effectiveness values for each hemi-field were obtained ( $A_{left}$  and  $A_{right}$ ) that basically reflect how well stimuli were perceived, under the chosen exposure duration, in the left and the right hemi-field. This parameter is relevant for the valid estimation of top-down control and spatial attentional bias, but not relevant for the current study and not considered further.

<sup>3</sup> The  $K$  value reported is the expected  $K$  given a particular distribution of the probability that on a given trial  $K = 1, 2, 3$ , or  $4$ .

participants whose  $t_0$  was estimated to be below 0 (4 out of 37), we refitted the data fixing  $t_0$  at 0. This new fit did not modify the mean value of K and C parameters (Supplementary Table S1) nor any analyses in this study (Supplementary Table S2).

### 2.3.3 IMAGING DATA ACQUISITION

Whole brain T1- and diffusion-weighted imaging data were acquired on a 3T Philips Ingenia scanner with a 32 channel head coil and a SENSE factor of 2. Diffusion images were acquired using a single-shot spin-echo echo-planar imaging sequence, resulting in one non-diffusion weighted image ( $b = 0$  s/mm<sup>2</sup>) and 32 diffusion weighted images ( $b = 800$  s/mm<sup>2</sup>, 32 non-collinear gradient directions) covering whole brain with: echo time (TE) = 61 ms, repetition time (TR) = 14206,980 ms, flip angle = 90°, field of view = 224 x 224 mm<sup>2</sup>, matrix = 112 x 112, 60 transverse slices, voxel size = 2 x 2 x 2 mm<sup>3</sup>. A whole head high-resolution T1-weighted anatomical volume was acquired using a 3D magnetization prepared rapid acquisition gradient echo sequence with the following parameters: repetition time = 9 ms; time to echo = 4 ms; inversion time, TI = 0 ms; flip angle = 8°; 170 sagittal slices; field of view = 240 mm<sup>2</sup>; matrix size = 240 × 240; reconstructed voxel size = 1 x 1 x 1 mm.

### 2.3.4 QUALITY CHECK

All acquired MRI images were visually inspected by two independent raters (A.M., C.S.) for excessive head motion, and apparent or aberrant artifacts. In addition to visual inspection of the raw data, we also used the fitting residuals (the sum-of-squared-error maps generated by DTIFIT) to identify data corrupted by artifacts. Artifacts include motion-induced artifacts, insufficient fat suppression (ghosting) artifacts, and extreme distortion artifacts. Furthermore, T2 images were examined to exclude potential lesions and white-matter abnormalities by experienced radiologists.

### 2.3.5 PREPROCESSING

Diffusion data preprocessing was performed using the FMRIB Diffusion Toolbox in the FSL software ([www.fmrib.ox.ac.uk/fsl](http://www.fmrib.ox.ac.uk/fsl); Jenkinson et al., 2012) after converting data from DICOM to nifti format using `mricron dcm2nii` (Rorden et al., 2007) as described in previous work (Meng et al., 2015). All diffusion-weighted images were first corrected for eddy current and head motion by registration to the  $b_0$  image and skull and non-brain tissue were removed using the brain extraction tool (BET).

T1-weighted images were preprocessed using the anatomical processing script from FSL which included reorientation, image cropping, bias field correction, linear (FLIRT, FMRIB's Linear Image Registration Tool) and non-linear (FNIRT, FMRIB's Non-Linear Image Registration Tool) registration

to MNI standard space. Output of this non-linear transformation included a structural-to-MNI standard space warp field and its inverse (MNI-to-structural). Anatomical preprocessing also included brain extraction (BET) and both tissue type and subcortical structure segmentations which were used to register diffusion weighted images to preprocessed structural T1-weighted images using boundary-based registration for echo planar imaging data thus yielding a diffusion-to-structural transformation matrix. In order to register diffusion weighted data to the MNI 152 template via structural scan, we combined the previously generated structural-to-MNI non-linear transformation matrix with the diffusion\_to\_structural transformation matrix, thus resulting in a diffusion-to-standard space transformation. This transformation will be used later on to transform the individual `fdt_paths`, the 3D image file containing the output connectivity distribution to the seed mask to standard space.

### 2.3.6 PROBABILISTIC TRACTOGRAPHY AND SEED AND TARGET MASKS CREATION

Overall, we used several FSL atlases to define the occipital cortices, thalamic and exclusion masks for each hemisphere in standard space. Those masks were then transformed into native space using the previously described non-linear mapping, and probabilistic tractography was performed to identify the streamlines from occipital cortex to the thalamus within each hemisphere discarding inter-hemisphere estimates. The resulting path was then normalized and transformed into standard space, where a posterior thalamus mask for each hemisphere was used to extract the mean probability of connection value which was then correlated with the previously described attention parameters.

### REGIONS OF INTEREST (ROIs) GENERATION

We used the MNI 152 2-mm label atlas combined with the Harvard Oxford 2-mm cortical atlas to create our cortical occipital mask in standard space. Masks of the right and left thalamus were created from the Oxford thalamic 30% 2-mm connectivity atlas which is based on the probability of anatomical connections between the thalamus and the cortex in MNI space (Behrens et al., 2003). Additionally, whole brain left and right hemisphere masks were created from the Talairach atlas and used as exclusion masks in the tractography process. All masks were transformed into the subjects native space using the reverse non-linear mapping previously obtained and nearest neighbor interpolation.

## ESTIMATION OF DIFFUSION PARAMETERS AND PROBABILISTIC TRACTOGRAPHY

Using the FDT toolbox from FSL, we first ran the function of Bayesian estimation of diffusion parameters obtained using sampling techniques (BedpostX) for each participant. It estimates the individual diffusion parameters at each voxel while automatically considering the number of crossing fibers per voxel (Behrens et al., 2003; Behrens et al., 2007). We used the default parameters implemented in FDT: 2 fibers per voxel, weight of 1, and burning period 1000. Using the ROIs created as described above, tractography was run for each hemisphere with the occipital ROI as seed and the thalamus as waypoint target mask using the probtrackx2 function from FSL. We also used an exclusion mask from the opposite hemisphere in order to ensure the ipsilateral nature of the tractography. We performed tractography separately from each occipital ROI to the thalamus. For each participant, 5000 streamlines were initiated per seed voxel with a path length of  $2000 \times 0.5$  mm steps, a curvature threshold of  $80^\circ$ , and loop checking criteria. The resulting image or `fdt_paths` represents the path connecting the seed region to the target, where the value in each voxel represents the number of streamlines generated from the seed region that pass through that voxel. Due to the differences in volume of each area across participants, we normalized the resulting tract estimates (`fdt_paths`) by dividing them by the `waytotal` (total number of streamlines generated from the seed region that reaches the target region) (Rilling et al., 2008), thus yielding a probability map of connectivity (Zhang et al. 2010, Arnold et al., 2012; Behrens et al., 2007; for review see Jbabdi et al., 2015). Those probability maps were then transformed back into standard space, so that they could be used for statistical analysis (Figure 1).

In order to assess the inter-individual variability of the thalamic probability maps, each individual probability map transformed into standard space was thresholded to exclude the lowest 20% of probability values voxels in order to reduce noise. Following this step, each individual's thresholded map was binarized and the mean of these maps was calculated. To visualize it, we thresholded this mean map to 0.9 to keep only voxels that were present in 90% of the individuals (supplementary material Figure S1 left). In a second step, we overlaid the posterior thalamic masks, which revealed that most of its voxels overlapped with the mean map, indicative of a relatively stable connectivity pattern among participants (supplementary material Figure S1 right).

### 2.3.7 ESTIMATION OF TOTAL INTRACRANIAL VOLUME (TIV)

In order to obtain volumetric measurements for the whole brain, T1 images were segmented into grey matter, white matter and cerebrospinal fluid tissue classes and normalized to the MNI 152 mm template using DARTEL (SPM12 software package, <http://www.fil.ion.ucl.ac.uk>). The segmented and normalized images were modulated to account for the structural changes resulting from the normalization process, thus indicating grey matter, white matter and cerebrospinal fluid volume. A measure of total intracranial volume was estimated by first computing and then adding up the totals (in

liters) of the warped, modulated, and unsmoothed grey-matter, white-matter and cerebrospinal-fluid segments with the in-built SPM Tissue Volumes Utility (Malone *et al.*, 2015).

### 2.3.8 STATISTICAL ANALYSES

For each individual connection probability map, posterior thalamus masks of each hemisphere were used to extract the mean probability of connection from these regions. A posterior thalamus mask was created for each hemisphere using the Talairach labels 2mm atlas, which, owing to the low resolution of MRI, contained the thalamic reticular nucleus as well as the pulvinar nucleus. Since normal distribution was not confirmed for all variables (via Kolmogorov-Smirnov test), Spearman partial correlation was used to assess the association among left and right posterior thalamus-occipital cortex connection probability and top down control/vSTM capacity. These analyses were performed using the SPSS statistics package version 21 (IBM). For all correlations, gender, handedness, age, crystallized IQ, and TIV were used as covariates of no interest.

### 2.3.9 CONTROL ANALYSES

In order to test the structural specificity of our connectivity results for the occipital region, we performed tractography from the motor cortex as control ROI to the thalamus. We used Brodmann areas 4a, 4p, and B6 from the Jülich atlas, separately for each hemisphere, combined with the Harvard-Oxford 2-mm cortical atlas to create the cortical motor masks for the left and the right hemisphere. Similarly, the Harvard-Oxford 2-mm cortical atlas combined with the MNI 152 2-mm label atlas were used to create left and right parietal cortex masks. Furthermore, in order to test the cognitive specificity of our results for vSTM capacity  $K$  and top-down control  $\alpha$ , in control analyses the TVA parameters processing speed  $C$  and spatial bias  $w_{lat}$  were correlated with left and right posterior thalamus-occipital cortex connection probability using Spearman partial correlation.

## 2.4 RESULTS

### 2.4.1 BEHAVIOURAL DATA

The mean vSTM storage capacity  $K$  value of our sample was 3.31 (SD = 0.39) (see Table 1), and the mean top down control  $\alpha$  value was 0.44 (SD = 0.14), consistent with highly similar previous findings in healthy participants (e.g., Finke et al., 2005; Kraft et al., 2015). Moreover, in line with the assumption of the TVA model (Bundesen 1990) that the two parameters reflect independent attentional functions, vSTM capacity and top down control were not significantly correlated with each other ( $r_s(35) = 0.28$ ;  $p = .10$ ).

### 2.4.2 POSTERIOR THALAMUS-OCCIPITAL CORTEX (PT-OC) STRUCTURAL CONNECTIVITY AND VSTM CAPACITY

In order to test our hypothesis that PT-OC connection probability would be significantly associated with vSTM capacity, we performed two separate Spearman correlation analyses between PT-OC connection probability obtained from tractography for the left and the right hemisphere and  $K$ , controlling for gender, age, handedness, IQ, and TIV. We found the left hemisphere PT-OC connection probability to be significantly negatively associated with  $K$  ( $r_s(30) = -0.38$ ;  $p = .03$ ), whereas there was no significant association between  $K$  and the right hemisphere PT-OC connection probability ( $r_s(30) = 0.02$ ;  $p = .91$ ; Figure 2 and Table 2).

### 2.4.3 POSTERIOR THALAMUS-OCCIPITAL CORTEX STRUCTURAL CONNECTIVITY AND ATTENTIONAL SELECTION

In order to test our hypothesis that PT-OC connection probability would be associated with top-down control, we performed separate Spearman correlation analyses between PT-OC connection probability obtained from tractography for the left and the right hemisphere and top-down control  $\alpha$ , again controlling for gender, age, handedness, IQ, and TIV. We observed a trend for a significant positive correlation between  $\alpha$  and right PT-OC structural connectivity ( $r_s(30) = 0.31$ ;  $p = .08$ ), that is: higher connectivity between posterior thalamus and occipital cortices tends to be related with less efficient top-down control. We did not find any association between left PT-OC structural connectivity and  $\alpha$  ( $r_s(30) = -0.06$ ;  $p = .74$ ; Figure 2 and Table 2).

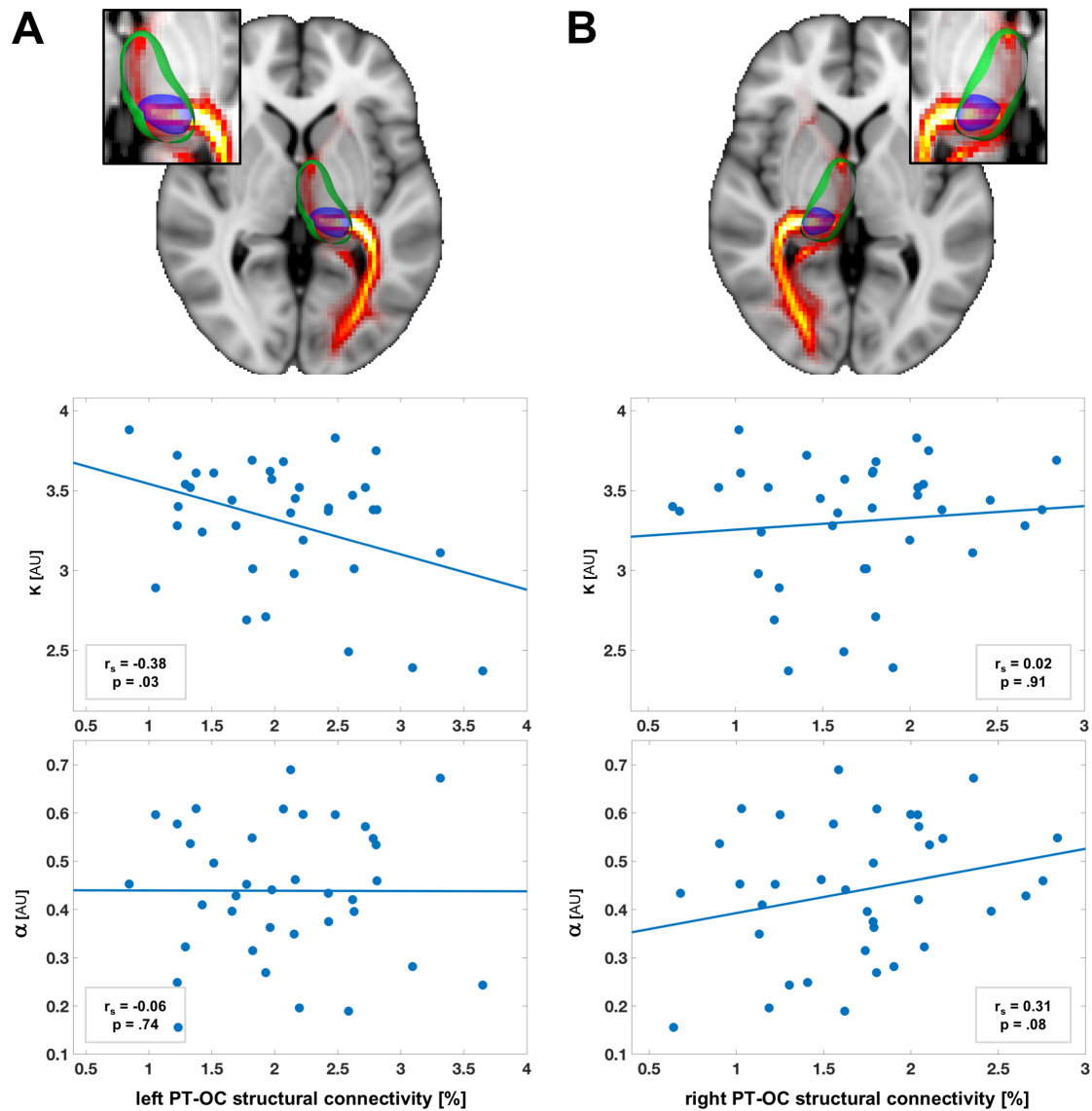


**Figure 2: Structural connectivity between posterior thalamus and occipital cortices is associated with vSTM capacity and top down control.** The first row illustrates probabilistic tractography between occipital cortices and left (A) or right (B) thalamus respectively. Green represents left and right thalamic masks and blue left and right posterior thalamic masks. The second and third rows show graphs representing vSTM capacity and top down control respectively, as a function of left or right structural connectivity. Data points were correlated by Spearman correlation with correlation coefficient  $r_s$  and significance level  $p$ . The lines in the graphs represent linear regression lines, for illustration.

### 2.4.4 CONTROL ANALYSES

#### ANALYSES OF CORTICAL SPECIFICITY: vSTM CAPACITY AND TOP DOWN CONTROL ARE NOT ASSOCIATED WITH POSTERIOR THALAMUS- MOTOR CORTEX STRUCTURAL CONNECTIVITY

In order to test the cortical specificity of the association between PT-OC structural connectivity and vSTM capacity, we investigated whether the parameters vSTM storage capacity and/or top-down control would also be associated with structural connectivity of the posterior thalamus with regions not supposed to be relevant for attentional weighting or visual short-term maintenance, i.e., with the left and the right motor cortex. We did not find any significant associations (highest  $r_s$ -value: 0.23; lowest  $p$ -value: .22; Table 2).

#### FUNCTIONAL SPECIFICITY, PT-OC STRUCTURAL CONNECTIVITY IS NOT ASSOCIATED WITH PROCESSING SPEED OR SPATIAL BIAS

In order to test whether the results obtained for vSTM storage capacity  $K$  and top-down control were cognitively specific, we additionally correlated left- and right-hemisphere PT-OC connection probability with the TVA parameters visual processing speed  $C$  and spatial bias  $w_{lat}$ , via Spearman partial correlations. We did not find any significant correlations (highest  $r_s$ -value: 0.24; lowest  $p$ -value: .19; Table 2).

|                          |           | <i>Test ROIs</i> |             |                |           | <i>Control ROIs</i> |           |                |           |
|--------------------------|-----------|------------------|-------------|----------------|-----------|---------------------|-----------|----------------|-----------|
|                          |           | Left PT-OC SC    |             | Right PT-OC SC |           | Left PT-MC SC       |           | Right PT-MC SC |           |
| <i>Test variables</i>    | <i>K</i>  | $r = -0.38$      | $p = .03^*$ | $r = 0.02$     | $p = .91$ | $r = 0.03$          | $p = .80$ | $r = -0.10$    | $p = .59$ |
|                          | $\alpha$  | $r = -0.06$      | $p = .74$   | $r = 0.31$     | $p = .08$ | $r = 0.01$          | $p = .99$ | $r = -0.23$    | $p = .22$ |
| <i>Control variables</i> | <i>C</i>  | $r = -0.17$      | $p = .36$   | $r = 0.09$     | $p = .64$ | $r = 0.09$          | $p = .62$ | $r = -0.01$    | $p = .96$ |
|                          | $w_{lat}$ | $r = 0.24$       | $p = .19$   | $r = 0.13$     | $p = .50$ | $r = 0.27$          | $p = .14$ | $r = 0.12$     | $p = .50$ |

**Table 2: Correlation between TVA parameters and posterior thalamus structural connectivity.**

Abbreviations: PT-OC: Posterior thalamus to occipital cortex; PT-MC: Posterior thalamus to motor cortex; SC structural connectivity. ROI: Region of interest. Correlations below  $p = .10$  are shown in bold, \* indicates  $p < .05$ .

## 2.5 DISCUSSION

According to the NTVA model (Bundesen et al., 2005), the pulvinar nucleus of the thalamus contains the priority map of objects where attentional weights are computed and bias the processing of objects in visual areas. Based on this assumption, we investigated whether posterior thalamus to occipital cortex structural connectivity was associated with top-down control in healthy individuals. Furthermore, the NTVA model suggests that posterior thalamic nuclei and, in particular, the TRN are relevant for vSTM capacity by sustaining the activity of visual cortical neurons representing the objects through a feedback loop. Accordingly, we also investigated whether posterior thalamus-occipital cortex structural connectivity was associated with vSTM capacity in healthy individuals.

We found evidence for the relevance of fiber tracts connecting the posterior thalamus and the visual cortex areas for both of these functions. In more detail, we observed a non-significant trend for estimates of top-down control  $\alpha$  to be related to the probability of connection between the right posterior thalamus and the right occipital cortex. Furthermore, we individual estimates of vSTM capacity were significantly inversely related to the probability of connection between the left posterior thalamus and the left occipital cortex. These associations were structurally specific to the occipital cortex, as the probabilities of connections between the thalamus and motor cortex did not show the respective associations. Furthermore, they were also cognitively specific, as control analyses for other visual attention functions (visual processing speed  $C$  and spatial bias  $w_{\text{lat}}$ ) failed to show the respective correlations.

Thus, our results imply that these fiber tracts do indeed serve specific roles in task-related attentional weighting and short-term maintenance, as assumed in the NTVA model, rather playing a more general, broad role in diverse attention functions.

### 2.5.1 TOP DOWN CONTROL IS ASSOCIATED WITH POSTERIOR THALAMUS – OCCIPITAL CORTEX STRUCTURAL CONNECTIVITY

Our finding of a trend-wise relation of the individual level of top-down control  $\alpha$  was to connectivity between posterior thalamus and occipital cortex can be taken as empirical support for the NTVA assumption that the pulvinar nucleus plays an important role in task-related attentional weighting (Bundesen et al., 2005). Specifically, NTVA assumes that, following the computation of attentional weights of the objects in the visual display, the pulvinar transmits weighted information to higher-order visual areas. From this, it follows that the connection between posterior thalamic areas and the occipital cortex would be relevant for the efficiency of task-related weighting. Moreover, our finding is in line with electrophysiological studies which have suggested that the pulvinar nucleus plays an important role in selective attention (Desimone et al., 1990; Robinson and Petersen 1992; Olshausen et

al., 1993; Shipp 2004; Saalman and Kastner, 2011; Saalman et al., 2012). For example, combining electrical recordings in the pulvinar nuclei and visual areas with tractography in monkeys, Saalman and colleagues (Saalman et al., 2012) found that the maintenance of attention in expectation of visual stimuli was heavily reliant on pulvino-cortical interactions. Our finding is also in line with those of Snow and colleagues (2009). Investigating task-related selection of visual targets in three patients with ventral pulvinar lesions, they found deficits in discriminating target features when in the presence of salient distractors –suggesting a role of the pulvinar in saliency-based competition of objects for selection, as assumed by NTVA.

### 2.5.2 VSTM CAPACITY IS ASSOCIATED WITH POSTERIOR THALAMUS – OCCIPITAL CORTEX STRUCTURAL CONNECTIVITY

Our finding of a significant association between vSTM capacity and posterior thalamus-occipital cortex connection probability is in line with the NTVA assumption of recurrent loops between posterior thalamus, and more specifically: the reticular nucleus, and visual cortices subserving reactivation and maintenance of selected visual object information (Bundesen 2005). In TVA, visual processing is conceived as a race between objects for representation in capacity-limited vSTM (Bundesen 1990). The objects that win the race are thought to be categorized in a vSTM map of locations situated in the posterior thalamus, more precisely: the TRN (Bundesen 2005). In consonance with Hebb (1949), for example, the NTVA suggests that in visual cortices, the activity of the neurons representing the winning objects is sustained and reactivated by a feedback loop gated by the TRN. Our findings go beyond previous TVA-based studies that revealed an association between microstructure in posterior white matter and vSTM capacity (Habekost and Rostrup 2007, Espeseth et al., 2014), in that they provide structurally more precise evidence for the importance of especially the connection between posterior thalamus and occipital cortex. In this regard, our findings further confirm the role of the tracts connecting the posterior thalamus to visual cortices for vSTM capacity, which was suggested in a previous study by Menegaux et al. (2017). Our findings are complementary to those of Golestani and colleagues, who found the microstructure of the posterior thalamic radiations as well as other posterior thalamic tracts, the optic radiations, to be relevant for individual vSTM capacity (Golestani et al., 2014).

The finding of a negative association between vSTM capacity and left PT-OC structural connectivity shows that vSTM capacity is associated with a characteristic of this pathway. Due to the largely unknown basis of the probability of connection value, it is not possible to identify the precise characteristic that renders the relation between the connectivity value and VSTM capacity. Indeed, the probability of connection between the occipital cortex and the posterior thalamus reflects the number of streamlines connecting those two ROIs. As the number of streamlines is not a direct measure of anatomical connectivity and as their relationship to the underlying anatomy is unclear (Jones et al.,

2013; Jbabdi & Johansen-Berg, 2011), lower connectivity values do not necessarily indicate lower strength of connection or fewer axons between PT and OC. Furthermore, it is important to note that here we use the term ‘probability of connection’ to refer to the probabilistic tractography score obtained by probtrackx. As explained by Jones and colleagues who prefer the term ‘stochastic tractography score’, the tractography score indicates how frequently a streamline between two points can be reconstructed, and there are many reasons why a streamline might not be successfully reconstructed (Jones et al., 2013). Differences in ‘true’ connection strength is one of them (Jones et al., 2010). Indeed, several factors can influence the number of streamlines such as the organization of myelin in regions bordering cortical grey matter (Reveley et al., 2015) as well as fanning fibers or crossing fibers. For example, fewer crossing fibers would yield increased connectivity values (Jbabdi & Johansen-Berg 2011; Thomas et al 2014; Reveley et al., 2015; Donahue et al., 2016). Dense white-matter fiber bundles at the grey matter/white matter boundary would impede tractography detection of weaker crossing fibers entering or exiting grey matter in sulcal fundi and thus influence the number of streamlines. This also applies to inter-individual differences in axon diameter distribution as well as the distance between the two regions of interest (Donahue 2016; probably Thomas, 2014; Behrens 2007). Considering the complex meaning of the probability of connection value obtained from probtrackx, our results can be taken to suggest that both vSTM capacity and, to a lesser extent, top-down control depend on the path between posterior thalamus and occipital cortex. However, the nature of the association, i.e., the precise underlying characteristics of the tracts that are related to the attention functions can only be revealed in further investigation. These could use, for example, diffusion MRI methods that can resolve intravoxel structure such as high angular resolution diffusion imaging (Tuch et al., 2002; Tuch et al., 2003)

### 2.5.3 LIMITATIONS

The present study has several limitations. As the sample consisted of relatively highly educated participants, the results might be impacted by a selection bias. This might have led to reduced variance in cognitive and structural measures and thus an underestimation of correlations that would be found in a less selective sample. Another limitation lies in the relatively small number of participants involved. Additional limitations include inherent tractography difficulties, such as the unknown directionality of connections (as pointed out above), the influence of distance on tractography, and false positive results of anatomical connections owing to various physical and biological factors (Thomas et al., 2014). Moreover, it has been shown that partial volume effect can affect tractography (Vos et al., 2011). Thus, the present results should be considered with care. Finally, we used a large ROI for the occipital region, which does not allow us to say which specific area of the occipital lobe is linked to the attentional measures.

---

## 2.6 CONCLUSION

We investigated whether the structural connectivity of posterior thalamus to occipital cortices is associated with vSTM capacity and top-down control of attention selection as suggested by the NTVA model. We found that vSTM capacity was significantly associated with structural connectivity of left posterior thalamus to occipital cortex, and a trend towards an association between the structural connectivity of right posterior thalamus to occipital cortex and top-down control. These findings constitute the first evidence in support of the assumption that thalamic structures and their connections to visual cortex are of relevance for both top-down control and vSTM capacity.

## ACKNOWLEDGMENTS

We thank Erika Künstler and Annette Abraham for their help with both the recruitment of participants, and the collection of TVA data. We are grateful to the staff of the Department of Neuroradiology in Munich particularly Dr. Christine Preibisch and Stephan Kaczmarz for showing us how to operate the scanner. Most importantly, we thank all our participants for their efforts to take part in this study. This study was supported by EU Marie Curie Training Network INDIREA (ITN- 2013-606901 to H.J.M., and K.F.), Deutsche Forschungsgemeinschaft (FI 1424/2-1 to K.F. and SO 1336/1-1 to C.S.), German Federal Ministry of Education and Science (BMBF 01ER0803 to C.S.), the Kommission für Klinische Forschung, Technische Universität München (KKF 8765162 to C.S), and a stipend of the Graduate school of Systemic Neurosciences (GSN LMU to A.M).

---

## REFERENCES

- Arend, I., Rafal, R., Ward, R.** 2008. Spatial and temporal deficits are regionally dissociable in patients with pulvinar lesions. *Brain*, 131(Pt 8) 2140-52.
- Arnold, J. F., Zwiers, M. P., Fitzgerald, D. A., van Eijndhoven, P., Becker, E. S., Rinck, M., Fernandez, G., Speckens, A. E., & Tendolkar, I.** 2012. Fronto-limbic microstructure and structural connectivity in remission from major depression. *Psychiatry Res*, 204(1), 40-48.
- Beck, A.T., Steer, R.A., Brown, G.K.,** 1996. *Manual for the Beck Depression Inventory-II*. Second Edition ed. The Psychological Corporation, San Antonio, TX.
- Behrens, T. E., Berg, H. J., Jbabdi, S., Rushworth, M. F., & Woolrich, M. W.** 2007. Probabilistic diffusion tractography with multiple fibre orientations: What can we gain? *Neuroimage*, 34(1), 144-155.
- Behrens, T. E., Johansen-Berg, H., Woolrich, M. W., Smith, S. M., Wheeler-Kingshott, C. A., Boulby, P. A., Barker, G. J., Sillery, E. L., Sheehan, K., Ciccarelli, O., Thompson, A. J., Brady, J. M., & Matthews, P. M.** 2003. Non-invasive mapping of connections between human thalamus and cortex using diffusion imaging. *Nat Neurosci*, 6(7), 750-757.
- Bundesen, C.,** 1990. A theory of visual attention. *Psychol. Rev.* 97, 523-547.
- Bundesen, C., Habekost, T., Kyllingsbaek, S.,** 2005. A neural theory of visual attention: bridging cognition and neurophysiology. *Psychol. Rev.*, 112, 291-328.
- Chechlacz, M., Gillebert, C.R., Vangkilde, S.A., Petersen, A., Humphreys, G.W.,** 2015. Structural Variability within Frontoparietal Networks and Individual Differences in Attentional Functions: An Approach Using the Theory of Visual Attention. *J. Neurosci.*, 35 (30), 10647-58.
- Cowan, N.,** 2001. The magical number 4 in short-term memory: a reconsideration of mental storage capacity. *Behav. Brain. Sci.* 24, 87-114.
- Danziger, S., Ward, R., Owen, V., Rafal, R.,** 2001-2002. The effects of unilateral pulvinar damage in humans on reflexive orienting and filtering of irrelevant information. *Behav. Neurol.*, 13, 95-104
- Danziger, S., Ward, R., Owen, V., Rafal, R.,** 2004. Contributions of the human pulvinar to linking vision and action. *Cogn Affect Behav Neurosci.* 4(1), 89-99.
- Desimone, R., Wessinger, M., Thomas, L., Schneider, W.** 1990. Attentional control of visual perception: cortical and subcortical mechanisms. *Cold Spring Harb. Symp. Quant. Biol.*, 55, 963-971

- Desimone, R., & Duncan, C.**, 1995. Neural mechanisms of selective visual attention. *Annu. Rev. Neurosci.* 18, 193-222
- Donahue, C.J., Sotiropoulos, S.N., Jbabdi, S., Hernandez-Fernandez, M., Behrens, T.E., Dyrby, T., Coalson, T., Kennedy, H., Knoblauch, H., Van Essen, D.C., Glasser, M.F.** 2016. Using Diffusion Tractography to Predict Cortical Connection Strength and Distance: A Quantitative Comparison with Tracers in the Monkey. *J. Neurosci.*, 36 (25), 6758-6770.
- Espeseth, T., Vangkilde, S.A., Petersen, A., Dyrholm, M., Westlye, L.T.**, 2014. TVA-based assessment of attentional capacities-associations with age and indices of brain white matter microstructure. *Front. Psychol.* 5, 1177.
- Finke, K., Bublak, P., Krummenacher, J., Kyllingsbæk, S., Müller, H.J., Schneider, W.X.**, 2005. Usability of a theory of visual attention (TVA) for parameter-based measurement of attention I: evidence from normal subjects. *J. Int. Neuropsychol. Soc.* 11, 832–842.
- Golestani, A.M., Miles, L., Babb, J., Castellanos, F.X., Malaspina, D., Lazar, M.**, 2014. Constrained by Our Connections: White Matter's Key Role in Interindividual Variability in Visual Working Memory Capacity. *J. Neurosci.* 34 (45), 14913-14918.
- Habekost, T., Rostrup, E.**, 2007. Visual attention capacity after right hemisphere lesions. *Neuropsychologia* 45, 1474-1488.
- Hebb, D. O.**, 1949. *Organization of behavior*. New York: Wiley
- Jbabdi, S., & Johansen-Berg, H.** (2011). Tractography: where do we go from here? *Brain Connect*, 1(3), 169-183
- Jbabdi, S., Sotiropoulos, S.N., Haber, S.N., Van Essen, D.C., Behrens, T.E.** 2015. Measuring macroscopic brain connections in vivo. *Nat Neurosci.* 18(11), 1546-55.
- Jenkinson, M., Beckmann, C. F., Behrens, T. E., Woolrich, M. W., & Smith, S. M.** (2012). FSL. *Neuroimage*, 62(2), 782-790.
- Jones, D.K.**, 2010. Challenges and limitations of quantifying connectivity in the human brain in vivo with diffusion MRI. *Imaging Med.*, 2, 341-355
- Jones, D.K., Knosche, T.R., Turner, R.**, 2013. White matter integrity, fiber count, and other fallacies: the do's and don'ts of diffusion MRI. *Neuroimage*, 73, 239-54.
- Karnath, H.O., Himmelbach, M., Rorden, C.**, 2002. The subcortical anatomy of human spatial neglect: putamen, caudate nucleus and pulvinar. *Brain*, 125(Pt 2), 350-360.

- Kraft, A., Irlbacher, K., Finke, K., Kaufmann, C., Kehler, S., Liebermann, D., Bundesen, C., Brandt, S.A., 2015.** Dissociable spatial and non-spatial attentional deficits after circumscribed thalamic stroke. *Cortex*, 64, 327–342.
- Kyllingsbæk, S., 2006.** Modeling visual attention. *Behavior. Research. Methods*, 38, 123–133.
- Lehr, S., 1977.** Mehrfachwahl-Wortschatz-Intelligenztest MWT-B. Manual. Straube-Verlag, Erlangen.
- Luck, S.J., Vogel, E.K., 1997.** The capacity of visual working memory for features and conjunctions. *Nature*, 390, 279–281.
- Malone, I.B., Leung, K.K., Clegg, S., Barnes, J., Whitwell, J.L., Ashburner, J., Fox, N.C., Ridgway, G.R., 2015.** Accurate automatic estimation of total intracranial volume: a nuisance variable with less nuisance. *Neuroimage*, 104, 366–72.
- Menegaux, A., Meng, C., Neitzel, J., Bauml, J. G., Muller, H. J., Bartmann, P., Wolke, D., Wohlschläger, A.M., 2017.** Impaired visual short-term memory capacity is distinctively associated with structural connectivity of the posterior thalamic radiation and the splenium of the corpus callosum in preterm-born adults. *Neuroimage*, 150, 68–76.
- Meng, C., Bäuml, J.G., Daamen, M., Jaekel, J., Neitzel, J., Scheef, L., Busch, B., Baumann, N., Boecker, H., Zimmer, C., Bartmann, P., Wolke, D., Wohlschläger, A.M., Sorg, C., 2015.** Extensive and interrelated subcortical white and gray matter alterations in preterm-born adults. *Brain Struct Funct* 221 (4), 2109–21.
- Oldfield, R.C., 1971.** The assessment and analysis of handedness: the Edinburgh inventory. *Neuropsychologia*. 9(1), 97–113.
- Olshausen, B.A., Anderson, C.H., Van Essen, D.C., 1993.** A neurobiological model of visual attention and invariant pattern recognition based on dynamic routing of information. *J. Neurosci.*, 13, 4700–4719
- Petersen, S.E., Robinson, D.L., Morris, J.D., 1987.** Contributions of the pulvinar to visual spatial attention. *Neuropsychologia*, 25 (1A), 97–105.
- Rafal, R.D., Posner, M.I., 1987.** Deficits in human visual spatial attention following thalamic lesions. *Proc. Natl. Acad. Sci. USA*, 84, 7349–7353
- Reveley, C., Seth, A.K., Pierpaoli, C., Silva, A.C., Yu, D., Saunders, R.C., Leopold, D.A., Ye, F.Q., 2015.** Superficial white matter fiber systems impede detection of long-range cortical connections in diffusion MR tractography. *Proc Natl Acad Sci U S A*, 112, 2820–2828.

- Rilling**, J.K., Glasser, M.F., Preuss, T.M., 2008. The evolution of the arcuate fasciculus revealed with comparative DTI. *Nat. Neurosci.*, 11(4), 426–428.
- Robinson**, D.L., Petersen, S.E., 1992. The pulvinar and visual salience. *Trends Neurosci.*, 15, 127-132
- Rorden**, C., Karnath, H.O., Bonilha, L., 2007. Improving lesion-symptom mapping. *J. Cog. Neurosci.*, 19(7), 1081-8.
- Saalmann**, Y.B., Kastner, S., 2011. Cognitive and perceptual functions of the visual thalamus. *Neuron*, 71 , 209-223
- Saalman**, Y.B., Pinsk, M.A., Wang, L., Li X., Kastner S., 2012. The pulvinar regulates information transmission between cortical areas based on attention demands. *Science*, 337, 753-756.
- Shipp**, S., 2003. The functional logic of cortico-pulvinar connections. *Philos. Trans. R. Soc. Lond. B Biol. Sci.*, 358,1605-1624.
- Shipp**, S., 2004. The brain circuitry of attention. *Trends Cogn. Sci.*, 8, 223-23
- Snow**, J.C., Allen, H.A., Rafal, R.D., Humphreys, G.D., 2009. Impaired attentional selection following lesions to human pulvinar: evidence for homology between human and monkey. *Proc. Natl. Acad. Sci. USA*, 106, 4054-4059.
- Strumpf**, H., Mangun, G.R., Boehler, C.N., Stoppel, C., Schoenfeld, M.A., Heinze, H.J., Hopf, J.M., 2013 *Hum Brain Mapp.*, 34(5), 1115-32.
- Thomas**, C., Ye, F.Q., Irfanoglu, M.O., Modi, P., Saleem, K.S., Leopold, D.A., Pierpaoli, C., 2014. Anatomical accuracy of brain connections derived from diffusion MRI tractography is inherently limited. *Proc Natl Acad Sci U S A*, 111,16574–16579.
- Tuch**, D.S., Reese, T.G., Wiegell, M.R., Makris, N., Belliveau, J.W., Wedeen, V.J., 2002. High angular resolution diffusion imaging reveals intravoxel white matter fibre heterogeneity. *Magn. Reson. Med.* 48, 577–582.
- Tuch**, D.S., Reese, T.G., Wiegell, M.R., Wedeen, V..J., 2003. Diffusion MRI of complex neural architecture. *Neuron*. 40, 885–895.
- Vogel**, E.K., Machizawa, M.G., 2004. Neural activity predicts individual differences in visual working memory capacity. *Nature*, 428,748–751
- Vos** S.B., Jones, D.K., Viergever, M.A., Leemans, A., 2011. Partial volume effect as a hidden covariate in DTI analyses. *Neuroimage*. 55(4), 1566-76.

- 
- Wiegand, I., Töllner, T., Dyrholm, M., Müller, H. J., Bundesen, C., & Finke, K. (2014b).** Neural correlates of age-related decline and compensation in visual attention capacity. *Neurobiol. Aging*, 35, 2161–2173.
- Wiegand, I., Töllner, T., Habekost, T., Dyrholm, M., Müller, H. J., & Finke, K. (2014a).** Distinct neural markers of TVA-based visual processing speed and short-term storage capacity parameters. *Cereb. Cortex*, 24, 1967-1978.
- Wilke, M., Turchi, J., Smith, K., Mishkin, M., Leopold, D.A., 2010.** Pulvinar inactivation disrupts selection of movement plans. *J. Neurosci.*, 30, 8650-8659.
- Wilke, M., Kagan, I., Andersen, R.A., 2013.** Effects of pulvinar inactivation on spatial decision-making between equal and asymmetric reward options. *J. Cogn. Neurosci.*, 25, 1270-1283
- Wurtz, R.H., Joiner, W.M., Berman, R.A., 2011.** Neuronal mechanisms for visual stability: progress and problems. *Philos Trans R Soc Lond B Biol Sci.*,366(1564),492-503.
- Zhang, D., Snyder, A. Z., Shimony, J. S., Fox, M. D., & Raichle, M. E. 2010.** Noninvasive functional and structural connectivity mapping of the human thalamocortical system. *Cereb Cortex*, 20(5), 1187-1194.
- Zhou, H., Schafer, R.J., Desimone R.,2016.** Pulvinar-Cortex Interactions in Vision and Attention. *Neuron*, 89(5), 209-220.
- Zihl, J., Von Cramon, D., 1979.** The contribution of the ‘second’ visual system to directed visual attention in man. *Brain*, 102,835-856

## 2.8 SUPPLEMENTARY MATERIAL

**Figure S1: Inter-individual variability of thalamic probability maps.**

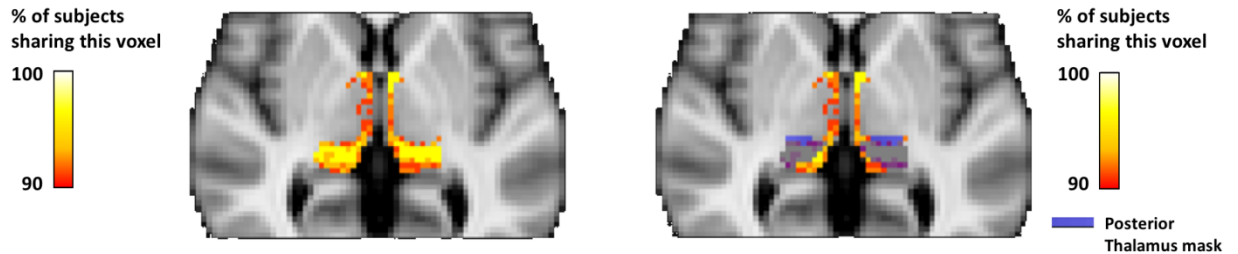


**Figure S1:** Yellow and orange colors represent voxels that are present in at least 90% of the participants; blue illustrates bilateral posterior thalamus mask.

**Table S1: Comparison of K and C parameters for  $t_0 < 0$  correction vs original value**

|          | $t_0 < 0$<br>set to 0 |           | $t_0 < 0$<br>unchanged |           |
|----------|-----------------------|-----------|------------------------|-----------|
|          | <i>M</i>              | <i>SD</i> | <i>M</i>               | <i>SD</i> |
| <b>K</b> | 3.306                 | 0.392     | 3.310                  | 0.397     |
| <b>C</b> | 24.733                | 8.661     | 24.361                 | 8.436     |

**Table S2: Correlation between K and C parameters and posterior thalamus structural connectivity for original  $t_0 < 0$  values**

|          |                        | Left PT-OC SC             | Right PT-OC SC   | Left PT-MC SC    | Right PT-MC SC    |
|----------|------------------------|---------------------------|------------------|------------------|-------------------|
| <b>K</b> | $t_0 < 0$<br>unchanged | <b>r = -0.38</b> p = .03* | r = 0.02 p = .91 | r = 0.02 p = .90 | r = -0.10 p = .60 |
| <b>C</b> | $t_0 < 0$<br>unchanged | r = -0.19 p = .29         | r = 0.08 p = .67 | r = 0.12 p = .51 | r = -0.01 p = .95 |

**Abbreviations:** PT-OC: Posterior thalamus to occipital cortex; PT-MC: Posterior thalamus to motor cortex; SC structural connectivity. Correlations below  $p = .10$  are shown in bold, \* indicates a  $p < .05$ .



## 3 STUDY II:

### AGING MODULATES THE ASSOCIATION BETWEEN VSTM CAPACITY AND THE STRUCTURAL CONNECTIVITY OF POSTERIOR THALAMUS TO OCCIPITAL CORTICES

This chapter contains a manuscript entitled “Aging modulates the association between vSTM capacity and the structural connectivity of posterior thalamus to occipital cortices” currently in preparation.

Authors: Aurore Menegaux, Felix J.B. Bäuerlein, Aliko Vania, Natan Napiorkowski , Julia Neitzel , Adriana L. Ruiz-Rizzo , Hermann J.,Müller , Christian Sorg , Kathrin Finke

#### **Contributions:**

The author of this thesis is the first author of this manuscript. **A.M.**, K.F. and C.S. designed this study, **A.M.**, J.N and A.R.R. acquired imaging data and N.N behavioral data, **A.M.** analyzed data with some help from A.V. supervised by **A.M.** as part of her bachelor thesis and with some tool provided by F.J.B.B., **A.M.** drafted the manuscript, **A.M.**, H.J.M., K.F. and C.S. wrote and revised the manuscript before submission.

## TITLE PAGE

### Title

Aging modifies the association between visual short-term memory capacity and the structural connectivity between posterior thalamus and occipital cortices

### Authors and Affiliations

Aurore Menegaux<sup>1,2,3</sup>, Felix J. B. Bäuerlein<sup>5</sup>, Aliko Vania<sup>1</sup>, Natan Napiorkowski<sup>1,2</sup>, Julia Neitzel<sup>1</sup>, Adriana L. Ruiz-Rizzo<sup>1</sup>, Hermann J Müller<sup>1,2</sup>, Christian Sorg<sup>3,4</sup> Kathrin Finke<sup>1,2,6</sup>

<sup>1</sup>Department of Psychology, General and Experimental Psychology, Ludwig-Maximilians-Universität München, Leopoldstrasse 13, 80802 Munich, Germany; <sup>2</sup>Graduate School of Systemic Neurosciences GSN, Ludwig-Maximilians-Universität, Großhaderner Strasse 2, 82152 Planegg, Germany; Departments of <sup>3</sup>Neuroradiology, <sup>4</sup>Psychiatry of the Klinikum rechts der Isar, Technische Universität München TUM, Ismaninger Strasse 22, 81675 Munich, Germany; <sup>5</sup>Department of Molecular Structural Biology, Max Planck Institute of Biochemistry, 82152 Martinsried, Germany <sup>6</sup>Hans Berger Department of Neurology, Friedrich-Schiller-University Jena, Germany.

### Corresponding author

Aurore Menegaux, Department of Psychology, General and Experimental Psychology, Ludwig-Maximilians-Universität München, Leopoldstrasse 13, 80802 Munich, Germany.

E-mail: aurore.menegaux@psy.lmu.de , phone: +49 89 2180 72567

### Counts

Number of words in abstract: 266

Number of figures: 2

Number of tables: 2

Number of Supplementary material: 2

## 3.1 ABSTRACT

Visual short-term memory (vSTM) capacity is the number of items that can be consciously perceived and stored into vSTM. vSTM capacity decreases with age; however, the neural underpinnings of such decrease are incompletely understood. According to the Neural Theory of Visual Attention, vSTM depends on the structural connectivity between posterior thalamus and visual occipital cortices. It has been shown that aging modifies the thalamo-cortical system. Thus, we aimed at investigating whether aging affects the association between vSTM capacity and the structural connectivity between the posterior thalamus and occipital cortices (PT-OC). In order to analyze this, 66 individuals aged 20 to 77 years underwent diffusion weighted imaging and a whole report task of briefly presented letter arrays, from which vSTM capacity estimates were derived by parametric modelling based on the Theory of Visual Attention (TVA). Probabilistic tractography was performed between occipital cortices and thalamus. We analyzed the relation of the resulting connection probability values with vSTM capacity, age, and their interaction via multiple regression analysis. We found both reduced vSTM capacity and aberrant PT-OC connection probability in aging. Critically, the relationship between vSTM capacity and PT-OC connection probability was significantly modified by age. In younger adults, vSTM capacity was negatively correlated with PT-OC connection probability while in older adults, this association was positive. Furthermore, we found reduced fractional anisotropy and increased mean diffusivity in PT-OC tracts with aging. This suggests that the inversion of the association between PT-OC connection probability and vSTM capacity with aging might reflect age-related changes in white matter properties. Thus, the effect of aging on vSTM capacity might be modulated by the microstructure and connectivity of white matter between posterior thalamus and occipital cortices.

**Keywords:** Diffusion tensor imaging, Probabilistic tractography, Neural theory of visual attention, Visual short-term memory capacity, Posterior thalamus, Aging

**Abbreviations:** vSTM, visual short-term memory; TVA, theory of visual attention; NTVA, neural theory of visual attention; DTI, diffusion tensor imaging; ROI, region of interest PT-OC, Posterior thalamus – occipital cortex ; SC, Structural connectivity; IQ, intelligence quotient

## 3.2 INTRODUCTION

Aging is associated with impairments in visual short term memory (vSTM) capacity (Jost et al., 2011; Verhaegen et al., 1993; Sander et al., 2011; McAvinue et al., 2012). vSTM capacity is the maximum number of objects that can be perceived simultaneously and stored into vSTM (Sperling 1960, Cowan 2001). Modelling performance in a psychophysical whole report task based on the computational Theory of Visual Attention (TVA) framework in which visual processing is described as a race between objects of the visual field to be represented into the vSTM store (Bundesen 1990), allows for parametric estimates of vSTM capacity, i.e. parameter  $K$ . Estimates of TVA parameter  $K$  using this methodology and framework are about 3 to 4 items in healthy young adults (e.g. Finke et al., 2005) and fit well to typical estimates of vSTM capacity delivered by alternative paradigms (Luke and Vogel 1997, Cowan et al. 2001, Vogel and Mechizawa 2004). McAvinue and colleagues (2012) have shown that vSTM capacity  $K$  linearly declined with increasing age. A significant reduction of this parameter has since been reproduced by various studies (Wiegand et al., 2014a; Wiegand et al., 2014b; 2018; Espeseth et al., 2014). It is incompletely understood, however, which brain mechanism alterations might lead to this decline. The current study addresses this question by focusing on posterior thalamo-cortical structural connectivity.

The neural theory of visual attention (NTVA) gives an interpretation of TVA at both the brain's cellular and systems level. NTVA proposes that 'visual' brain regions such as occipital cortices, thalami as well as white matter tracts connecting those regions are of particular relevance for vSTM capacity in healthy individuals (Bundesen et al., 2005). According to TVA, visual processing is conceived as a race between objects to be consciously perceived and stored into vSTM. The winner objects of the race are assumed to be categorized in a vSTM map of location positioned in the posterior thalamus and particularly in the TRN. In line with for example Hebb (1949), the NTVA assumes that the activity of the neurons representing the winner objects in visual cortices is sustained and reactivated by a feedback loop gated by the TRN (Bundesen et al., 2005). Given the critical role of posterior thalamus and visual cortices, it can be inferred from NTVA that the structural connectivity between those two regions is decisive for vSTM capacity (Bundesen et al., 2005). Evidence for a critical role of white matter connections in vSTM storage using the TVA framework comes from a study by Habekost and colleagues (2007) who found deficits in vSTM capacity in patients with lesions to posterior tracts. First empirical support for the suggested relevance of particularly the thalamus and posterior thalamic tracts comes from studies of Kraft and colleagues (Kraft et al., 2015), who found reduced vSTM capacity in patients with thalamic lesions, and Menegaux and colleagues (Menegaux et al., 2017) who found that the microstructure of posterior thalamic radiations was associated with vSTM capacity  $K$  in healthy young individuals. Nevertheless, the association between vSTM capacity and posterior thalamo-cortical connectivity in aging has not yet been studied.

Aging-related volumetric changes have been well documented (Courchesnes et al., 2000; Ge et al., 2002; Raz and Rodrigue, 2006). It has been shown that aging is accompanied by widespread reductions of grey matter volume and increases in Cerebrospinal fluid (CSFV) starting in early adulthood (Salat et al., 2011; Walhovd et al., 2011). However, the age-related changes in white matter volume follow a complex trajectory. Several studies have found an increase in white matter volume until the fourth or fifth decade of life, interpreted as ongoing myelination (Courchesnes et al., 2000; Ge et al., 2002; Bartzokis et al., 2004), followed by a decrease with an acceleration in late adulthood (Courchesnes et al., 2000; Raz et al., 2005). However, volumetric studies do not provide information regarding the mechanisms responsible for those age-related white matter changes. In contrast, Diffusion tensor imaging (DTI) allows inferences about white matter microstructure by quantifying the magnitude and directionality of water diffusion in tissues (Pierpaoli & Basser 1996; Pierpaoli 1996). By the use of a tensor, a 3x3 matrix, diffusion in all 3 dimensions can be quantified and several measures derived. These include fractional anisotropy (FA), which describes how directional diffusion is (Basser 1995), mean diffusivity (MD), radial diffusivity (RD), which represents the diffusivity perpendicular to axonal fibers and axial diffusivity (AD), which represents the diffusion parallel to the axon fibers. Predominant findings on age-related white matter diffusivity changes have been decreased FA and increased MD in widespread tracts including the inferior fronto-occipital fasciculus, sagittal stratum and posterior thalamic radiations in cross-sectional (Pfefferbaum 2000; O'Sullivan et al., 2001; Malloy et al., 2007; Hugenschmidt et al., 2008; Vernooij et al., 2008; Westlye et al., 2010; Bennett, I.J., et al., 2010; for review see Wozniak & Lim 2006; Fama et al., 2015) and longitudinal studies (Barrick et al., 2010; Teipel et al., 2010). Furthermore, while it has been repeatedly reported that RD increases with aging (Baghat and Beaulieu, 2004; Zhang et al., 2010; Bennett, I.J., et al., 2010), findings on AD where more mixed and both increases and decreases have been reported (Zahr et al., 2009; Bennett et al., 2010; Sullivan et al., 2010a; Sullivan et al., 2010b; Burzynska et al., 2010). Interestingly, particularly in posterior thalamic areas, changes in RD and AD have been reported with aging (Kumar et al., 2013) and alterations in thalamo-cortical projections' volume have been found (Hughes et al., 2012).

Those changes in white matter diffusivity with aging likely reflect microstructural alterations such as increase of brain water content, disruption of axon structure, demyelination, or rarefaction of fibers (Minati et al. 2007). Post-mortem histological studies have shown that axonal and myelin degeneration take place in aging brains along with other changes in the cellular environment, such as accumulation of cellular debris and formation of glial scars (Meier-Ruge et al., 1992; Aboitiz et al., 1996; Peters et al., 2002). Given the pronounced white matter diffusivity changes, particularly in posterior thalamic areas, investigating their role in age-related vSTM capacity seems highly relevant. It is known e.g. from the previously mentioned study by Menegaux and colleagues (Menegaux et al., 2017) that when changes in white matter occur, the relationship between white matter connectivity and VSTM capacity can change. Indeed, in preterm born adults where thalamo-cortical microstructure and connectivity has been shown to be impaired compared to term-born ones, the association between posterior thalamic

---

radiations microstructure and vSTM capacity was changed compared to term born ones. Similar white matter-cognition relationship changes might also be found in other conditions affecting WM diffusivity, such as normal aging. Thus, we investigated whether the association between the structural connectivity of posterior thalamus to occipital cortices and vSTM capacity was similar throughout the lifespan or whether it changes with aging.

In order to examine this question, healthy individuals, aged 18 to-77 years, underwent both diffusion weighted imaging and a TVA-based whole report task of briefly presented letter arrays. Structural connectivity values were obtained by performing probabilistic tractography on DWI scans from occipital cortices to posterior thalamus, separately for each hemisphere. Estimates of vSTM capacity parameter  $K$  were derived from verbal letter report of the whole report task. The relationship between the structural connectivity of posterior thalamus to occipital cortices and vSTM capacity was analyzed by means of regression and partial correlation analyses.

---

## 3.3 MATERIAL AND METHODS

### 3.3.1 PARTICIPANTS

The present study included 66 healthy adults aged 20 to 77 years, 32 of whom were females (mean age:  $48.8 \pm 19.6$  years; mean education  $12.1 \pm 1.6$  years; Table 1). 60 participants were right-handed, 4 were left-handed and 2 were ambidextrous according to the Edinburgh Handedness Inventory (Oldfield 1971). Written informed consent was obtained from all participants and the study was approved by the ethics committees of the psychology department of the Ludwig Maximilians Universität München (LMU Munich) and the Medical Department of the Technische Universität München (TUM). Initially, 108 adults (aged 19 to 78 years) of the Munich INDIREA aging cohort<sup>4</sup> were recruited for the study. The Mini Mental State Examination (MMSE; Folstein et al., 1975) was used as screening for cognitive impairments in participants aged 60 years and above (i.e., a MMSE score below 27), and the Beck Depression Inventory (BDI; Beck et al., 1996) for screening for symptoms of depression in all participants (i.e., a BDI score above 19). From the original cohort, eleven participants dropped out before participating in all sessions, three participants were excluded because of high BDI test scores, one because of a low MMSE score, two because of uncorrected visual acuity deficits, five because of too low accuracy in the whole report task, ten due to artefacts in their diffusion weighted imaging data, two because of incomplete diffusion-weighted imaging datasets and eight participants for lacking to undergo diffusion weighted imaging assessment. All of the 66 remaining participants had no previous or current psychiatric (e.g. anxiety disorder, schizophrenia) or neurological conditions (e.g. brain injury, stroke), diabetes, or depression. Diffusion weighted imaging was performed during one session at the Department of Neuroradiology of the TUM Klinikum rechts der Isar. In a separate, psychophysical-testing session at the Department of Psychology of the LMU Munich, visual attention functioning was assessed using the whole-report task. Event-related EEG potentials were also assessed during the task, but not analyzed for the current study. Additionally participants completed the MMSE, and filled out demographic, and BDI questionnaires. The average time between sessions was 2.6 months.

---

<sup>4</sup> INDIREA: ‘Individualised Diagnostics and Rehabilitation of Attentional Disorders’ European Marie Curie funded Initial Training Network. All participants underwent extensive behavioral (i.e., attention, memory and intelligence functions), neuroimaging (i.e., structural, functional and diffusion MRI), and electroencephalography assessment.

| Variable           | N = 66 |       |              |
|--------------------|--------|-------|--------------|
|                    | M      | SD    | Range        |
| Gender (F/M)       | 32/34  |       |              |
| Handedness (R/L/B) | 60/4/2 |       |              |
| Education (years)  | 12.1   | 1.65  | 8.50-14      |
| Age (years)        | 48.8   | 19.56 | 20 -77       |
| K                  | 3.22   | 0.39  | 2.29 – 3.83  |
| C                  | 23.26  | 8.41  | 9.71 – 47.01 |
| t0                 | 12.82  | 13.93 | 0.00 – 67.13 |
| Crystallized IQ    | 102.07 | 16.58 | 72.5 – 140.0 |

**Table 1: Sample characteristics**

### 3.3.2 TVA-BASED BEHAVIOURAL ASSESSMENT OF VSTM CAPACITY

#### GENERAL ASSESSMENT PROCEDURE

The whole report task was conducted in a dimly-lit sound-attenuated chamber (Industrial Acoustics Company) with simultaneous EEG recordings<sup>1</sup>. Stimuli were presented to participants on a 24'' LED screen (800 x 600 pixel resolution, 100-Hz refresh rate) at a distance of 65 cm.

Due to the special requirements of event-related components assessment, some of the experimental trials in whole and partial report were repeated more often than others. Furthermore, for the event-related EEG assessment it was also necessary to ensure balanced visual stimulation in both hemifields in the whole report task. Thus, symbols were presented in the visual hemifield opposite to the target stimuli. These specific manipulations, however, should not affect the TVA parameters derived from fitting report accuracy in the different conditions.

Each subject completed a session of 1.5 to 2 hours which included EEG preparation, presentation of written instructions and stimuli used in the experiment, a procedure for adjustment of the individual exposure durations and approximately 45 minutes of testing procedure.

At the beginning of each trial, a fixation point (a white circle, size of 0.9° of the visual angle in diameter with a white dot in the centre) was presented in the centre of the display for a duration randomly drawn from 10 to 240 ms. Participants were instructed to fixate this point throughout the whole trial blocks. Subsequently, red and/or blue letters were briefly presented on a black background.

Letters' exposure durations were determined individually for each participant in a preceding short practice session in order to ensure a comparable level of task difficulty across participants. The letters were randomly chosen from the following set of letters {A, B, D, E, F, G, H, J, K, L, M, N, O, P, R, S, T, V, X, Z} and appeared only once in a given trial. After stimulus presentation, a white question mark appeared in the centre of the screen, indicating the start of a verbal letter report. The verbal report of individual letters was performed in arbitrary order and without speed constraint. In order to avoid too much guessing participants were instructed to report only letters they were fairly certain they had seen. Following each block, participants received feedback related to the accuracy of the letters they reported and not related to the overall performance level reached in the task. The desired range of 70-90% was indicated by green colour coding on a report accuracy chart. In order to avoid too liberal or too conservative responding, participants were instructed by the experimenter to try to refrain from guessing and report only the letters he/she was relatively sure to have seen when accuracy dropped below 70%, and to try to name more letters (i.e. to be less anxious to report wrong letters) when it reached 90%. During both whole and partial report tasks, the experimenter was sitting behind the participant, entered the letters reported by the participant on a keyboard and manually started a new trial by a key press.

### WHOLE REPORT TASK

On each trial, four letters were briefly presented on an imaginary semi-circle with a radius of  $5.27^\circ$  of the visual angle either on the left or on the right of a fixation point and participants were instructed to report orally as many of them as possible. Four blue symbols (composed of random letter parts; see Figure 1) of the same luminance were displayed on the symmetrical semicircle on the other side of fixation. Diameters of letters and symbols were  $1.3^\circ$  of visual angle. At the beginning of each block of trials, a white arrow pointed towards the side on which the stimuli would appear in this block. The target side in the first block was counterbalanced across participants and then alternated throughout the experiment. Seven conditions were used. In five conditions, the stimulus array was followed by masks (see figure 1) that consisted of eight red-blue scattered squares of  $1.3^\circ$  of visual angle appearing at each stimulus location with a duration of 900 ms. In two unmasked conditions, stimuli were followed by a blank screen with a fixation point shown for 900 ms. The masked letter arrays were presented for five different, individually adjusted exposure durations. In addition, as mentioned above, two unmasked conditions were used, one with the second shortest exposure duration and one with an exposure duration of 200 ms. In the unmasked conditions the exposure durations are effectively prolonged compared to masked conditions due to visual persistence (Sperling, 1960). Thus, the five masked conditions and two unmasked conditions resulted in seven different effective exposure durations. Different experimental conditions were equally distributed across blocks of trials and were displayed in randomized order within the block (Figure 1).

The exposure adjustment phase consisted of 48 trials divided into 4 blocks of 12 twelve triples of trials. Each triple consisted of two trials that were not used for adjustment, but simply for familiarizing the participant with the task. These were either unmasked trials with exposure duration of 200 ms or masked ones with exposure duration of 250 ms. One trial in each triple was used for adjustment; this was masked and initially displayed for 80 ms.

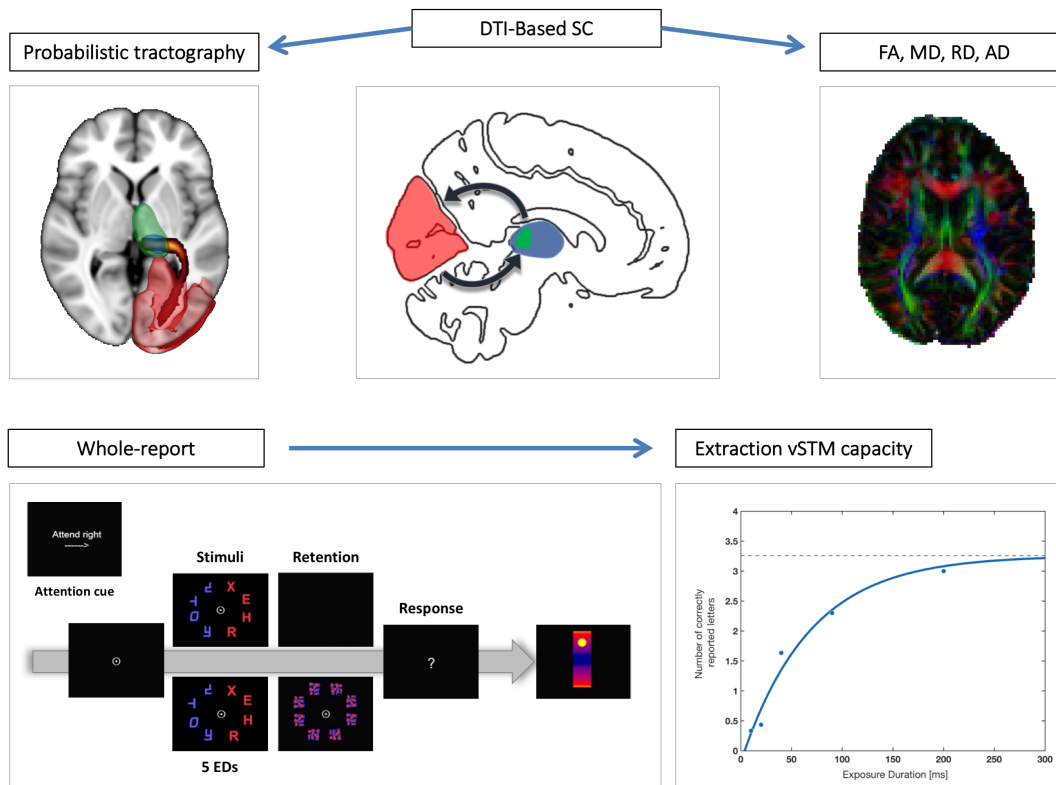


**Figure 1: Presentation of the model, task and methods used in our study.** On the top row in the middle, the regions of interest derived from the NTVA model of Bundesen are shown in red representing the occipital cortex, the whole thalamus in blue and the posterior thalamus in green. On the top left corner, a 3D representation of probabilistic tractography between the left occipital cortex and the left thalamus is shown for one individual. The top right corner shows an example of an individual's FA image modulated by his V1 map which is the principal eigenvector of the tensor. On this modulated FA image, white matter tracts with a left-right orientation are shown in red, tracts with an antero-posterior orientation in green and tracts with an up-down orientation in blue. On the bottom left corner, an example of the whole report task is shown. On the bottom right corner, a vSTM capacity K fit is represented for one subject.

Each time the participant reported at least one correct letter in this trial, exposure duration was decreased by 10 ms until the lowest exposure duration was identified. Based on this value a set of 4 additional exposure durations was chosen from the predefined sets.

The testing phase consisted of 10 experimental blocks, each including 40 trials. For each exposure duration 30 trials were used, with the exception of the condition with unmasked trials presented for 200 ms, where 220 trials were used.

### ESTIMATION OF VISUAL SHORT TERM MEMORY CAPACITY

Modeling of the participant's vSTM capacity was done using the TVA computational model, implemented in the *libTVA* toolbox for Matlab (Mads Dyrholm, [www.machlea.com/mads/libtva.html](http://www.machlea.com/mads/libtva.html)). Detailed descriptions of the fitting procedure can be found in Dyrholm et al., 2011. The TVA based whole report fitting procedure models the probability of correct letter report in terms of an exponential growth function with increasing (effective) exposure duration. The variation of exposure duration was intended to generate a broad range of performance which specified the whole probability distribution of the number of correctly reported elements as a function of the effective exposure duration. The asymptote of the function represents vSTM capacity or parameter  $K$  which indicates the maximum number of elements that can be simultaneously represented in visual short-term memory (VSTM). Three additional parameters which are of no particular interest in this study were estimated as this was necessary in order to reveal valid estimates of vSTM storage capacity based on the TVA model: Visual processing speed (parameter  $C$ ), the rate of visual information uptake (in elements per second) which is represented by the slope of the function at its origin; perceptual threshold (parameter  $t_0$ ) which indicates the visual perceptual threshold, i.e the longest ineffective exposure duration (in ms) below which information uptake is effectively zero and parameter  $\mu$ , representing the prolongation of the effective exposure duration (in ms) on unmasked trials.

### 3.3.3 IMAGING DATA ACQUISITION AND PREPROCESSING

#### IMAGING DATA ACQUISITION

Whole brain T1- and diffusion-weighted imaging data were acquired on a 3T Philips Ingenia scanner with a 32 channel head coil and a SENSE factor of 2. Diffusion images were acquired using a single-shot spin-echo echo-planar imaging sequence, resulting in one non-diffusion weighted image ( $b = 0$  s/mm<sup>2</sup>) and 32 diffusion weighted images ( $b = 800$  s/mm<sup>2</sup>, 32 non-collinear gradient directions) covering whole brain with: echo time (TE) = 61 ms, repetition time (TR) = 14206,980 ms, flip angle = 90°, field of view = 224 x 224 mm<sup>2</sup>, matrix = 112 x 112, 60 transverse slices, voxel size = 2 x 2 x 2 mm<sup>3</sup>. A whole head high-resolution T1-weighted anatomical volume was acquired using a 3D magnetization prepared rapid acquisition gradient echo sequence with the following parameters: repetition time = 9 ms; time to echo = 4 ms; inversion time, TI = 0 ms; flip angle = 8°; 170 sagittal slices; field of view = 240 mm<sup>2</sup>; matrix size = 240 × 240; reconstructed voxel size = 1 x 1 x 1 mm<sup>3</sup>.

## QUALITY CHECK

All acquired MRI images were visually inspected by two independent raters (A.M., A.V.) for excessive head motion, and apparent or aberrant artifacts. In addition to visual inspection of raw data, we also used the fitting residuals (the sum-of-squared-error maps generated by DTIFIT) to identify data corrupted by artifacts. Artifacts include motion-induced artifacts, insufficient fat suppression (ghosting) artifacts, and extreme distortion artifacts thus leading to the exclusion of five participants. Furthermore, T2 images were examined to exclude potential lesions and white matter abnormalities by experienced radiologists.

## PREPROCESSING

Diffusion data preprocessing was performed using FMRIB Diffusion Toolbox in the FSL software ([www.fmrib.ox.ac.uk/fsl](http://www.fmrib.ox.ac.uk/fsl); Jenkinson et al., 2012) after converting data from DICOM to niftii format by using `mricron dem2nii` (Rorden et al., 2007) as described in previous work (Meng et al., 2015). All diffusion-weighted images were corrected for eddy current and head motion by registration to b0 image and skull and non-brain tissue were removed using the Brain Extraction Tool (BET). The tensor model was then applied voxel by voxel using the tensor model fit (Smith et al., 2004) in order to obtain voxelwise FA and MD maps. Lambda 1, lambda 2 and lambda 3 maps were also obtained from the tensor fitting procedure and used to calculate RD and AD maps. RD maps were obtained by averaging lambda 2 and lambda 3 maps and AD by renaming lambda 1 maps.

T1-weighted images were preprocessed using the anatomical processing script from FSL which included reorientation, image cropping, bias field correction, linear (FLIRT, FMRIB's Linear Image Registration Tool) and non-linear (FNIRT, FMRIB's Non-Linear Image Registration Tool) registration to the MNI standard space. Non-linear transformation output included a structural -to-MNI standard space warp field and its inverse (MNI-to-structural). Preprocessing also included brain extraction (BET) and both tissue type and subcortical structure segmentations which were used to register diffusion weighted images to preprocessed structural T1-weighted images using boundary-based registration for echo planar imaging data thus yielding a diffusion-to-structural transformation matrix. In order to register diffusion weighted data to the MNI 152 template via structural scan, we combined the previously generated structural-to-MNI non-linear transformation matrix with the `diffusion_to_structural` transformation matrix thus resulting in a diffusion-to-standard space transformation. This transformation will be used in a later step to transform the individual `fdt_paths`, the 3D image file containing the output connectivity distribution to the seed mask, to standard space.

### PROBABILISTIC TRACTOGRAPHY

Overall, we used several FSL atlases to define the occipital cortices, posterior thalami and exclusion masks for each hemisphere in standard space. Those masks were then transformed into native space using the previously described non-linear mapping and probabilistic tractography was performed to identify the streamlines from occipital cortex to the posterior thalamus within each hemisphere discarding inter-hemisphere estimates. The resulting path was then normalized and transformed into standard space where a posterior thalamus mask for each hemisphere was used to extract the mean probability of connection value which was then correlated with the previously described vSTM capacity parameter  $K$ .

### REGIONS OF INTEREST (ROI) GENERATION

We used the MNI 152 2-mm label atlas combined with the Harvard Oxford 2-mm cortical atlas to create cortical occipital masks in standard space. Masks of the right and left posterior thalamus containing pulvinar nuclei were created from the Talairach atlas. Whole brain left and right hemisphere masks were also created from the MNI 152 2mm atlas and used as exclusion masks in the tractography process. All masks were transformed into the subjects' native space using the reverse non-linear mapping previously obtained and nearest neighbor interpolation.

### ESTIMATION OF DIFFUSION PARAMETERS AND PROBABILISTIC TRACTOGRAPHY

Using the FDT toolbox from FSL, we first ran the function of Bayesian estimation of diffusion parameters obtained using sampling techniques (BedpostX) for each subject. It estimates the individual diffusion parameters at each voxel while considering the number of crossing fibers per voxel (Behrens et al., 2003; Behrens et al., 2007). We used the default parameters implemented in FDT: 2 fibers per voxel, weight of 1 and burning period 1000. Using the previously created ROIs as described above, tractography was run for each hemisphere with the occipital ROI as seed and the posterior thalamus as waypoint target mask using `probtrackx2` function from FSL. We also used an exclusion mask from the opposite hemisphere in order to ensure the ipsilateral nature of the tractography. We performed tractography separately from each occipital ROI to the posterior thalamus. For each participant, 5000 streamlines were initiated per seed voxel with a path length of  $2000 \times 0.5$  mm steps, a curvature threshold of  $80^\circ$  and loop checking criteria. The resulting image or `fdt_paths` represents the path connecting the seed region to the target where the value in each voxel represents the number of streamlines generated from the seed region that pass through that voxel. Due to the differences in volume of each area across subjects, we normalized the resulting tract estimates (`fdt_paths`) by dividing it by the `waytotal` (total number of streamlines generated from the seed region that reaches the target region; Rilling et al., 2008) thus resulting in a probability map of connectivity

(Zhang et al. 2010; Arnold et al., 2012, Behrens et al., 2007; for review see Behrens et al., 2015). Those probability maps were then transformed back into standard space so they can be used for statistical analysis (Figure 1).

### 3.3.4 EXTRACTION OF FA, MD, AD, AND RD MAPS FROM PATH PROBABILITY MAPS

Native FA, MD, ad AD and RD maps were transformed into standard space using the nonlinear transformation described previously. A mask of the tracts between posterior thalamus and occipital cortex for left and right hemispheres were obtained using the individual fdt paths maps from probtrackx transformed to standard space. The average paths of our cohort for left and right PT-OC tracts were calculated with fslmaths and thresholded above 0.03. The average left and right tract masks were then binarized before being used to extract the mean FA and MD values for each subject using fslmeants command.

### 3.3.5 ESTIMATION OF TISSUE TYPE AND TOTAL INTRACRANIAL VOLUMES

In order to obtain volumetric measurements for the whole brain, T1 images were segmented into grey matter (GM), white matter (WM) and cerebrospinal fluid (CSF) tissue classes and normalized to the MNI 152 mm template using DARTEL (SPM12 software package, <http://www.fil.ion.ucl.ac.uk>). The segmented and normalized images were modulated to account for the structural changes resulting from the normalization process, thus indicating GM, WM and CSF volume. Grey and white matter images were smoothed with an 8mm full-width at half-maximum filter (FWHM). Total intracranial volume was estimated by first computing and then adding up the totals (in liters) of the warped, modulated and smoothed GM, WM, and CSF segments with the in-built SPM Tissue Volumes Utility (Malone et al., 2015).

### 3.3.6 STATISTICAL ANALYSIS

For each individual connection probability map of posterior thalamus previously normalized and transformed into standard space, the mean probability of connection was extracted for each hemisphere, thus resulting in left or right PT-OC connection probabilities. Those values were then used to investigate the role of left or right PT-OC structural connectivity in the reduction of vSTM capacity with aging, using a regression model with vSTM capacity as dependent variable and age, PT-OC connection probability and interaction between both variables as independent variables. Gender, handedness, CSFV and crystallized IQ were also included in the model as covariates. These analyses were done using the SPSS statistics package version 21 (IBM).

### 3.3.7 SLIDING WINDOW ANALYSIS

In order to investigate more in depth the association between vSTM capacity and left PT-OC connection probability with age, we used a sliding window approach: Participants were sorted according to age. The sliding window contained a subgroup of 24 participants: The association between vSTM capacity and left PT-OC connection probability was calculated by Pearson partial correlation in this subgroup, controlling for age, gender, handedness, IQ and CSFV. The window was then consecutively shifted by one participant to get an ‘older’ group of 24 subjects and the partial correlation repeated for each shift. In Figure 2, the mean age of the sliding window subgroup versus the correlation coefficient of the partial correlation is represented (See Figure 2 A).

In order to test the reliability of the sliding window analysis, we performed bootstrapping analyses. We repeated the analysis sequentially by excluding each subject separately once, to test whether outliers might have influenced the results. We found a very similar pattern, suggesting that the results were not driven by non-representative outliers (see supplementary material figure 1B). We then repeated the sliding window analysis for different window sizes, varying from 20 to 35 subjects, and found a congruent pattern of results, which suggested that the results are reliable and do not depend on the selected window size (Supplementary fig 1A).

## 3.4 RESULTS

### 3.4.1 AGING MODULATES THE ASSOCIATION BETWEEN PT-OC STRUCTURAL CONNECTIVITY AND vSTM CAPACITY

In order to test whether our sample was representative with respect to brain changes that are normally shown in aging individuals and in order to identify variables that needed to be used as control variables in the later analyses, we first assessed age effects on brain structure, namely on brain volume. Using voxel based morphometry we found that CSF volume was significantly increased ( $r = 0.79$ ;  $p < .001$ ) while GM volume was significantly reduced with increasing age ( $r = -0.57$ ;  $p < .001$ ) (See supplementary figure 1). As this was to be expected based on previous studies (Salat et al., 1999; Salat et al., 2011; Walhovd et al., 2011), we can conclude that the brain changes in our sample are representative for those that are to be expected in healthy aging individuals.

In order to investigate the role of PT-OC structural connectivity in the reduction of vSTM capacity with aging, a regression model with Age, PT-OC connection probability and interaction between both variables, Gender, Handedness, CSFV and IQ was used. The last four variables were included in the model, in order to control for gender, handedness, general cognitive performance, and brain volume effects. We tested the model for left and right PT-OC connectivity separately, in order to account for potential side effects of age as suggested by previous studies (Silver et al., 1997; Huster et al., 2009; Johnson et al., 2014). Concerning right PT-OC connectivity, we found that the model was not a significant predictor of vSTM capacity  $F(7.58) = 2.25$ ;  $p = .087$ . We therefore not further analyzed this model. Concerning left PT-OC connectivity, we found that the overall model was a significant predictor of (23.8% of variance in) vSTM capacity, demonstrating the reliability of this model to explain age-related variance in vSTM capacity (Table 2). In accordance with previous studies (McAvinue et al., 2012; Wiegand et al., 2014; Wiegand et al., 2014) we found that vSTM storage capacity  $K$  declined with increasing age in our participant group ( $\beta_1 = -0.047$ ;  $p = .001$ ). We then aimed to investigate whether PT-OC structural connectivity was associated with vSTM, as suggested by the NTVA theory and previous findings (Kraft et al., 2015; Menegaux et al., 2017). We found left PT-OC connection probability to be significantly associated with vSTM capacity ( $\beta_2 = -42.370$ ;  $p = .032$ ). Finally, we tested whether the association between PT-OC connectivity and vSTM  $K$  connectivity changed with aging

We found a significant interaction between Age x left PT-OC connection probability ( $\beta_3 = 0.952$ ;  $p = .009$ ), demonstrating that age affects the relationship between posterior thalamus-occipital cortex connectivity and vSTM capacity.

| Dependent variable = vSTM capacity                   |                |              |                     |
|--|----------------|--------------|---------------------|
| Predictors   | $\beta$ values | P value      | 95% CI              |
| Age  | <b>-0.047</b>  | <b>0.001</b> | [-0.075 , -0.020 ]  |
| Left PT-OC structural connectivity                   | <b>-42.37</b>  | <b>0.032</b> | [-81.066 , -3.674 ] |
| Interaction Age x left PT-OC Structural connectivity | <b>0.95</b>    | <b>0.009</b> | [ 0.243 , 1.661 ]   |
| Gender   | -0.05          | 0.609        | [-0.261 , 0.155 ]   |
| Handedness   | -0.16          | 0.180        | [-0.400 , 0.077 ]   |
| IQ   | <b>0.008</b>   | <b>0.019</b> | [ 0.001 , 0.015 ]   |
| CSFV   | 2.159          | 0.063        | [-0.118 , 4.435 ]   |

**Table 2: Regression table**

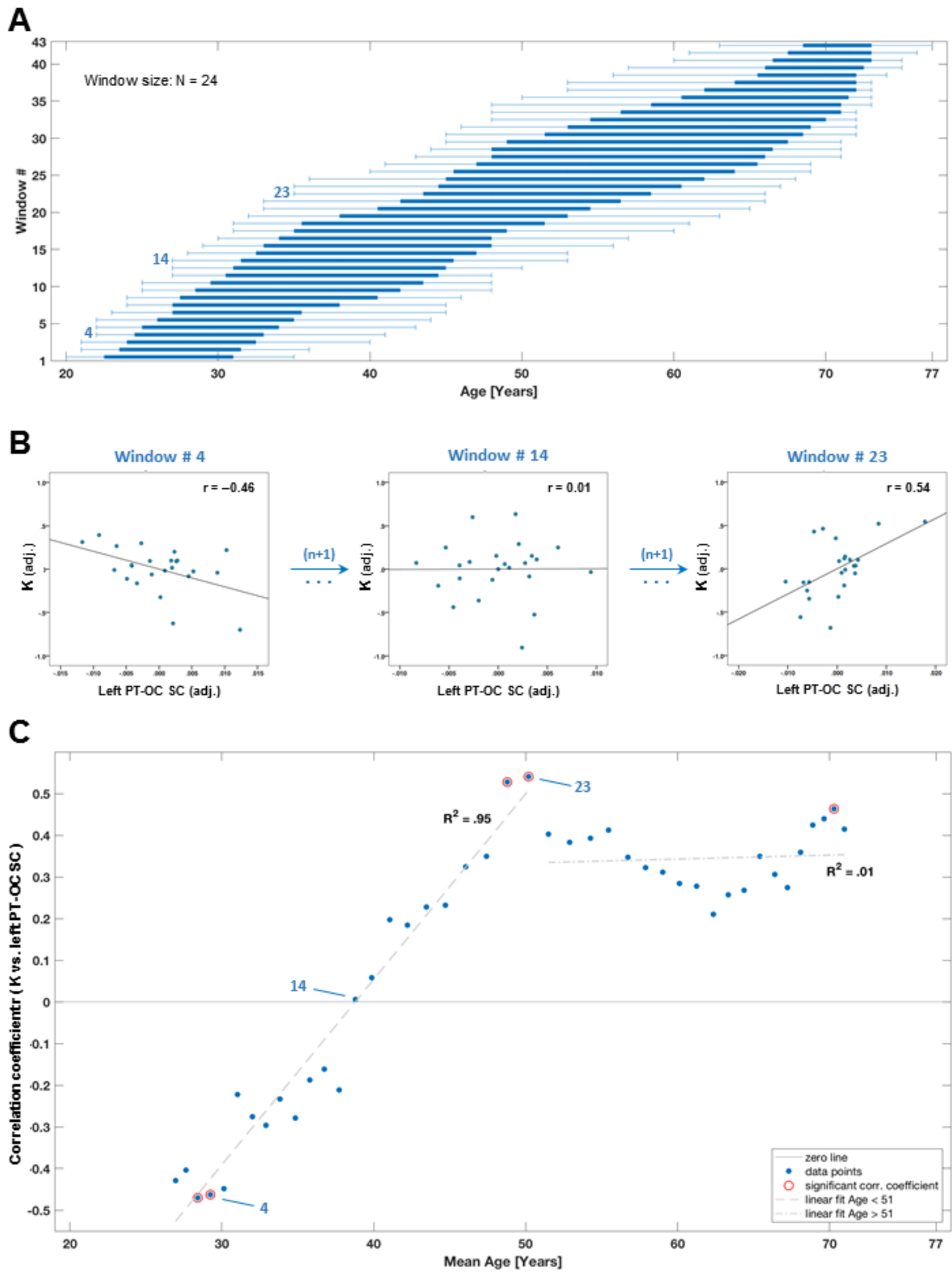
### 3.4.2 THE AGE EFFECT ON THE ASSOCIATION BETWEEN LEFT PT-OC STRUCTURAL CONNECTIVITY AND VSTM CAPACITY: SHIFT AND ALTERATION OF MICROSTRUCTURE

In order to investigate the association between PT-OC connection probability and vSTM capacity with increasing age in more depth, we applied a sliding window approach. This allowed tracking the association between PT-OT connectivity and vSTM capacity as a pseudo-continuous function of age. The window was slid until the age of 77 years (the oldest participant's age), resulting in the plot presented in figure 2C. We found that the association between vSTM capacity and left PT-OC structural connectivity was linearly inverting from a negative association in the youngest groups to a positive association around an age of 50 years. Up from this age, the positive association remained significant throughout. As illustrated in figure 2B, window number 4, we found that in young individuals with a mean age of 28 years, vSTM capacity  $K$  was significantly negatively correlated with left PT-OC structural connectivity ( $r = -0.46$ ;  $p < .05$ ) whereas in individuals with a mean age of 50 years (see window 14 in figure 2), it was significantly positively correlated with left PT-OC structural connectivity ( $r = 0.54$ ;  $p < .05$ ). Similarly, we found that for individuals with a mean age of 70 years, vSTM capacity was significantly positively associated with left PT-OC structural connectivity ( $r = 0.45$ ;  $p < .05$ ).

Considering this somewhat surprising inverse association between vSTM capacity and left PT-OC connection probability in younger compared to older individuals, the well-known aging effects on white matter microstructure (Pfefferbaum et al., 2000; Hugenschmidt et al., 2008; Westlye et al., 2010) and previous studies suggesting that white matter microstructure mediates the impact of age on attention functions such as processing speed (Salami et al., 2012), we speculated that the inverse

association to vSTM capacity that we found might be caused by changes in white matter properties of left PT-OC tract. Although we cannot fully test such speculation, we investigated whether the microstructure of the tracts connecting the left posterior thalamus to the left occipital cortex was altered with increasing age. We found that the mean FA of the tracts connecting the left posterior thalamus to the left occipital cortex was significantly reduced with increasing age ( $r = -0.54$ ;  $p < .001$ ) while MD was significantly increased ( $r = 0.63$ ;  $p < .001$ ). Similarly, RD and AD were also significantly increased with age ( $r = 0.60$ ;  $p < .001$ ;  $r = 0.36$ ;  $p = .003$  respectively) (See supplementary figure S2).

**Figure 2: Aging modulates the association between vSTM capacity and the left structural connectivity of posterior thalamus to occipital cortex.** **A** illustrates the sliding window approach used in this study: participants were ranked by age and the first 24 individuals constituted the first window which was shifted consecutively by one participant. In **B**, three examples of correlations between  $K$  and left PT-OC SC in different age windows as indicated in (A) are shown. The correlation coefficient  $r$  is presented in the upper right corner of the individual plots. In **C** these correlation coefficients are plotted against the mean age of the window group. Significant correlations between  $K$  and left PT-OC SC are indicated with a red circle, the dotted lines represent linear fits.



## 3.5 DISCUSSION

Using a whole-report paradigm and TVA -based modeling together with probabilistic tractography in a group of healthy participants aged 20 to 77 years, we investigated the effect of age on the association between the structural connectivity of posterior thalamus to occipital cortices and vSTM capacity  $K$ . We found that the association between left PT-OC connection probability and vSTM capacity differed throughout the lifespan. Indeed, in younger individuals at an age below 30 years, vSTM capacity was significantly negatively associated with left PT-OC structural connectivity. In older individuals above the age of 50, this association was reversed, i.e. the higher the connection probability between left posterior thalamus and left occipital cortex, the higher the vSTM capacity  $K$ . When exploring the microstructural properties of the left PT-OC tracts, we found that FA was significantly decreased with age while MD, AD and RD were significantly increased. This suggested that age modifies the microstructural properties of the tracts connecting the left posterior thalamus to the left occipital cortex. Such changes might underlie the altered relationship between thalamo-cortical connectivity and vSTM capacity  $K$ . Altogether, to the best of our knowledge, our findings provide first evidence for the significant impact of aging not only on vSTM capacity  $K$  and the structural connectivity between posterior thalamus and occipital cortices, but also on the relationship between these measures.

### 3.5.1 AGING MODULATES THE ASSOCIATION BETWEEN PT-OC STRUCTURAL CONNECTIVITY AND VSTM CAPACITY

In order to investigate whether aging affects the association between vSTM capacity and PT-OC connection probability, two different analyses were carried out, i.e. a multiple regression with vSTM capacity as independent variable and age, PT-OC connection probability and interaction between both variables as independent variables as well as a sliding window approach.

We found that left PT-OC connection probability was a significant predictor of vSTM capacity. This is in line with findings from Habekost and Rostrup (2006) and Kraft and colleagues (2015) who found that vSTM capacity was reduced in a group of patients with thalamic lesions.

Our finding is in agreement with the NTVA assumption that posterior thalamus and visual cortices are relevant for vSTM capacity. Indeed, according to NTVA, the activity of visual neurons coding for the objects that won the race is assumed to be sustained and reactivated by a feedback loop gated by the TRN (Bundesen et al., 2005). Our finding of a significant association between vSTM capacity and PT-OC connection probability suggests that, independently of age, connections from posterior thalamus to occipital cortices are relevant for vSTM capacity. The fact that left PT-OC connection probability is a significant predictor of vSTM capacity also fits with findings from Menegaux and colleagues (Menegaux et al., 2017) who found that the microstructure of posterior thalamic radiations, as

reflected by FA, was significantly associated with vSTM capacity in a group of healthy young adults aged 26 years. Together, these findings suggest that tracts connecting posterior thalamus to occipital cortices and their microstructure are critical for vSTM capacity.

The main finding of this study is the significant interaction effect found between age and left PT-OC structural connectivity on vSTM capacity suggesting that the association between vSTM capacity and left PT-OC connection probability is modified by age. This interaction effect remained significant when controlled for the potential effects of CSF volume and IQ. The modification of the association between vSTM capacity and a brain correlate, here PT-OC structural connectivity, with age had previously been suggested by electroencephalographic findings of a weaker association between vSTM capacity and contralateral delay activity in older compared to younger adults (Wiegand et al., 2013; Sander et al., 2011; Duarte et al., 2013). It also fits to previous findings that in populations with changes in white matter connectivity the association between vSTM capacity and posterior thalamic radiations microstructure might change compared to young healthy groups. In particular, these results fit to those from a previous study that used the same TVA-based methodology in preterm-born adults who are known to exhibit changes in thalamo-cortical connectivity (Menegaux et al., 2017). Indeed, Menegaux and colleagues found that the association between FA in posterior thalamic radiations and vSTM capacity was inverse in preterm compared to term-born adults (Menegaux et al., 2017). Arguably, modifications of thalamo-cortical tracts microstructure in older participants might also affect the association between thalamo-cortical connectivity and vSTM capacity  $K$ . However, although the significant interaction effect between age and left PT-OC connection probability on vSTM capacity suggested that aging affects this structure-function association, it did not provide information regarding the direction of change. Thus, in order to investigate the direction of this interaction, we examined the association between vSTM capacity  $K$  and PT-OC connection probability as a pseudo continuous function of age using a sliding window approach. This yielded intriguing findings as it showed that the association between vSTM capacity  $K$  and PT-OC structural connectivity was continuously inverted from negative to positive with increasing age.

### 3.5.2 THE ASSOCIATION BETWEEN VSTM CAPACITY AND LEFT PT-OC STRUCTURAL CONNECTIVITY IS CONTINUOUSLY INVERSED WITH AGE: POTENTIALLY RELEVANT MICROSTRUCTURAL ALTERATIONS.

This continuum across aging suggests that there is a ceaseless process influencing PT-OC connectivity so that the association with vSTM capacity  $K$  is changed. Interestingly, it has been well documented that aging affects white matter microstructure (Pfefferbaum et al., 2000; Hugenschmidt et al., 2008; Westlye et al., 2010) and that white matter microstructure can mediate the impact of age on attention functions such as processing speed (Salami et al., 2012). Thus, a change in white matter microstructure could be the critical mechanism behind the continuous inversion from negative to

positive of the association between vSTM capacity and left PT-OC structural connectivity. While this speculative hypothesis cannot be tested in our sample, we examined whether in our older participants age-related microstructural changes of PT-OC tracts would be found. Interestingly, we found that FA in left PT-OC tracts was reduced and MD, RD, AD increased in older compared to younger participants. These findings are in line with those of Kumar and colleagues (2013) who found increased AD in bilateral posterior thalamus white matter of older participants and of Hugenschmidt and colleagues (2008) and Westlye and colleagues (2010) who found reduced FA in posterior thalamic radiations of older compared to younger adults. A reduced FA value might be interpreted as a decrease in the organization of white matter caused by various processes such as demyelination, axonal degradation or gliosis (Beaulieu 2002, Concha et al., 2006; Lebel et al., 2008; Assaf et al., 2008). The conjunction of decreased FA with increased MD, RD and AD is in line with findings from Burzynska and colleagues (2010) and would preferentially suggest a decrease in fiber organization which might be caused by axonal loss or gliosis (Beaulieu et al., 2002; Concha 2006; Lebel 2008 et Assaf 2008).

Another interesting finding in our sample is the absence of significant changes in WM volume with age which is in agreement with several studies that have shown slight increases in white matter volume until mid-adulthood (Van Buchem et al., 1999; Bartzokis et al., 2001; Chechik G et al., 1999) before a strong decrease starting around the age of 65 years (Westlye et al., 2010). This opposite pattern between FA and volume is interesting as it has been shown in mice that both were related to myelination to some degree (Peters et al., 2000; Peters and Sethares, 2002). Such pattern might result from several factors such as redundant myelination (Peters et al., 2000); fluid bubbles in myelin sheets (Peters and Sethares 2002), or complexity of circuitry. The increase in WM volume until mid-adulthood might result from the increased complexity of myelinated fibers, with more occurrence of fiber crossing as a higher number of fiber crossing would reduce the FA while increasing the volume (Tuch et al., 2005). Although the link between FA, MD and myelin has sometimes been questioned (Arshad et al., 2011), previous studies have found a quadratic relationship between magnetic transfer ratio and age with a slight increase until 40s and then a decrease also suggesting an increase in myelin content until mid-adulthood (Van der Flier et al., 2002). Interestingly, we found that the switch from a negative to a positive association between vSTM capacity  $K$  and PT-OC structural connectivity also occurred around 40 years. Thus we speculate that the switch of the direction of association between vSTM capacity  $K$  and PT-OC structural connectivity with aging might be due to a change in microstructural properties of PT-OC tracts such as myelination or increased complexity of myelinated fibers. A higher number of crossing fibers could also explain the increase in axial diffusivity (Douaud et al., 2011).

Together, those findings suggest strong changes in microstructural properties of the tracts connecting posterior thalamus to occipital cortices and make those tracts an ideal candidate to mediate the effect of aging on vSTM capacity. This would fit with previous findings on the mediating role of white matter integrity in age-behavior relationships (Raz et al., 2005; Burgmans et al., 2011; Brickman et al.,

2012; Salami et al., 2012; Samanez-Larkin et al., 2012). Further studies using MTR and/or diffusion MRI methods that can resolve intravoxel structure such as high angular resolution diffusion imaging (Tuch et al., 2003) could help bring further information regarding the affected white matter characteristics.

### 3.5.3 LIMITATIONS

Our study has several limitations: First, we used a cross sectional sample. Thus, although we could examine the effect of age on PT-OC structural connectivity with vSTM capacity between individuals, we cannot generalize our findings to intra-individual changes over the lifespan (Salthouse et al., 2011). Moreover, it is difficult to interpret our DTI-based results in terms of underlying microscopic changes since the number of streamlines generated by probtrackx is not a direct measure of anatomical connectivity and their relationship to the underlying anatomy is quite unclear (Jones 2010; Jones et al., 2013; Jbabdi and Johansen-berg, 2011). Several factors can influence the number of streamlines such as the organization of myelin in regions bordering cortical grey matter (Reveley et al., 2015) fanning fibers, crossing fibers with fewer crossing fibers leading to increased connectivity values (Jbabdi and Johansen-Berg, 2011; Thomas et al., 2014; Reveley et al., 2015; Donahue et al., 2016). Moreover, dense white matter fiber bundles at the grey matter/white matter boundary would hinder the tractography detection of weaker crossing fibers entering or exiting grey matter in sulcal fundi and thus influence the number of streamlines. Crossing fibers are also a limitation of the tensor model and thus will affect FA, MD, RD and AD values as well.

## 3.6 CONCLUSION

We investigated whether aging affects the association between vSTM capacity and the structural connectivity of posterior thalamus to visual cortices. In addition to a reduced vSTM capacity and aberrant PT-OC connection probability, we found that the relationship between vSTM capacity  $K$  and PT-OC connection probability was significantly modified by age. In young adults, vSTM capacity  $K$  was significantly negatively associated with PT-OC connection probability while in older adults, this association was positive. Interestingly, we also found reduced fractional anisotropy and increased mean diffusivity in PT-OC tracts with aging which suggested that the inversion of the association between PT-OC connection probability and vSTM capacity  $K$  with aging might reflect age-related changes in white matter properties. These results suggest that the effect of aging on vSTM capacity might be modulated by the microstructure and connectivity of white matter between posterior thalamus and occipital cortices.

---

## ACKNOWLEDGMENTS

We thank, Erika Künstler and Annette Abraham for their help with the recruitment, and data collection of the TVA data. We are grateful to the staff of the Department of Neuroradiology in Munich particularly Dr. Christine Preibisch and Stephan Kaczmarz for showing us how to operate the scanner. Most importantly, we thank all our study participants for their efforts to take part in this study. This study was supported by EU Marie Curie Training Network INDIREA (ITN- 2013-606901 to H.J.M., and K.F.), Deutsche Forschungsgemeinschaft (FI 1424/2-1 to K.F. and SO 1336/1-1 to C.S.), German Federal Ministry of Education and Science (BMBF 01ER0803 to C.S.) and the Kommission für Klinische Forschung, Technische Universität München (KKF 8765162 to C.S.).

---

## REFERENCES

- Aboitiz, F., Rodriguez, E., Olivares, R., Zaidel, E., 1996.** Age-related changes in fibre composition of the human corpus callosum: sex differences. *NeuroReport* 7, 1761–1764.
- Arnold, J. F., Zwiers, M. P., Fitzgerald, D. A., van Eijndhoven, P., Becker, E. S., Rinck, M., Fernandez, G., Speckens, A. E., & Tendolkar, I. 2012.** Fronto-limbic microstructure and structural connectivity in remission from major depression. *Psychiatry Res*, 204(1), 40-48.
- Assaf, Y., Blumenfeld-Katzir, T., Yovel, Y., Basser, P.J., 2008.** AxCaliber: a method for measuring axon diameter distribution from diffusion MRI. *Magn. Reson Med.*, 59, 1347-1354.
- Bartzokis, G., Sultzer, D., Lu, P.H., Nuechterlein, K.H., Mintz, J., Cummings, J.L., 2004.** Heterogeneous age-related breakdown of white matter structural integrity: implications for cortical “disconnection” in aging and Alzheimer’s disease. *Neurobiol Aging*, 25, 843–51.
- Barrick, T.R., Charlton, R.A., Clark, C.A., Markus, H.S., 2010.** White matter structural decline in normal ageing: a prospective longitudinal study using tract-based spatial statistics. *Neuroimage*, 51, 565–577.
- Basser, P.J., 1995.** Inferring microstructural features and the physiological state of tissues from diffusion-weighted images. *NMR Biomed.* 8(7-8), 333-44.
- Basser, P.J., Mattiello, J., LeBihan, D., 1994.** MR diffusion tensor spectroscopy and imaging. *Biophys J.* 66, 259–267.
- Beaulieu, C., 2002.** The basis of anisotropic water diffusion in the nervous system—a technical review. *NMR Biomed.* 15 (7–8), 435–455.
- Beck, A.T., Steer, R.A., Brown, G.K., 1996.** Manual for the Beck Depression Inventory-II. Second Edition ed. The Psychological Corporation, San Antonio, TX.
- Behrens, T. E., Berg, H. J., Jbabdi, S., Rushworth, M. F., & Woolrich, M. W. 2007.** Probabilistic diffusion tractography with multiple fibre orientations: What can we gain? *Neuroimage*, 34(1), 144-155.
- Behrens, T. E., Johansen-Berg, H., Woolrich, M. W., Smith, S. M., Wheeler-Kingshott, C. A., Boulby, P. A., Barker, G. J., Sillery, E. L., Sheehan, K., Ciccarelli, O., Thompson, A. J., Brady, J. M., & Matthews, P. M. 2003.** Non-invasive mapping of connections between human thalamus and cortex using diffusion imaging. *Nat Neurosci*, 6(7), 750-757.

- Bennett, I.J., Madden, D.J., Vaidya, C.J., Howard, D.V., Howard, J.H., 2010.** Age-Related Differences in Multiple Measures of White Matter Integrity: A Diffusion Tensor Imaging Study of Healthy Aging. *Hum Brain Mapp.* 31(3), 378–390.
- Bhagat, Y.A., Beaulieu, C., 2004.** Diffusion anisotropy in subcortical white matter and cortical gray matter: changes with aging and the role of CSF-suppression. *J Magn Reson Imaging.* 20, 216–227.
- Bundesen, C., 1990.** A theory of visual attention. *Psychol. Rev.* 97, 523-547.
- Bundesen, C., Habekost, T., Kyllingsbaek, S., 2005.** A neural theory of visual attention: bridging cognition and neurophysiology. *Psychol. Rev.*, 112, 291-328.
- Burzynska, A.Z., Preuschhof, C., Backman, L., Nyberg, L., Li, S.C., Lindenberger, U., Heekeren, H.R., 2010.** Age-related differences in white-matter microstructure: Region-specific patterns of diffusivity. *Neuroimage.* 49(3),2104-12.
- Chechik G., Meilijson, I., Ruppin, E., 1999.** Neuronal regulation: A mechanism for synaptic pruning during brain maturation. *Neural Comput.* 11(8), 2061-80.
- Concha, L., Gross, D.W., Wheatley, B.M., Beaulieu, C., 2006.** Diffusion tensor imaging of time-dependent axonal and myelin degradation after corpus callosotomy in epilepsy patients. *Neuroimage.* 32,1090–1099.
- Courchesne, E., Chisum, H.J., Townsend, J., Cowles, A., Covington, J., Egaas, B., Harwood, M., Hinds, S., Press, G.A., 2000.** Normal brain development and aging: quantitative analysis at in vivo MR imaging in healthy volunteers. *Radiology.* 216(3), 672–82.
- Cowan, N., 2001.** The magical number 4 in short-term memory: a reconsideration of mental storage capacity. *Behav. Brain. Sci.* 24, 87-114.
- Desimone, R., & Duncan, C., 1995.** Neural mechanisms of selective visual attention. *Annu. Rev. Neurosci.* 18, 193-222.
- Duarte, A., Hearons, P., Jiang, Y., Delvin, M.C., Newsome, R.N., Verhaeghen, P., 2013.** Retrospective attention enhances visual working memory in the young but not the old: an ERP study. *Psychophysiology* 50(5), 465-476.
- Dyrholm, M., Kyllingsbaek, S., Espeseth, T., Bundesen, C. 2011.** Generalizing parametric models by introducing trial-by-trial parameter variability: The case of TVA. *Journal of Mathematical Psychology* 55(6), 416-29.

- Espeseth, T., Vangkilde, S.A., Petersen, A., Dyrholm, M., Westlye, L.T., 2014.** TVA-based assessment of attentional capacities-associations with age and indices of brain white matter microstructure. *Front. Psychol.* 5, 1177.
- Fama, R., Sullivan, E.V., 2015.** Thalamic structures and associated cognitive functions: Relations with age and aging. *Neurosci Biobehav Rev.*, 54, 29–37.
- Finke, K., Bublak, P., Krummenacher, J., Kyllingsbæk, S., Müller, H. J., & Schneider, W. X. (2005).** Usability of a theory of visual attention (TVA) for parameter-based measurement of attention I: Evidence from normal subjects. *Journal of the International Neuropsychological Society*, 11, 832-842.
- Folstein, M.F., Folstein, S.E., McHugh, P.R. 1975.** "Mini-mental state". A practical method for grading the cognitive state of patients for the clinician. *J Psychiatr Res* 12(3), 189-98.
- Ge, Y., Grossman, R.I., Babb, J.S., Rabin, M.L., Mannon, L.J., Kolson, D.L., 2002.** Age-related total gray matter and white matter changes in normal adult brain. Part I: volumetric MR imaging analysis. *AJNR Am J Neuroradiol.* 23(8),1327-33.
- Golestani, A.M., Miles, L., Babb, J., Castellanos, F.X., Malaspina, D., Lazar, M., 2014.** Constrained by Our Connections: White Matter's Key Role in Interindividual Variability in Visual Working Memory Capacity. *J. Neurosci.* 34 (45), 14913-14918.
- Habekost, T., Rostrup, E., 2007.** Visual attention capacity after right hemisphere lesions. *Neuropsychologia* 45, 1474-1488.
- Hebb, D. O., 1949.** Organization of behavior. New York: Wiley
- Hugenschmidt, C.E., Peiffer, A.M., Kraft, R.A., Casanova, R., Deibler, A.R., Burdette, J.H., Maldjian, J.A., Laurienti, P.J., 2008.** Relating imaging indices of white matter integrity and volume in healthy older adults. *Cereb Cortex*, 18, 433-442.
- Hughes, E.J., Bond, J., Svrckova, P., Makropoulos, A., Ball, G., Sharp, D.J., Edwards, A.D., Hajnal, J.V., Counsell, S.J. 2012.** Regional changes in thalamic shape and volume with increasing age. *NeuroImage.* 63,1134–1142.
- Huster, R.J., Westerhausen, R., Kreuder, F., Schweiger, I., Wittling, W., 2009.** Hemispheric and gender related differences in the midcingulum bundle: a DTI study. *Hum Brain Mapp.* 30, 383–391.
- Jbabdi, S., Sotiropoulos, S.N., Haber, S.N., Van Essen, D.C., Behrens, T.E. 2015.** Measuring macroscopic brain connections in vivo. *Nat Neurosci.* 18(11), 1546-55.
- Jenkinson, M., Beckmann, C. F., Behrens, T. E., Woolrich, M. W., & Smith, S. M. (2012).** FSL. *Neuroimage*, 62(2), 782-790.

- Johnson, R.T.,** Yeatman, J.D., Wandell, B.A., Buonocore, M.H., Amaral, D.G., Nordahl, C.W., 2014. Diffusion properties of major white matter tracts in young, typically developing children. *Neuroimage*, 88,143–154.
- Jones, D.K.,** 2010. Challenges and limitations of quantifying connectivity in the human brain in vivo with diffusion MRI. *Imaging Med.*, 2, 341-355.
- Jones, D.K.,** Knosche, T.R., Turner, R., 2013. White matter integrity, fiber count, and other fallacies: the do's and don'ts of diffusion MRI. *Neuroimage*, 73, 239-54.
- Jost, K.,** Bryck, R. L., Vogel, E. K., & Mayr, U. (2011). Are Old Adults Just Like Low Working Memory Young Adults? Filtering Efficiency and Age Differences in Visual Working Memory. *Cerebral Cortex*, 21, 1147-1154.
- Kraft, A.,** Irlbacher ,K., Finke, K., Kaufmann, C., Kehrer, S., Liebermann, D., Bundesen, C., Brandt, S.A., 2015. Dissociable spatial and non-spatial attentional deficits after circumscribed thalamic stroke. *Cortex*, 64, 327–342.
- Kumar, R.,** Chavez, A.S., Macey, P.M., Woo, M.A., Harper, R.M., 2013. Brain axial and radial diffusivity changes with age and gender in healthy adults. *Brain Res.* 1512, 22-36.
- Kyllingsbæk, S.,** 2006. Modeling visual attention. *Behavior. Research. Methods*, 38, 123–133.
- Lebel, C.,** Walker, L., Leemans, A., Phillips, L., Beaulieu, C., 2008. Microstructural maturation of the human brain from childhood to adulthood. *Neuroimage*. 40(3), 1044-55.
- Luck, S.J.,** Vogel, E.K., 1997. The capacity of visual working memory for features and conjunctions. *Nature*, 390, 279–281.
- Malloy, P.,** Correia, S., Stebbins, G., Laidlaw, D.H.,2007. Neuroimaging of white matter in aging and dementia. *Clin Neuropsychol.*, 21(1), 73-109.
- Malone, I.B.,** Leung, K.K., Clegg, S., Barnes, J., Whitwell, J.L., Ashburner, J., Fox, N.C., Ridgway, G.R., 2015. Accurate automatic estimation of total intracranial volume: a nuisance variable with less nuisance. *Neuroimage*, 104, 366-72.
- McAvinue, L.P.,** Habekost, T., Johnson, K.A., Kyllingsbaek, S., Vangkilde, S., Bundesen, C., Robertson, I.H. 2012. Sustained attention, attentional selectivity, and attentional capacity across the lifespan. *Atten Percept Psychophys*, 74(8), 1570-82.
- Menegaux, A.,** Meng, C., Neitzel, J., Bauml, J. G., Muller, H. J., Bartmann, P., Wolke, D., Wohlschläger, A.M., 2017. Impaired visual short-term memory capacity is distinctively associated

with structural connectivity of the posterior thalamic radiation and the splenium of the corpus callosum in preterm-born adults. *Neuroimage*, 150, 68–76.

**Meng, C.**, Bäuml, J.G., Daamen, M., Jaekel, J., Neitzel, J., Scheef, L., Busch, B., Baumann, N., Boecker, H., Zimmer, C., Bartmann, P., Wolke, D., Wohlschläger, A.M., Sorg, C., 2015. Extensive and interrelated subcortical white and gray matter alterations in preterm-born adults. *Brain Struct Funct* 221 (4), 2109-21.

**Meier-Ruge, W.**, Ulrich, J., Bruhlmann, M., Meier, E., 1992. Age-related white matter atrophy in the human brain. *Ann. N. Y. Acad. Sci.* 673, 260–269.

**Minati, L.**, Grisoli, M., Buzzone, M.G., 2007. MR spectroscopy, functional MRI, and diffusion-tensor imaging in the aging brain: a conceptual review. *J. Geriatr. Psychiatry Neurol.* 20, 3–21.

**Oldfield, R.C.**, 1971. The assessment and analysis of handedness: the Edinburgh inventory. *Neuropsychologia*. 9(1), 97-113.

**O'Sullivan, M.**, Jones, D.K., Summers, P.E., Morris, R.G., Williams, S.C., Markus, H.S., 2001. Evidence for cortical "disconnection" as a mechanism of age-related cognitive decline. *Neurology*. 57, 632–638.

**Peters A.** 2002. The effects of normal aging on myelin and nerve fibers: a review. *Journal of Neurocytology*. 31, 581–593.

**Pfefferbaum, A.**, Sullivan, E.V., Hedehus, M., Lim, K.O., Adalsteinsson, E., Moseley, M., 2000. Age-related decline in brain white matter anisotropy measured with spatially corrected echo-planar diffusion tensor imaging. *Magn. Reson. Med.*, 44 ,259-268.

**Pierpaoli, C.**, Basser, P.J., 1996. Toward a quantitative assessment of diffusion anisotropy. *Magn Reson Med.*, 36(6), 893-906.

**Pierpaoli, C.**, Jezzard, P., Basser, P.J., Barnett, A., Di Chiro, G., 1996. Diffusion tensor MR imaging of the human brain. *Radiology*, 201, 637–648.

**Pierpaoli, C.**, Barnett, A., Pajevic, S., Chen, R., Penix, L.R., Virta, A., Basser, P., 2001. Water diffusion changes in Wallerian degeneration and their dependence on white matter architecture. *Neuroimage*. 2001, 6(1), 1174-85.

**Raz, N.**, Lindenberger, U., Rodrigue, K.M., Kennedy, K.M., Head, D., Williamson, A., Dahle, C., Gerstorf, D., Acker, J.D., 2005. Regional brain changes in aging healthy adults: general trends, individual differences and modifiers. *Cereb Cortex*, 15, 1676–89.

- Raz**, N., Rodrigue, K.M., 2006. Differential aging of the brain: patterns, cognitive correlates and modifiers. *Neurosci Biobehav Rev.* , 30(6), 730–4.
- Rilling**, J.K., Glasser, M.F., Preuss, T.M., 2008. The evolution of the arcuate fasciculus revealed with comparative DTI. *Nat. Neurosci.*, 11(4), 426–428.
- Rorden**, C., Karnath, H.O., Bonilha, L., 2007. Improving lesion-symptom mapping. *J. Cog. Neurosci.*, 19(7), 1081-8.
- Salat**, D.H., Kaye, J.A., Janowsky, J.S., 1999. Prefrontal gray and white matter volumes in healthy aging and Alzheimer disease. *Arch Neurol.* 56(3),338-44.
- Salat**, D.H., Chen, J.J., Van der Kouwe, A.J., Greve, D.N., Fischl, B., Rosas, H.D., 2011. Hippocampal degeneration is associated with temporal and limbic gray matter/white matter tissue contrast in Alzheimer's disease. *Neuroimage*, 54(3), 1795-802.
- Sander**, M.C., Werkle-Bergner, M., Lindenberger, U., 2011. Contralateral delay activity reveals life-span age differences in top-down modulation of working memory contents. *Cereb. Cortex*, 22, 2809-2819.
- Silver**, N.C., Barker, G.J., MacManus, D.G., Tofts, P.S., Miller, D.H., 1997. Magnetisation transfer ratio of normal brain white matter: a normative database spanning four decades of life. *J. Neurol. Neurosurg. Psychiatry*, 62, 223-228.
- Smith**, S., Jenkinson, M., Woolrich, M., Beckmann, C., Behrens, T., Johansen-Berg, H., Bannister, P., DeLuca, M., Drobnjak, I., Flitney, D., Niazy, R., Saunders, J., Vickers, J., Zhang, Y., DeStefano, N., Brady, J., Matthews, P., 2004. Advances in functional and structural MR image analysis and implementation as FSL. *NeuroImage*, 23(S1):208–219.
- Sperling**, G., 1960. The information available in brief visual presentations. *Psychological monographs: General and applied.* 74:1.
- Sullivan** E.V., Rohlfing, T., Pfefferbaum, A., 2010a. Quantitative fiber tracking of lateral and interhemispheric white matter systems in normal aging: relations to timed performance. *Neurobiol. Aging.* 31(3),464-81
- Sullivan** E.V., Zahr, N.M., Rohlfing, T., Pfefferbaum, A., 2010b. Fiber tracking functionally distinct components of the internal capsule. *Neuropsychologia*, 48(14),4155-63.
- Teipel**, S.J., Meindl, T., Wagner, M., Stieltjes, B., Reuter, S., Hauenstein, K.H., Filippi, M., Ernemann, U., Reiser, M.F., Hampel, H., 2010. Longitudinal changes in fiber tract integrity in healthy aging and mild cognitive impairment: a DTI follow-up study. *J Alzheimers Dis.* 22,507–522.

- Tuch**, D.S., Reese, T.G., Wiegell, M.R., Wedeen, V.J., 2003. Diffusion MRI of complex neural architecture. *Neuron*. 40, 885–895.
- Tuch**, D.S., Salat, D.H., Wisco, J.J., Zaleta, A.K., Hevelone, N.D., Rosas, H.D., 2005. Choice reaction time performance correlates with diffusion anisotropy in white matter pathways supporting visuospatial attention. *Proc. Natl. Acad. Sci. U S A* 102, 12212–12217.
- Van Buchem** M.A., McGowan, J.C., Grossman, R.I., 1999. Magnetization transfer histogram methodology: its clinical and neuropsychological correlates. *Neurology*. 53(5 Suppl 3),S23-8.
- Van der Flier**, W., van den Heuvel, D., Weverling-Rijnsburger, A., Bollen, E., Westendorp, R., van Buchem, M., Middelkoop, H.A., 2002. Magnetization transfer imaging in normal aging, mild cognitive impairment, and Alzheimer’s disease. *Ann Neurol*, 52, 62–7.
- Verhaegen**, P., Marcoen, A., Goossens, L., 1993. Facts and fiction about memory aging: A quantitative integration of research findings. *Journal of Gerontology: Psychological Sciences*, 48,157-171.
- Vernooij**, M.W., de Groot, M., van der Lugt, A., Ikram, M.A., Krestin, G.P., Hofman, A., Niessen, W.J., Breteler, M.M., 2008. White matter atrophy and lesion formation explain the loss of structural integrity of white matter in aging. *Neuroimage*, 43(3), 470-7..
- Vogel**, E.K., Machizawa, M.G., 2004. Neural activity predicts individual differences in visual working memory capacity. *Nature*.428,748--751.
- Walhovd**, K.B., Westlye, L.T., Amlie, I., Espeseth, T., Reinvang, I., Raz, N., Agartz, I., Salat, D.H., Greve, D.N., Fischl, B., Dale, A.M., Fjell, A.M.,2011. Consistent neuroanatomical age-related volume differences across multiple samples. *Neurobiol Aging*. 32(5),916-32.
- Westlye**, L.T., Walhovd, K.B., Dale, A.M., Bjørnerud, A., Due-Tønnessen, P., Engvig, A., Grydeland, H., Tamnes, C.K., Østby, Y., Fjell, A.M., 2010. Life-span changes of the human brain white matter: diffusion tensor imaging (DTI) and volumetry. *Cereb Cortex*.,20(9),2055-68.
- Wiegand**, I., Töllner, T., Dyrholm, M., Müller, H. J., Bundesen, C., & Finke, K. (2014a). Neural correlates of age-related decline and compensation in visual attention capacity. *Neurobiol. Aging*, 35, 2161–2173.
- Wiegand**, I., Töllner, T., Habekost, T., Dyrholm, M., Müller, H. J., & Finke, K. (2014b). Distinct neural markers of TVA-based visual processing speed and short-term storage capacity parameters. *Cereb. Cortex*, 24, 1967-1978.

- Wiegand, I.**, Lauritzen, M.J., Osler, M., Mortensen, E.L., Rostrup, E., Rask, L., Richard, N., Horwitz, A., Benedek, K., Vangkilde, S., Petersen, A., 2018. EEG correlates of visual short-term memory in older age vary with adult lifespan cognitive development. *Neurobiol. Aging*, 62, 210-220.
- Wozniak, J.R., Lim, K.O.**, 2006. Advances in white matter imaging: a review of in vivo magnetic resonance methodologies and their applicability to the study of development and aging. *Neurosci Biobehav Rev.* 2006, 30(6), 762-74.
- Zahr, N.M., Rohlfsing, T., Pfefferbaum, A., Sullivan, E.V.**,2009. Problem solving, working memory, and motor correlates of association and commissural fiber bundles in normal aging: A quantitative fiber tracking study. *Neuroimage*. 44,1050–1062.
- Zhang, Y., Du, A.T., Hayasaka, S., Jahng, G.H., Hlavin, J., Zhan, W., Weiner, M.W., Schuff, N.**, 2010. Patterns of age-related water diffusion changes in human brain by concordance and discordance analysis. *Neurobiol Aging*. 31(11), 1991-2001.
- Zhang, D., Snyder, A. Z., Shimony, J. S., Fox, M. D., & Raichle, M. E.** 2010. Noninvasive functional and structural connectivity mapping of the human thalamocortical system. *Cereb Cortex*, 20(5), 1187-1194.

## 3.7 SUPPLEMENTARY MATERIAL

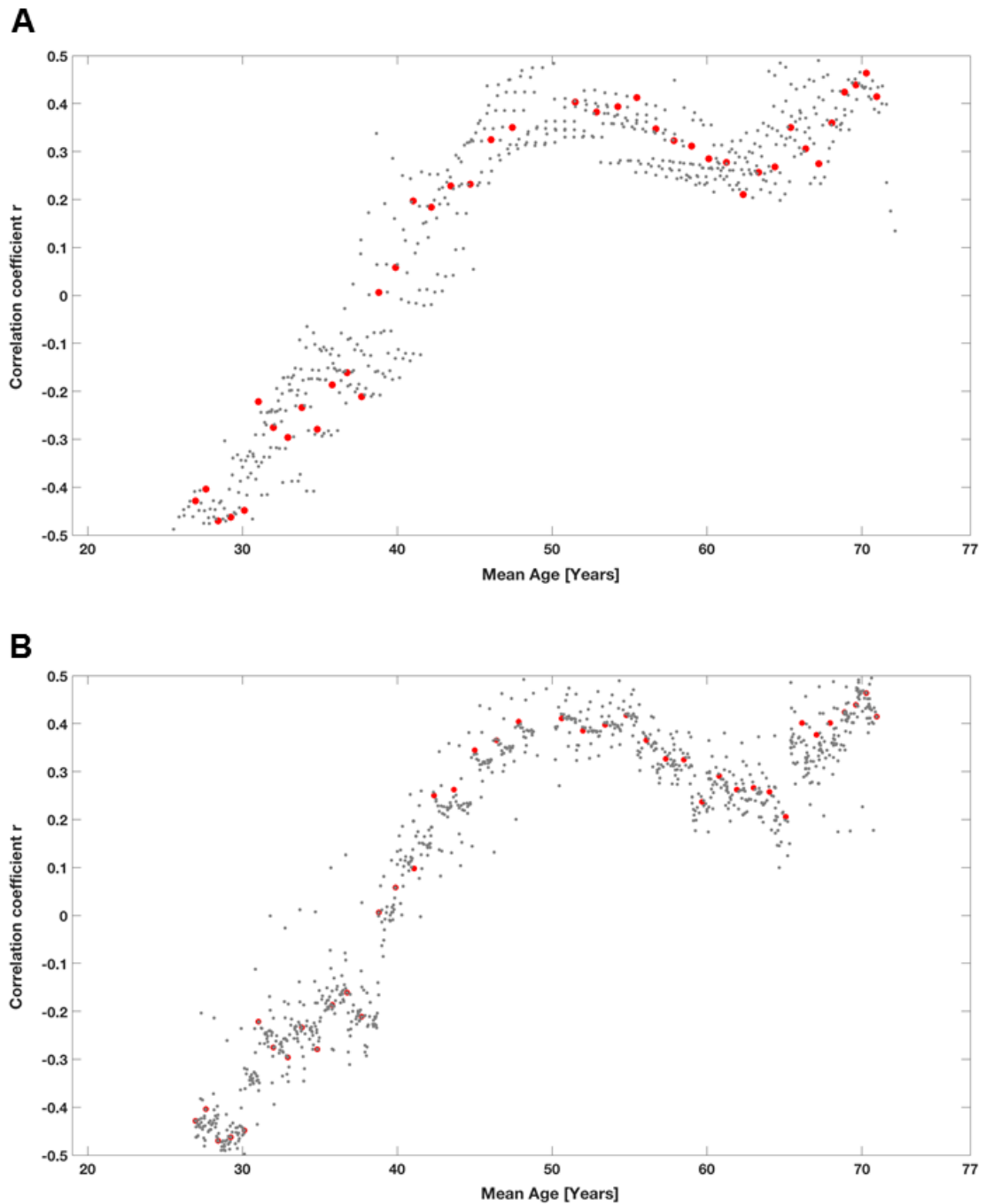


**Figure S1: Bootstrapping analyses showing the reliability of the sliding window analysis. A:** representation of the sliding window analysis for different window sizes, varying from 20 to 35. **B:** to test whether outliers might have influenced the results, the sliding window analysis was repeated, by analyzing a subsample, excluding a different participant in each run.

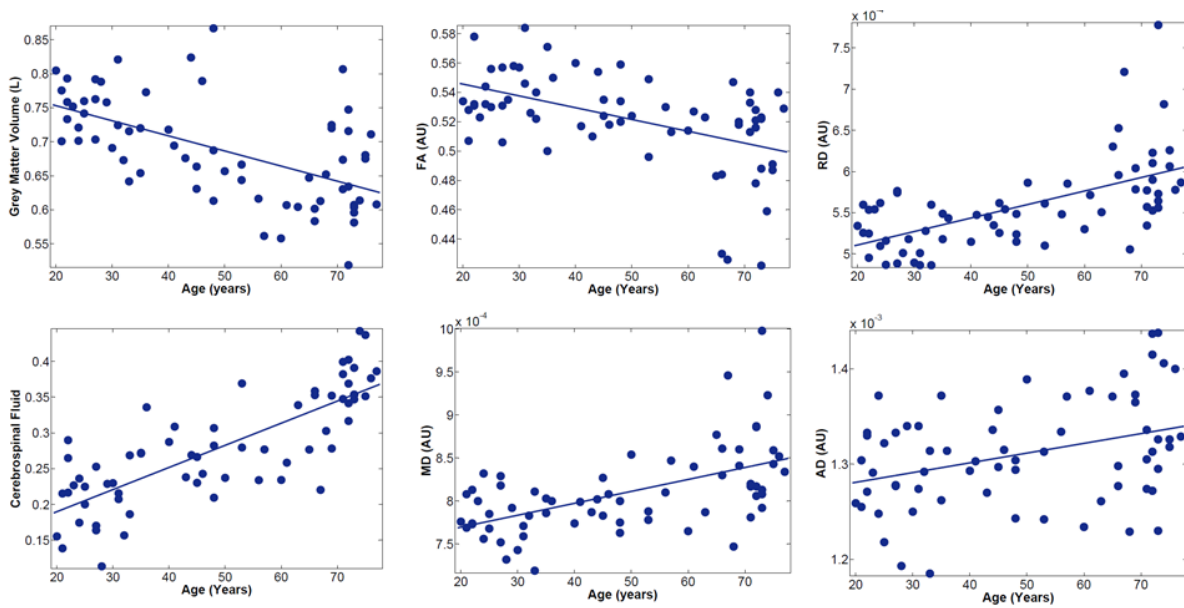


**Figure S2: Structural and diffusion alterations in aging.** The first column shows graphs representing the grey matter volume and cerebrospinal fluid volume, respectively, as a function of age. In the second and third column, linear plots of white matter microstructure measures as a function of age are shown.

## 4 STUDY III:

### IMPAIRED VISUAL SHORT-TERM MEMORY CAPACITY IS DISTINCTIVELY ASSOCIATED WITH STRUCTURAL CONNECTIVITY OF THE POSTERIOR THALAMIC RADIATION AND THE SPLENIUM OF THE CORPUS CALLOSUM IN PRETERM-BORN ADULTS

This chapter contains a manuscript entitled “Impaired visual short-term memory capacity is distinctively associated with structural connectivity of the posterior thalamic radiation and the splenium of the corpus callosum in preterm-born adults” which has been published in *NeuroImage* in 2017. It also contains unpublished supplementary material used to answer some comments made by a reviewer of this paper. We added it as we believe it shows additional control steps we have taken to ensure the reliability of our findings.

Authors: Aurore Menegaux, Chun Meng, Julia Neitzel, Josef G. Bäuml, , Hermann J.Müller, Peter Bartmann, Dieter Wolke, Afra M. Wohlschläger, Kathrin Finke, Christian Sorg

#### **Contributions:**

The author of this thesis is the first author of this manuscript. K.F. and C.S. designed this study, P.B. and D.W. recruited participants, J.G.B and C.M. acquired imaging data and J.N. behavioral data, A.M. analyzed the data under the supervision of C.M., A.M. drafted the manuscript and. A.M., C.M., H.J.M., P.B., D.W., A.M.W., K.F. and C.S. wrote and revised the manuscript before submission.



Contents lists available at ScienceDirect

NeuroImage

journal homepage: [www.elsevier.com/locate/neuroimage](http://www.elsevier.com/locate/neuroimage)

## Impaired visual short-term memory capacity is distinctively associated with structural connectivity of the posterior thalamic radiation and the splenium of the corpus callosum in preterm-born adults



Aurore Menegaux<sup>a,e,\*</sup>, Chun Meng<sup>b,d,e</sup>, Julia Neitzel<sup>a,b,e</sup>, Josef G. Bäuml<sup>b</sup>, Hermann J. Müller<sup>a,e</sup>, Peter Bartmann<sup>f</sup>, Dieter Wolke<sup>g,h</sup>, Afra M. Wohlschläger<sup>b,d,e</sup>, Kathrin Finke<sup>a,e,i,1</sup>, Christian Sorg<sup>b,c,1</sup>

<sup>a</sup> Department of Psychology, General and Experimental Psychology, Ludwig-Maximilians-Universität München, Leopoldstrasse 13, 80802 Munich, Germany

<sup>b</sup> Department of Neuroradiology, Klinikum rechts der Isar, Technische Universität München TUM, Ismaninger Strasse 22, 81675 Munich, Germany

<sup>c</sup> Department of Psychiatry, Klinikum rechts der Isar, Technische Universität München TUM, Ismaninger Strasse 22, 81675 Munich, Germany

<sup>d</sup> TUM-Neuroimaging Center of Klinikum rechts der Isar, Technische Universität München TUM, Ismaninger Strasse 22, 81675 Munich, Germany

<sup>e</sup> Graduate School of Systemic Neurosciences GSN, Ludwig-Maximilians-Universität München, Biocenter, Großhaderner Strasse 2, 82152 Munich, Germany

<sup>f</sup> Department of Neonatology, University Hospital Bonn, Bonn, Germany

<sup>g</sup> Department of Psychology, University of Warwick, Coventry, United Kingdom

<sup>h</sup> Warwick Medical School, University of Warwick, Coventry, United Kingdom

<sup>i</sup> Hans Berger Department of Neurology, Friedrich-Schiller-University Jena, Germany

### ARTICLE INFO

#### Keywords:

Preterm birth  
Theory of Visual Attention  
Visual short-term memory capacity  
Diffusion tensor imaging  
Posterior thalamic radiation  
Compensation

### ABSTRACT

Preterm birth is associated with an increased risk for lasting changes in both the cortico-thalamic system and attention; however, the link between cortico-thalamic and attention changes is as yet little understood. In preterm newborns, cortico-cortical and cortico-thalamic structural connectivity are distinctively altered, with increased local clustering for cortico-cortical and decreased integrity for cortico-thalamic connectivity. In preterm-born adults, among the various attention functions, visual short-term memory (vSTM) capacity is selectively impaired. We hypothesized distinct associations between vSTM capacity and the structural integrity of cortico-thalamic and cortico-cortical connections, respectively, in preterm-born adults.

A whole-report paradigm of briefly presented letter arrays based on the computationally formalized Theory of Visual Attention (TVA) was used to quantify parameter vSTM capacity in 26 preterm- and 21 full-term-born adults. Fractional anisotropy (FA) of posterior thalamic radiations and the splenium of the corpus callosum obtained by diffusion tensor imaging were analyzed by tract-based spatial statistics and used as proxies for cortico-thalamic and cortico-cortical structural connectivity.

The relationship between vSTM capacity and cortico-thalamic and cortico-cortical connectivity, respectively, was significantly modified by prematurity. In full-term-born adults, the higher FA in the right posterior thalamic radiation the higher vSTM capacity; in preterm-born adults this FA-vSTM-relationship was inverted. In the splenium, higher FA was correlated with higher vSTM capacity in preterm-born adults, whereas no significant relationship was evident in full-term-born adults.

These results indicate distinct associations between cortico-thalamic and cortico-cortical integrity and vSTM capacity in preterm- and full-term-born adults. Data suggest compensatory cortico-cortical fiber re-organization for attention deficits after preterm delivery.

### Introduction

Preterm birth is associated with an increased risk for lasting

impairments in both brain structure and cognitive functions (Baron and Rey-Casserly, 2010; D'Onofrio et al., 2013). Among cognitive functions, attention is particularly affected, as evidenced by pro-

**Abbreviations:** vSTM, visual short-term memory; TVA, theory of visual attention; FA, fractional anisotropy; DTI, diffusion tensor imaging; ROI, region of interest; TFCE, threshold-free cluster enhancement; BLS, bavarian longitudinal study; IQ, intelligence quotient

\* Corresponding author.

E-mail address: [aurore.menegaux@psy.lmu.de](mailto:aurore.menegaux@psy.lmu.de) (A. Menegaux).

<sup>1</sup> Finke and Sorg contributed equally to the study.

<http://dx.doi.org/10.1016/j.neuroimage.2017.02.017>

Received 21 September 2016; Accepted 6 February 2017

Available online 07 February 2017

1053-8119/© 2017 Elsevier Inc. All rights reserved.

nounced attentional impairments along childhood following preterm delivery (Anderson and Doyle, 2003; Atkinson and Braddick, 2007). Concerning brain structure, white matter integrity is particularly affected, as demonstrated by widespread changes (e.g., in posterior thalamic radiations, corpus callosum, and superior longitudinal fasciculus) in fractional anisotropy (FA) from infancy (Ball et al., 2012, 2013b) to adulthood (Vangberg et al., 2006; Skranes et al., 2007; Constable et al., 2008; Eikenes et al., 2011; Mullen et al., 2011; Meng et al., 2015; for review see Ment et al., 2009; Pandit et al., 2013).

As concerns lasting impairments in attention and their relation with lasting brain changes after preterm delivery, a recent study has linked selective attentional deficits in preterm-born adults to functional connectivity changes of intrinsic posterior brain networks (Finke et al., 2015). Attention parameters were estimated based on the computational Theory of Visual Attention (TVA; Bundesen, 1990). In TVA, visual processing is conceived as a parallel-competitive race of visual objects towards selection, that is, representation in a capacity-limited visual short-term memory (vSTM) store. Bottom-up and top-down biases determine the relative ‘attentional weights’ for objects. The probability of selection is determined by an object’s processing rate  $v$ , which depends on its attentional weight ( $w$ ), sensory effectiveness, and the capacity of the vSTM store (if the store is filled, the selection process terminates). By means of TVA model-based fitting of performance accuracy in simple psychophysical tasks (requiring verbal report of briefly presented letter arrays), separable, independent latent parameters underlying an individual’s performance can be extracted. Finke et al. (2015) showed that specifically parameter vSTM capacity  $K$ , which reflects the number of items that can be categorized in parallel and transferred to vSTM (Cowan, 2001; Luck and Vogel, 1997), was reduced in preterm- compared to term-born adults, while other parameters, such as visual processing speed  $C$  and attentional selectivity measures, were preserved. Of note, in the preterm group, vSTM capacity was linked with brain changes in intrinsic networks in a compensatory way: the more pronounced the functional connectivity changes of bilateral posterior brain networks (e.g., dorsal attention network), the higher the individual’s vSTM capacity. Similar evidence for compensatory activation following preterm birth comes from a number of other studies (Gimenez et al., 2005; Peterson et al., 2002; Nosarti et al., 2006). For example, Froudist-Walsh et al. (2015) found changes in task-related activity during an N-back task, in which adults who suffered perinatal brain injury exhibited reduced activation in frontoparietal areas, though without differing from controls in performance level. Accordingly, Finke et al. (2015) took their results to suggest that brain alterations following prematurity promote the compensatory recruitment of alternative brain networks. It has been shown that, beyond local activity, functional connectivity depends on underlying white matter structural connectivity (Honey et al., 2009; Hagmann et al., 2008; Kringelbach et al., 2014), which provides a backbone for the coherence of ongoing activity fluctuations. Thus, the question arises whether and how the underlying white matter integrity is linked to vSTM capacity in preterm-born adults. The current study focuses on this question.

According to a neural interpretation of TVA (the Neural TVA, NTVA), visual brain regions, such as thalamus, occipital cortices and posterior parts of temporal and parietal cortices, and their inter-regional structural connectivity subserves vSTM processes in healthy individuals (Bundesen et al., 2005). In line with, for instance, Hebb (1949), it is assumed that when visual objects enter vSTM, the activation of those neurons within posterior parts of the cortex that are initially coding and representing these winner objects is sustained and re-activated in a feedback loop. The thalamus and particularly the thalamic reticular nucleus, where the vSTM map of objects is assumed to be located, are suggested to play a key role in gating these thalamocortical feedback loops (Magen et al., 2009; Todd and Marois, 2004; Xu and Chun, 2006). Given the critical role of such recurrent feedback loop activity, the integrity of cortico-thalamic and

cortico-cortical white matter circuits of the thalamo-cortical systems would be expected to be decisive for vSTM capacity (Bundesen et al., 2005). Although Habekost and Rostrup (Habekost and Rostrup, 2007) observed specific alterations in the TVA-based estimates of vSTM capacity following posterior white matter damage, the specific role of posterior cortico-thalamic and cortico-cortical fiber tracts that is implied in NTVA remains to be documented.

As demonstrated by animal studies of prematurity, **preterm** birth leads to a disturbed brain maturation by impairing the maturation of subplate neurons, GABAergic interneurons, oligodendrocytes and astrocytes (Dean et al., 2013; Komitova et al., 2013). In particular, the premyelinating oligodendrocytes affected by hypoxia or ischemia lead to a loss or a maturational delay of their cellular targets resulting in hypomyelination or axonal damage (Ment et al., 2009). This is reflected in preterm infants by the absence of normal maturational increase in FA (Miller 2002). Correspondingly, cortico-thalamic and cortico-cortical tracts of the thalamo-cortical system are substantially re-organized after preterm delivery (Ball et al., 2012, 2013a). Indeed, using tract-based spatial statistics, Ball and colleagues have provided evidence that preterm birth altered thalamocortical development through reduction of white matter microstructure and changes in thalamic volume (Ball et al., 2012). Using a similar methodology, Meng and colleagues found lasting changes in white matter microstructure in preterm-born adults, associated with both subcortical grey matter volume reduction and lower IQ (Meng et al., 2015). Using probabilistic tractography, Ball et al. (2013) documented a reorganization of connectivity after preterm birth with reduced cortico-thalamic connectivity and increased local cortico-cortical connectivity in infants. These findings suggest a distinct trajectory of brain organization in preterm-, as compared to full-term-, born individuals, with some changes, particularly in cortico-cortical connectivity, potentially reflecting compensation.

Based on (i) such complex and permanent patterns of brain reorganization, (ii) on the altered relationship between vSTM capacity and functional connectivity in the posterior brain (Finke et al., 2015), and (iii) on the fact that functional connectivity depends on underlying structural connectivity (e.g. Honey et al., 2009), we hypothesized that the linkage of microstructure of posterior brain circuits with vSTM capacity might be changed, too, in preterm-, as compared to full-term-, born adults. Furthermore, we assumed that the way these relationships are changed might differ between cortico-thalamic fibers microstructure on the one hand and cortico-cortical fibers on the other. Specifically, (i) with respect to cortico-thalamic tracts microstructure in full-term-born adults, based on the NTVA thalamo-visual cortex vSTM loop model, we expected greater integrity of tracts connecting thalamus and posterior cortex, that is, of the posterior thalamic radiations, to be associated with higher vSTM capacity. Accordingly, we used the posterior thalamic radiations as a proxy for cortico-thalamic structural connectivity. Given profound changes of cortico-thalamic connectivity in preterm-born adults (Meng et al., 2015), this relationship could be changed in the preterm group. (ii) Based on findings of changes in cortico-cortical connectivity in preterm-born infants (Ball et al., 2014) and compensatory functional connectivity changes in bilateral posterior intrinsic networks in preterm-born adults (Finke et al., 2015), we hypothesized that the role of cortico-cortical structural connectivity for vSTM capacity might also be changed (i.e., be potentially enhanced) for preterm- as compared to term-born adults. We analyzed FA in a main cortico-cortical fiber tract, the splenium of the corpus callosum, as a simple proxy for cortico-cortical connectivity. The corpus callosum is classically regarded as important for compensatory functional recovery following brain damage, as it provides an interhemispheric connection to contralateral homologous brain systems (Bartolomeo and de Schotten, 2016). We focused on the splenium of the corpus callosum as it supports interactions between bilateral posterior visual intrinsic networks. Parallel activation of homologous vSTM systems has been shown to improve vSTM storage

in healthy individuals (Delvenne and Holt, 2012; Umemoto et al., 2010) and, notably, also to enhance parameter  $K$  in TVA-based paradigms (Kraft et al., 2013, 2015). FA in the splenium of the corpus callosum has been shown to be related to the degree of such a bilateral processing advantage (Davis and Cabeza, 2015). Thus, especially in preterm-born adults, FA of the corpus callosum might be critical for a potential compensatory hemispheric interaction between parallel vSTM storage systems with relatively independent resources in both hemispheres (e.g., Sereno and Kosslyn, 1991).

In order to test these hypotheses, 28 pre- and 27 full-term born young adults were assessed by both diffusion tensor imaging (DTI) and a TVA-based whole-report task. To sample white matter structural connectivity, FA of water diffusion was investigated using tract-based spatial statistics in the mentioned regions of interest (ROD), specifically, posterior thalamic radiations (proxy for cortico-thalamic connectivity) and the splenium of the corpus callosum (proxy for cortico-cortical connectivity). Parameter  $K$ , representing vSTM capacity in TVA, was estimated based on whole report of briefly presented letter arrays. White matter FA values of both ROIs, respectively, were explored in relation to vSTM capacity and prematurity using ANCOVA.

## Material and methods

### Participants

#### Sample description

Participants were recruited from the Bavarian Longitudinal Study (BLS) (Riegel et al., 1995; Wolke and Meyer, 1999), which investigates a geographically defined whole-population sample of neonatal at-risk children and healthy term controls. 28 preterm-born and 27 term-born young adults were recruited, all born between January 1985 and March 1986 (25 to 27 years old) (for demographics and clinical data, see Table 1). Participants represent a sub-sample of a previous study of our group, for which DTI data were assessed beyond attention assessment (Finke et al., 2015). While the previous study aimed at answering which particular attention functions are impaired in preterm-born adults (i.e. vSTM capacity), the current study focused on the underlying structural connectivity of vSTM capacity deficits. Full-term- and preterm-born participant groups were matched in terms of sex, age, visual acuity, socioeconomic background, and maternal age. Exclusion criteria for participating in the study were non-correctable reduction of sight in either eye and the presence of psychiatric disorders that are known to affect attention, such as ADHD, autism, schizophrenia, or major depression. All participants had normal or corrected-to-normal vision and were not color-blind. Participants were examined at the Department of Neuroradiology, Klinikum rechts der Isar, Technische

Universität München, Germany. The study was approved by the local ethics committee of the Klinikum Rechts der Isar. All participants provided informed consent to be entered in the study.

#### Measure of prematurity

Gestational age was estimated from maternal reports of the last menstrual period and serial ultrasounds during pregnancy. When the two measures differed by more than two weeks, clinical assessment using the Dubowitz method was applied (Dubowitz et al., 1970).

#### Cognitive evaluation

All participants were tested for global cognitive functioning at the age of 26 years by trained psychologists. This included a short version of the German Wechsler Adult Intelligence scale-III (WAIS-III) (Von Aster et al., 2006), permitting computation of Full Scale Intelligence Quotient (IQ).

#### Theoretical TVA framework and TVA-based behavioural assessment of vSTM capacity

##### Computational TVA framework

In TVA, visual processing is conceived as a race: objects are processed in parallel and compete for being selected, that is, represented in vSTM for conscious report. vSTM capacity  $K$  quantifies the number of items that can be categorized and selected in parallel and transferred into the vSTM store (Cowan, 2001; Habekost and Starrfelt, 2009; Luck and Vogel, 1997; Sperling, 1960). Note that three additional parameters, visual processing speed  $C$ , minimum effective exposure duration (visual threshold)  $t_0$ , and effective additional exposure duration in unmasked displays  $\mu$ , were also determined. While not being in the focus of the present study, these parameters play a role for valid estimation of parameter vSTM capacity  $K$ . All parameters are obtained from the fitting of the accuracy of letter report across the different conditions of a so-called whole-report task. For a formal description of TVA and the TVA equations, maximum likelihood model fitting and software, see Kyllingsbæk (2006).

##### Assessment procedure

As described previously in Finke et al., (Finke et al., 2015), we used a whole-report task (conducted in a dimly lit room). Stimuli were presented briefly to participants on a 17 in. screen (1024×1280 pixel resolution, 60 Hz refresh rate). A chin rest was used to maintain viewing distance at 50 cm. Participants were instructed to fixate a central white cross (0.3° visual angle) presented for 300 ms. Then, after a gap of 100 ms, red and/or green letters (0.5° high×0.4° wide) were briefly presented on a black background. Three different individual

**Table 1**  
Sample characteristics.

|              | Preterm group |           |              | Full-term group |           |              | Statistical comparison |
|--------------|---------------|-----------|--------------|-----------------|-----------|--------------|------------------------|
|              | n=26          |           |              | n=21            |           |              |                        |
|              | <i>M</i>      | <i>SD</i> | <i>Range</i> | <i>M</i>        | <i>SD</i> | <i>Range</i> |                        |
| gender (f/m) | 14/12         |           |              | 10/11           |           |              | p=.67                  |
| age (years)  | 26.6          | ± 0.53    | 25.8–27.6    | 26.7            | ± 0.54    | 25.9–27.9    | p=.64                  |
| GA (weeks)   | 30.6          | ± 2.43    | 27–36        | 39.6            | ± 0.95    | 38–42        | <b>p &lt; .01</b>      |
| IQ           | 93.8          | ± 9.62    | 72–117       | 101             | ± 11.3    | 77–117       | <b>p=.03</b>           |
| $t_0$        | 7.31          | ± 15.2    | 0–53.8       | 1.49            | ± 2.85    | 0–9.42       | p=.10                  |
| $C$          | 26.3          | ± 190.1   | 9.8–53.3     | 27.1            | ± 8.11    | 17.2–47.5    | p=.76                  |
| $\mu$        | 98.3          | ± 40.8    | 49–220       | 99.8            | ± 32.1    | 36–194       | p=.89                  |
| $K$          | 2.76          | ± 0.35    | 1.98–3.83    | 3               | ± 0.43    | 2.47–3.89    | <b>p=.02</b>           |

#### Abbreviations:

m: male, f: female; GA: gestational age; IQ: Wechsler Intelligence Test for Adults at 26 years of age,  $t_0$ : visual threshold in ms,  $\mu$ : duration of iconic memory in ms,  $C$ : visual processing speed,  $K$ : visual short-term memory storage capacity. Statistical comparisons: gender: chi-squared statistics; age, IQ: t-tests;  $K$ ,  $C$ ,  $t_0$ ,  $\mu$ : permutation tests; GA: nonparametric Mann-Whitney-U-test.

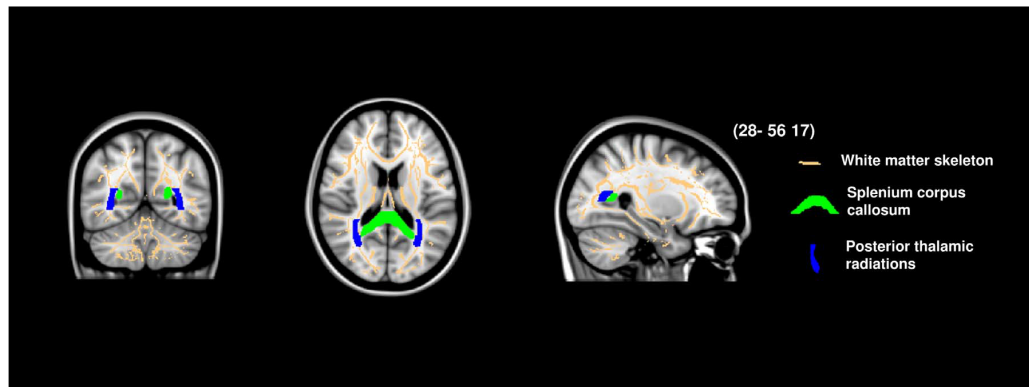


**Fig. 1. Regions of interest (ROI) for visual short term memory capacity.** Coronal, axial, and sagittal views illustrating the localization of posterior thalamic radiations and the splenium of the corpus callosum superimposed on the T1-weighted brain image of MNI152 structural standard template and group-generated white matter skeleton. Brown color indicates the common skeleton over preterm- and full-term born groups. Blue color shows bilateral posterior thalamic radiations and green represents the splenium of the corpus callosum.

letter exposure durations were determined in a practice session prior to the experiment proper to meet a set criterion value (i.e., about one letter named correctly at the intermediate, unmasked exposure duration). The letters were randomly chosen from a pre-specified set (“ABEFHJKLMNPRSTWXYZ”), with the same letter appearing only once on a given trial. Each participant received the same displays in the same sequence. Stimuli were either masked at the end of the exposure duration or unmasked. In unmasked conditions, the effective exposure durations are prolonged by several hundred milliseconds due to “iconic” memory buffering. Participants were asked to identify and verbally report as many stimuli as possible. They were free to report individual letters in any order they liked, without stress on response speed. The experimenter entered the responses on the keyboard. The total number of trials was 192, separated into blocks of 48 trials each. Within each block, the different trial types were presented equally often in randomized order. For more details regarding the assessment procedure see Kyllingsbæk (2006).

#### Statistical analysis

As  $K$  was not normally distributed, we used a permutation test with  $10^5$  iterations to confirm that  $K$  was lower in the preterm group than in the term group, as shown previously by Finke et al. (2015). In the same way, a permutation test was used to assess between-group differences in  $C$ ,  $t_0$ , and  $\mu$ .

#### Diffusion imaging and data analysis

##### Image acquisition

Both T1 and diffusion-weighted imaging data were obtained using a 3 T Philips scanner with an 8-channel phased-array head coil. A whole-head, high-resolution T1-weighted image was acquired using a magnetization-prepared rapid acquisition gradient echo sequence with the following parameters: echo time (TE)=3.9 ms, repetition time (TR)=7.7 ms, flip angle=15°, field of view=256×256 mm<sup>2</sup>, matrix=256×256, 180 sagittal slices, slice thickness=1 mm, and 0 mm inter-slice gap, voxel size=1×1×1 mm<sup>3</sup>. Diffusion images were acquired using a single-shot spin-echo echo-planar imaging sequence, resulting in one non-diffusion weighted image ( $b=0$  s/mm<sup>2</sup>) and 32 diffusion weighted images ( $b=1000$  s/mm<sup>2</sup>, 32 non-collinear gradient directions) covering whole brain with: echo time (TE)=47 ms, repetition time (TR)=20,150 ms, flip angle=90°, field of view=224×224 mm<sup>2</sup>, matrix=112×112, 75 transverse slices, slice thickness = 2 mm, and 0 mm inter-slice gap, voxel size=2×2×2 mm<sup>3</sup>.

##### Quality Check

Each image was visually checked by three independent raters (C.M., C.S., A.M.) prior to further processing (see also Meng et al., 2015). Beyond visual inspection of raw data, we also used the fitting residuals (the sum-of-squared-error maps generated by DTIFIT) to identify data corrupted by artifacts. Artifacts include motion-induced artifacts and insufficient fat suppression (ghosting) artifacts. DTI data were classified as data with none, moderate, and severe visible artifacts, respectively. Only data without artifacts were included in the study, that is, out of the 28 preterm- and 27 term-born participants, seven subjects were excluded due to ghost artifacts and one subject due to a motion artifact. Our final cohort consisted of 26 preterm- and 21 term-born young adults.

##### Preprocessing

Diffusion data preprocessing was performed using FMRIB Diffusion Toolbox in the FSL software ([www.fmrib.ox.ac.uk/fsl](http://www.fmrib.ox.ac.uk/fsl)) after converting data from DICOM to niftii format by using dcm2nii as described in previous work (Meng et al., 2015). All diffusion-weighted images were first corrected for eddy current and head motion by registration to b0 image. Using the Brain Extraction Tool (BET), skull and non-brain tissue were removed. The tensor model was then applied voxel by voxel to obtain FA maps.

##### Skeletonized FA generation

Voxel-wise statistical analysis of the FA data was carried out using Tract Based Spatial Statistics (TBSS). All subjects' FA were non-linearly registered and aligned to the Montreal Neurological Institute Standard Space (MNI 152). Next, the mean FA image of all subjects was created and used to generate an across-all-subjects skeleton, which represents the white matter tracts common to all subjects. We thresholded the skeleton for FA > 0.2 to keep the main white matter tracts only and then projected each subject's FA image onto the skeleton to obtain individual FA maps.

##### ROI generation

We used the whole-brain skeleton to create our ROIs (Fig. 1). Using `fsstats` command, we extracted the splenium of the corpus callosum as well as bilateral posterior thalamic radiations including optic radiations separately, from the JHU-ICBM-DTI-81 white matter labels atlas (Mori et al., 2005). Using `fsmaths` command, we first combined the splenium of the corpus callosum with the FA skeleton obtained previously to obtain a splenium of the corpus callosum skeleton mask. We repeated the process using both posterior thalamic radiations instead of the splenium of the corpus callosum to obtain a posterior thalamic radiation skeleton mask.

### Statistical analysis

General linear model and nonparametric permutation testing (5000 random permutations) were adopted to perform statistical analyses on the ROI's FA using FSL's *randomize* script (<http://fsl.fmrib.ox.ac.uk/fsl/fslwiki/randomize/>) (Anderson and Robinson 2001). The design matrix we used was representative of an ANCOVA with main effects of group and vSTM storage parameter  $K$  and the interaction effect of group and  $K$  on FA. The statistical threshold was set at  $P_{FWE} < 0.05$ , with multiple comparison correction threshold-free cluster enhancement (TFCE) (Smith and Nichols, 2009). In order to control for the influence of general cognitive performance, we added in a second analysis IQ as a covariate-of-no-interest in the ANCOVA model. In order to visualize the association between vSTM storage  $K$  and FA in each group separately, we used *fslmeans* command to extract for each subject a mean FA value from TBSS significant interaction voxels of each ROI. Then we plotted each individual FA value and its vSTM storage  $K$  score, and applied linear fitting and Spearman correlation in each group separately using Matlab (MathWorks). Group differences in mean FA were analysed by ANCOVA including Full-scale IQ as additional co-variate using SPSS statistics package version 21 (IBM).

## Results

### VSTM capacity is reduced in preterm-born adults

As previously reported by Finke et al. (2015), vSTM capacity  $K$  was significantly lower in the preterm- compared to the full-term-born group ( $p=0.023$ ) (see Table 1). Also in line with Finke et al. (2015), visual processing speed ( $C$ ) and minimum effective exposure duration ( $t0$ ) did not differ significantly between the two groups. There was also no difference for the parameter of no interest, effective additional exposure duration in unmasked displays ( $\mu$ ).

### Preterm birth modulates the relationship between vSTM capacity and FA in posterior thalamic radiation

To investigate whether there was a distinct association between vSTM capacity  $K$  and cortico-thalamic fibers' integrity in preterm- and full-term-born adults, we performed a voxel-wise analysis of the interaction between prematurity (preterm-born group, term-born group) and vSTM capacity  $K$  on posterior thalamic radiation FA values by means of ANCOVA modeling and permutation testing (Fig. 2). We found a significant interaction between prematurity and vSTM capacity  $K$  on FA in a cluster of voxels (264 voxels) in the posterior part of the right posterior thalamic radiation (Fig. 2a,  $P_{FWE} < 0.05$  TFCE corrected).

**Control analyses.** (i) To assess whether the interaction between prematurity and vSTM capacity  $K$  arises independently of general cognitive performance, we repeated the interaction analysis including Full-scale IQ as additional co-variate of no interest (Fig. 2b). The interaction effect remained significant, indicating the specificity of the distinct link between cortico-thalamic fibers' FA and vSTM capacity  $K$  across preterm- and full-term-born adults. To examine the direction of this interaction, we extracted the average FA value within that cluster separately for the term-born and the preterm-born group, plotted it and correlated it to vSTM capacity  $K$ , using Spearman correlation. In full-term-born adults, the association between vSTM capacity  $K$  and FA was significantly positive ( $\rho=0.57$ ;  $p < 0.01$ ), whereas in preterm-born subjects it was significantly negative ( $\rho=-0.49$ ;  $p=0.01$ ) (Fig. 2c). (ii) To examine FA group differences for the relevant (interaction) cluster, we tested for the main effect of prematurity. We found a significant main effect of prematurity on mean FA, with FA being reduced in preterm-born adults ( $p < 0.016$ ), which is in line with previous findings (Meng et al., 2015). We did not find any significant difference in mean FA between groups over the whole tract ( $p=0.34$ ).

### Preterm birth modulates the relationship between vSTM capacity and FA in the splenium of the corpus callosum

To investigate the distinct association between vSTM capacity  $K$  and cortico-cortical fibers' integrity in preterm- and full-term-born adults, we performed a voxel-wise analysis of the interaction between prematurity and  $K$  on splenium FA values by using the same approach as for the posterior thalamic radiations (Fig. 3). We found a significant interaction between prematurity and  $K$  on FA in two clusters of voxels (354 voxels in total) within the posterior part of the splenium (Fig. 3a,  $P_{FWE} < 0.05$  TFCE corrected).

**Control analyses:** (i) To test whether the interaction between prematurity and vSTM capacity  $K$  occurs independently of general cognitive performance, we repeated the ANCOVA-based interaction analysis including Full-scale IQ as additional co-variate of no interest. We found a trend towards significance for the interaction between  $K$  and prematurity (Fig. 3b,  $P_{FWE} < 0.06$ , TFCE corrected), suggesting specificity of the distinct link between cortico-cortical fibers' FA and vSTM capacity across preterm- and full-term-born adults. To examine the direction of interaction, we extracted the average FA value within that cluster separately for the term-born and the preterm-born group, plotted it and correlated it to vSTM capacity  $K$ , using Spearman correlation. This showed that within these clusters, average FA was significantly positively associated with vSTM capacity  $K$  in the preterm-born group ( $\rho=0.51$ ;  $p < 0.01$ ), while no significant association was found in the term-born group ( $\rho=-0.14$ ;  $p=0.56$ ) (Fig. 3c). (ii) To examine FA group differences for the relevant (interaction) cluster, we tested for the main effect of prematurity. We found a significant main effect of prematurity on mean FA, with FA being reduced in preterm-born adults ( $p=0.046$ ), which is in line with previous findings (Meng et al., 2015). We did not find any significant difference in mean FA between groups over the whole tract ( $p=0.59$ ).

## Discussion

The present study tested the hypothesis that cortico-cortical and cortico-thalamic fibers' integrity of posterior brain circuits would be distinctively linked with vSTM capacity in preterm-born, in comparison with full-term-born, adults. Diffusion tensor imaging DTI and TVA-based whole-report were applied in preterm- and full-term-born adults. We found that prematurity modulated the relationship between vSTM capacity and cortico-cortical and cortico-thalamic fibers' microstructure, respectively. For cortico-thalamic connectivity we found a reversed relationship between FA and vSTM storage capacity in preterm- compared to full-term born adults: Full-term-born adults with higher FA in a posterior part of the right posterior thalamic radiation exhibited higher vSTM capacity, while a significantly negative relationship was revealed for preterm-born adults. For cortico-cortical connectivity, too, we found a change in the FA-vSTM-relationship between full-term and preterm-born adults: preterm-born adults with higher FA in a right part of the splenium exhibited higher vSTM capacity, while no significant relationship was evident for full-term-born adults. This pattern of results provides first evidence of distinct structural connectivity underlying vSTM capacity in preterm-born adults compared to term-born individuals. The data suggest that, in preterm-born adults, the re-organization of cortico-cortical and cortico-thalamic tracts is differentially linked with vSTM capacity, and that the splenium in particular plays a role in compensatory re-organization.

### Prematurity modulates the relationship between vSTM capacity and posterior thalamic radiation microstructure

Our hypothesis of a distinct link of posterior brain white matter with vSTM capacity  $K$  in preterm-born, in comparison with full-term-born, adults was supported by the finding that the association between

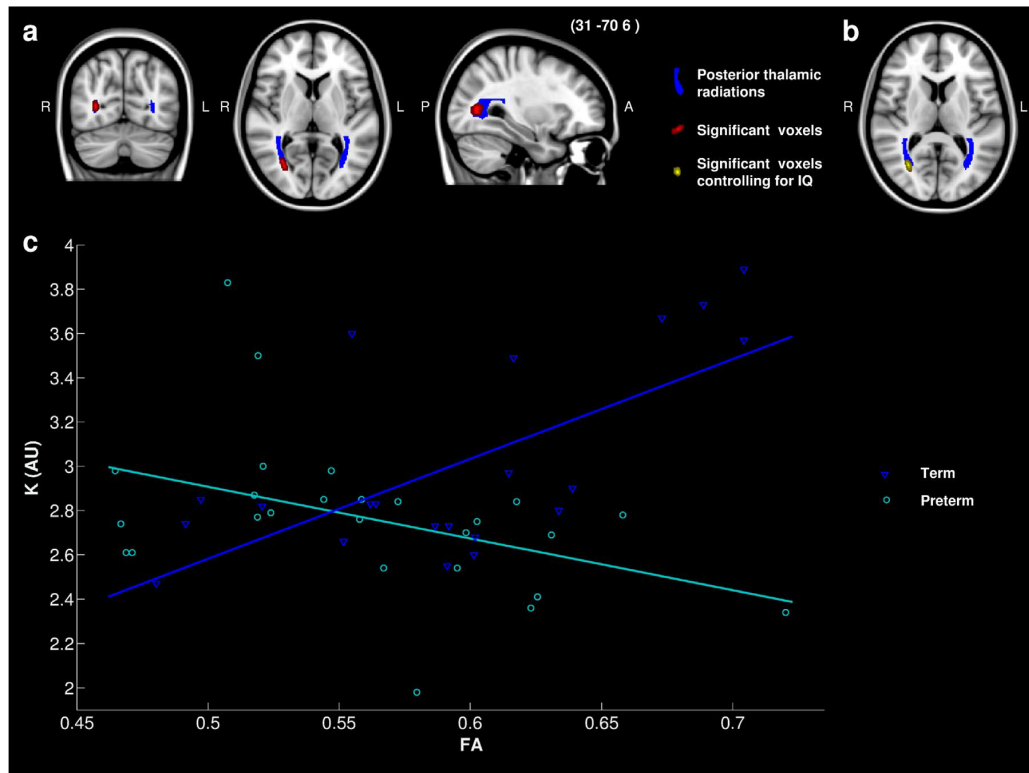


**Fig. 2. Prematurity modulates the association between vSTM capacity and FA in posterior thalamic radiation.** **a)** In the upper panel, coronal, axial, and sagittal views illustrate a significant interaction between prematurity and vSTM capacity  $K$  on fractional anisotropy (FA). Blue color shows the posterior thalamic radiations. Red color indicates where prematurity and  $K$  significantly interacted on FA (permutation test,  $P < 0.05$ , FWE corrected). MNI coordinates were provided near the sagittal view. **b)** Axial view representing the significant interaction between prematurity and  $K$  on FA. The same color code as in a) is used. Additionally, yellow shows the significant voxels where prematurity and  $K$  interact on FA when controlling for IQ (permutation test,  $P < 0.05$ , FWE corrected). **c)** For visualization of the direction of association in each group separately vSTM capacity  $K$  and averaged FA of significant voxels in a) were illustrated in a scatter plot.

FA in a posterior part of the posterior thalamic radiation and  $K$  differed significantly between the two groups (Fig. 2a). Since this result remained significant even when we controlled for the influence of IQ (Fig. 2c), this interaction appears to be independent of the general level of cognitive ability. Our finding of a significant association of FA in part of the right posterior thalamic radiation of healthy full-term-born adults with TVA parameter  $K$  goes beyond previous TVA-based studies that documented a relationship between posterior white matter microstructure and vSTM capacity  $K$  (Habekost and Rostrup, 2007; Espeseth et al., 2014) and the relevance of right hemispheric tracts in particular (Chechlacz et al., 2015). We establish a role for a specific tract: the posterior thalamic radiation, which connects the thalamus with the posterior visual brain. We thus provide direct empirical support for the NTVA notion of a recurrent thalamo-cortical feedback loop that sustains the activity in visual areas representing objects in vSTM (Bundesen et al., 2005). Our findings are in line with those of Golestani et al. (2014), who reported an association between visual working memory performance in a different paradigm and white matter microstructure of the optic radiations (as part of the posterior thalamic radiations) and posterior thalamus in healthy adults.

Our finding of a negative association in preterm-born adults as well as a reduction of FA in the preterm group indicates that the relationship between this central fiber tract in the thalamo-cortical loop system and vSTM maintenance is compromised after preterm delivery. Prior studies on the role of FA in the posterior thalamus and the optic radiation with visual functions in preterm newborns found that, at this

stage of development, changes in FA are related to impaired visual and attentional functions (Bassi et al., 2008; Groppo et al., 2014). These findings support the assumption that the thalamo-cortical system is critically damaged following preterm birth. Our results are in line with those of Karolis et al. (2016), who reported altered cortico-thalamic loops in adults born preterm. Additionally, our results are in agreement with those of Meng et al. (2015), who reported a widespread reduction of white matter microstructure in preterm-born adults in several tracts (e.g., in the splenium of the corpus callosum) and in cortico-thalamic tracts such as the posterior thalamic radiations. Moreover, although the negative association between  $K$  and FA in the preterm group might seem somewhat surprising, other studies have previously reported different directions of correlations (positive vs. negative) between microstructural properties of WM pathways and individual differences in cognitive abilities (Tuch et al., 2005; Roberts et al., 2010; Chechlacz et al., 2015). Jones et al. (2013), reported that changes in FA can reflect changes in myelination, axon diameter, packing density or membrane permeability, that is, higher FA might not invariably reflect higher integrity of a tract. Nevertheless, the well-known impairment in white matter microstructure demonstrated after preterm birth (Ball et al., 2012; Meng et al., 2015) leads us to suggest that lower FA is associated with lower integrity of the posterior thalamic radiations in preterm-born adults.

This, in summary, provides evidence that posterior thalamic radiations support vSTM capacity in the healthy adult brain. Following preterm delivery, this support is compromised.

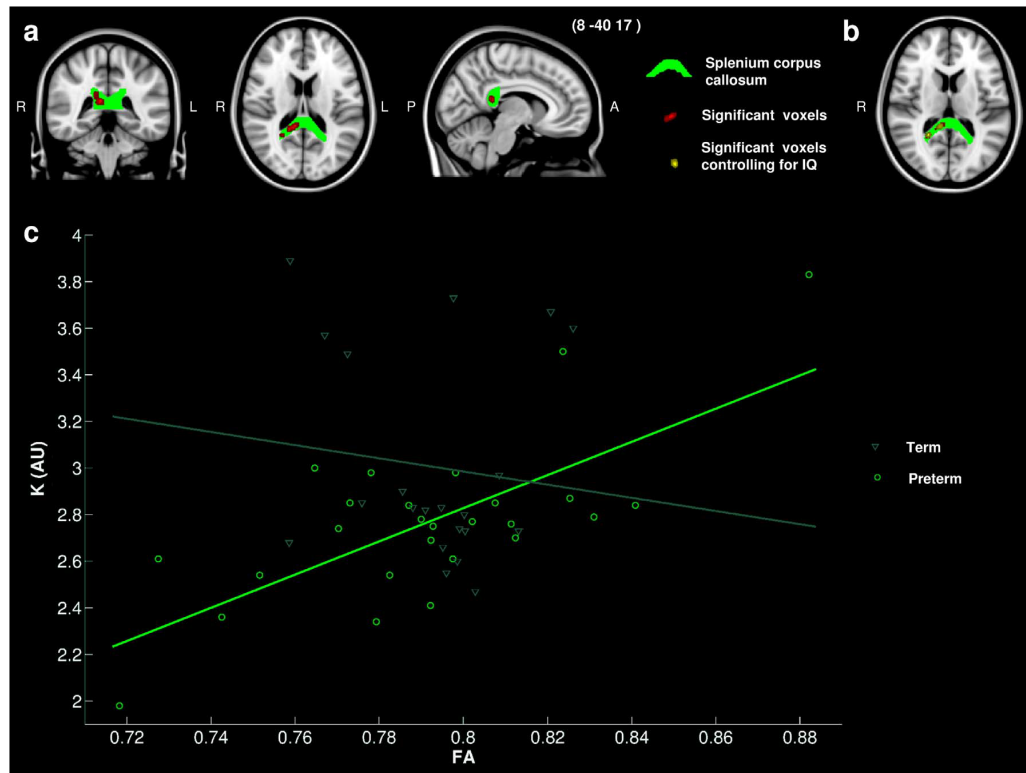


**Fig. 3. Prematurity modulates the association between vSTM capacity and FA in the splenium of the corpus callosum.** **a)** In the upper panel, coronal, axial, and sagittal views illustrate a significant interaction between prematurity and vSTM capacity  $K$  on fractional anisotropy (FA). Green color indicates the splenium of the corpus callosum, red color indicates where prematurity and  $K$  significantly interacted on FA (permutation test,  $P < 0.05$ , FWE corrected). MNI coordinates were provided near the sagittal view. **b)** axial view representing the significant interaction between prematurity and  $K$  on FA. The same color code as in **a)** is used. Additionally, yellow shows the significant voxels where prematurity and  $K$  interact on FA controlling for IQ (permutation test,  $P < 0.05$ , FWE corrected). **c)** For visualization of the direction of association in each group separately, vSTM capacity  $K$  and averaged FA of significant voxels in **a)** were illustrated in a scatter plot.

#### *Prematurity modulates the relationship between vSTM capacity and the splenium of the corpus callosum microstructure*

We found evidence that prematurity increases the relevance of FA in a right part of the splenium of the corpus callosum for vSTM capacity  $K$  (Fig. 3a) as only in the preterm (but not in the full-term) group, higher FA was associated with higher storage capacity  $K$  (Fig. 3b). These interaction results remained near-significant even when we controlled for IQ (TFCE corrected,  $p < 0.06$ ), implying that they are relatively independent of general cognitive abilities. The splenium FA was reduced in preterm-born adults, indicative of compromised microstructure. Thus, the positive correlation between  $K$  and FA suggests that, when the splenium of the corpus callosum is still relatively intact despite preterm delivery, the role of this fiber tract can be reorganized so as to support the vSTM system in a compensatory manner. Our results are in agreement with findings of compensatory intrinsic functional connectivity changes in bilateral posterior brain networks in the same cohort of preterm-born adults (Finke et al., 2015). Finke et al. (2015) found that preterm-born adults with relatively preserved vSTM storage functions exhibited a stronger difference in intrinsic functional connectivity compared to term-born adults. While these results had already implied complex reorganization of intrinsic connectivity in posterior networks, the current results suggest that structural cortico-cortical and cortico-thalamic changes reflect, and support, this reorganization. More specifically, reduced cortico-thalamic connectivity as reflected by a reduction of FA in the posterior thalamic radiation in preterm-born adults is in line with intrinsic functional connectivity changes in typical vSTM networks

previously documented by Finke et al. (2015). Furthermore, the splenium might play an enhanced role in interhemispheric transfer especially between those compensatory bilateral posterior intrinsic networks that had also been documented in the Finke et al. (2015) study. This is in line with a role of the corpus callosum in functional recovery following brain damage by interconnecting homologous brain systems (Bartolomeo and de Schotten, 2016). In preterm-born adults in particular, the splenium might support transfer between otherwise relatively independent vSTM systems in the two hemispheres (e.g., Kraft et al., 2013, 2015), thus providing a means to activate bilateral systems and so increase storage capacity resources. – Taken together, the findings of the two studies provide converging evidence for the proposal that the damaged original, or typical, vSTM network is not functional to the same degree by adults born preterm as compared to full-term-born adults. Furthermore, it appears that especially adults with relatively preserved vSTM storage function might rather employ a compensatory bilateral posterior intrinsic network that at least in part relies on structural connections provided by the splenium of the corpus callosum. Studies on task-related activation during performance of N-back working memory tasks appear to support our proposal: Froudust-Walsh et al. (2015) found that preterm-born adults who suffered perinatal brain injury and who, despite reduced activation in typical frontoparietal working memory areas, displayed relatively normal N-back performance exhibited enhanced activity in the perisylvian cortex. And Daamen et al. (2015) found enhanced deactivations of posterior parietal areas of the default mode network in preterm- compared to term-born adults. Finally, with respect to the relationship between structural connectivity and cognition, and similar to the present

findings, Lindqvist et al. (2011) found a positive correlation between FA in the splenium of the corpus callosum and visual performance in preterm-, but not in full-term-, born adolescents. Importantly, however, in our participants, visual screening prior to inclusion and normal visual thresholds ( $t0$ ) and visual processing speed ( $C$ ) in the TVA-based testing rule out that the reduced vSTM capacity is attributable to more basic visual deficits. Given this, the findings of Lindqvist and colleagues and of our study are complementary in indicating that at least from adolescence and up to adulthood, the splenium of the corpus callosum plays an important role in the compensatory recruitment of structural networks supporting both perception and short-term storage of visual information in preterm-born individuals.

Finally, Ceschin et al. (2015) proposed that thalamo-cortical and interhemispheric connectivity are likely playing a synergistic role in the development of visual functions in preterm-born infants. In line with this assumption, we found a significant modulation of the relationship between vSTM capacity and cortico-cortical and cortico-thalamic connectivity by preterm birth. Thus, in light of our results, it appears likely that a compensatory vSTM network, in preterm-born adults, relies less on cortico-thalamic connectivity (as this “original” network is disrupted in preterm infants) and more on interhemispheric cortico-cortical, that is, the splenium of the corpus callosum, connectivity.

#### Methodological issues and limitations

First, individuals with severe impairments or multiple complications in the initial BLS sample were more likely to be excluded in the initial screening for MRI and visual attention testing (e.g., visual acuity) or they declined to participate in MRI scanning. Accordingly, there is sample bias in the current study towards preterm-born adults with reduced neonatal complications and higher IQ. Therefore, our findings of linked structural connectivity and vSTM capacity, and in particular of ‘compensatory’ splenium integrity, might not hold for preterm-born adults in general. Severely impaired preterm-born individuals might not have the same compensatory mechanisms, or such mechanisms might be disrupted. Further studies on subgroups and longitudinal studies are necessary to clarify this. Second, despite many advantages, the use of TBSS-based analysis of fiber integrity combine with the use of the JHU-ICBM atlas has several limitations, as reported by Bach et al. (2014). Most prominently, skeletonised structural connectivity approaches mainly investigate major fiber pathways across subjects, but it is nevertheless difficult to label the white matter skeleton for specific tracts due to crossing fibers or high inter-subject variability. Indeed, although the ROI we used is labeled posterior thalamic radiation, we cannot exclude the possibility that other tracts might be present within it. Additionally, although TBSS uses nonlinear registration to align each subject’s individual FA to the FMRIB58 FA 1mm standard template, the registration might not be optimal for individuals with large ventricles such as preterm-born adults. Given this, the region-of-interest labels we used to link white matter with vSTM capacity should be evaluated with care. Furthermore, all our results were obtained using TFCE and are thus also influenced by the size of the skeleton sheet structure. Moreover, we found differences in the relationship of FA and vSTM storage only in subparts of both posterior thalamic radiations and the splenium of the corpus callosum. Accordingly, our findings do not indicate that the role of these fiber tracts is, in general, changed; rather, they imply that some fibers of these bundles are restructured following preterm delivery.

Finally, we interpreted higher FA representing higher integrity of the tract. However, as mentioned by Jones et al. (2013), it is under debate whether FA is a sufficient measure of fiber integrity. Given that FA is a measure influenced by axon diameter, axon density, and myelination, interpretations of reduced FA in terms of reduced microstructure should be considered with care.

#### Conclusion

The Splenium and posterior thalamic radiation integrity are distinctively linked with vSTM capacity in preterm-born adults, in comparison with full-term born adults. In particular, the splenium integrity is positively associated with vSTM capacity exclusively in preterm-born subjects, indicative of a specific compensatory re-organization of the vSTM loop system.

#### Acknowledgments

We thank all current and former members of the Bavarian Longitudinal Study Group who contributed to general study organization, recruitment, and data collection, management and subsequent analyses, including (in alphabetical order): Stephan Czeschka, Henning Böcker, Marcel Daamen, Claudia Grünzinger, Christian Koch, Diana Kurze, Sonja Perk, Andrea Schreier, Antje Strasser, Julia Trummer, and Eva van Rossum. We are grateful to the staff of the Department of Neuroradiology in Munich and the Department of Radiology in Bonn for their help in data collection. We are grateful to Petra Redel for organizing the assessment of attentional parameters. Most importantly, we thank all our study participants and their families for their efforts to take part in this study. This study was supported by EU Marie Curie Training Network INDIREA (ITN- 2013–606901 to H.J.M., and K.F.), Deutsche Forschungsgemeinschaft (FI 1424/2-1 to K.F. and SO 1336/1-1 to C.S.), Chinese Scholar Council (CSC, File No: 2010604026 to C.M.), German Federal Ministry of Education and Science (BMBF 01ER0801 to P.B. and D.W., BMBF 01EVO710 to A.M.W., BMBF 01ER0803 to C.S.) and the Kommission für Klinische Forschung, Technische Universität München (KKF 8765162 to C.S.).

#### References

- Anderson, P., Doyle, L.W., 2003. Neurobehavioral outcomes of school-age children born extremely low birth weight or very preterm in the 1990s. *J. Am. Med. Assoc.* 289 (24), 3264–3272.
- Anderson, M.J., Robinson, J., 2001. Permutation tests for linear models. *Austral. N. Z. J. Stat.* 43, 75–88.
- Atkinson, J., Braddick, O., 2007. Visual and visuo-cognitive development in children born very prematurely. *Prog. Brain Res.* 164, 123–149.
- Bach, M., Laun, F.B., Leemans, A., Tax, C.M., Biessels, G.J., Stieltjes, B., Maier-Hein, K.H., 2014. Methodological considerations on tract-based spatial statistics (TBSS). *Neuroimage* 100, 358–369.
- Ball, G., Boardman, J.P., Rueckert, D., Aljabar, P., Arichi, T., Merchant, N., Gousias, I.S., Edwards, A.D., Counsell, S.J., 2012. The effect of preterm birth on thalamic and cortical development. *Cereb. Cortex* 22, 1016–1024.
- Ball, G., Boardman, J.P., Aljabar, P., Pandit, A., Arichi, T., Merchant, N., Rueckert, D., David Edwards, A., Counsell, S.J., 2013a. The influence of preterm birth on the developing thalamocortical connectome. *Cortex J. Devot. Study Nerv. Syst. Behav.* 49, 1711–1721.
- Ball, G., Srinivasan, L., Aljabar, P., Counsell, S.J., Durighel, J., Hajnal, J.V., Rutherford, M.A., Edwards, A.D., 2013b. Development of cortical microstructure in the preterm human brain. *Proc. Natl. Acad. Sci. USA* 110, 9541–9546.
- Ball, G., Aljabar, P., Zebari, S., Tusor, N., Arichi, T., Merchant, N., Robinson, E.C., Ogunjipe, E., Rueckert, D., Edwards, A.D., Counsell, S.J., 2014. Rich-club organization of the newborn human brain. *Proc. Natl. Acad. Sci. USA* 111 (20), 7456–7461.
- Baron, I.S., Rey-Casserly, C., 2010. Extremely preterm birth outcome: a review of four decades of cognitive research. *Neuropsychol. Rev.* 20, 430–452.
- Bartolomeo, P., de Schotten, M.T., 2016. Let thy left brain know what thy right brain doeth: inter-hemispheric compensation of functional deficits after brain damage. *Neuropsychologia*, (S0028-3932(16)30215-9). 10.1016.
- Bassi, L., Ricci, D., Volzone, A., Allsop, J.M., Srinivasan, L., Pai, A., Ribes, C., Ramenghi, L.A., Mercuri, E., Mosca, F., Edwards, A.D., Cowan, F.M., Rutherford, M.A., Counsell, S.J., 2008. Probabilistic diffusion tractography of the optic radiations and visual function in preterm infants at term equivalent age. *Brain* 131, 573–582.
- Bundesen, C., 1990. A theory of visual attention. *Psychol. Rev.* 97, 523–547.
- Bundesen, C., Habekost, T., Kyllingsbaek, S., 2005. A neural theory of visual attention: bridging cognition and neurophysiology. *Psychol. Rev.* 112, 291–328.
- Ceschin, R., Wisniewski, J.L., Paquette, L.B., Nelson, M.D., Bilim, S., Panigrahy, A., 2015. Developmental synergy between thalamic structure and interhemispheric connectivity in the visual system of preterm infants. *Neuroimage Clin.* 8, 462–472.
- Chechlacz, M., Gillebert, C.R., Vangjilde, S.A., Petersen, A., Humphreys, G.W., 2015. Structural Variability within Frontoparietal Networks and Individual Differences in Attentional Functions: an Approach Using the Theory of Visual Attention. *J.*

- Neurosci. 35 (30), 10647–10658.
- Constable, R.T., Ment, L.R., Vohr, B.R., Kesler, S.R., Fulbright, R.K., et al., 2008. Prematurely born children demonstrate white matter microstructural differences at 12 years of age, relative to term control subjects: an investigation of group and gender effects. *Pediatrics* 121, 306–316.
- Cowan, N., 2001. The magical number 4 in short-term memory: a reconsideration of mental storage capacity. *Behav. Brain. Sci.* 24, 87–114.
- Daamen, M., Bäuml, J.G., Scheef, L., Sorg, C., Busch, B., Baumann, N., Bartmann, P., Wolke, D., Wohlschläger, A., Boecker, H., 2015. Working memory in preterm-born adults: load-dependent compensatory activity of the posterior default mode network. *Hum. Brain. Mapp.* 36 (3), 1121–1137.
- Davis, S.W., Cabeza, R., 2015. Cross-hemispheric collaboration and segregation associated with task difficulty as revealed by structural and functional connectivity. *J. Neurosci.* 35 (21), 8191–8200.
- D'Onofrio, B.M., Class, Q.A., Rickert, M.E., Larsson, H., Langstrom, N., Lichtenstein, P., 2013. Preterm birth and mortality and morbidity: a population-based quasi-experimental study. *JAMA Psychiatry* 70, 1231–1240.
- Dean, J.M., McClendon, E., Hansen, K., Azimi-Zonooz, A., Chen, K., Riddle, A., Gong, X., Sharifnia, E., Hagen, M., Ahmad, T., Leigland, L.A., Hohimer, A.R., Kroenke, C.D., Back, S.A., 2013. Prenatal cerebral ischemia disrupts MRI-defined cortical microstructure through disturbances in neuronal arborization. *Sci. Transl. Med.* 5 (168), 168ra7.
- Delvenne, J.F., Holt, J.L., 2012. Splitting attention across the two visual fields in visual short-term memory. *Cognition* 122 (2), 258–263.
- Dubowitz, L.M., Dubowitz, V., Goldberg, C., 1970. Clinical assessment of gestational age in the newborn infant. *J. Pediatr.* 77, 1–10.
- Eikenes, L., Lohaugen, G.C., Brubakk, A.M., Skranes, J., Haberg, A.K., 2011. Young adults born preterm with very low birth weight demonstrate widespread white matter alterations on brain DTI. *NeuroImage* 54, 1774–1785.
- Espeseth, T., Vangkilde, S.A., Petersen, A., Dyrholm, M., Westlye, L.T., 2014. TVA-based assessment of attentional capacities—associations with age and indices of brain white matter microstructure. *Front. Psychol.* 5, 1177.
- Finke, K., Neitzel, J., Bäuml, J.G., Redel, P., Müller, H.J., Meng, C., Jaekel, J., Daamen, M., Scheef, L., Busch, B., Baumann, N., Boecker, H., Bartmann, P., Habekost, T., Wolke, D., Wohlschläger, A., Sorg, C., 2015. Visual attention in preterm-born adults: specifically impaired attentional sub-mechanisms that link with altered intrinsic brain networks in a compensation-like mode. *NeuroImage* 107, 95–106.
- Froudust-Walsh, S., Karolis, V., Caldinelli, C., Brittain, P., Kroll, J., Rodriguez-Toscano, E., Tesse, M., Colquhoun, M., Howes, O., Dell'Acqua, F., Thiebaut de Schotten, M., Murray, R., Williams, S., Nosarti, C., 2015. Very early brain damage leads to remodelling of the working memory system in adulthood: a combined fMRI/tractography study. *J. Neurosci.* 35 (48), 15787–15799.
- Gimenez, M., Junge, C., Vendrell, P., Caldu, X., Narberhaus, A., Bargallo, N., Falcon, C., Botet, F., Mercader, J.M., 2005. Hippocampal functional magnetic resonance imaging during a face-name learning task in adolescents with antecedents of prematurity. *NeuroImage* 25, 561–569.
- Golestani, A.M., Miles, L., Babb, J., Castellanos, F.X., Malaspina, D., Lazar, M., 2014. Constrained by Our Connections: white Matter's Key Role in Inter individual Variability in Visual Working Memory Capacity. *J. Neurosci.* 34 (45), 14913–14918.
- Groppe, M., Ricci, D., Bassi, L., Merchant, N., Doria, V., Arichi, T., Allsop, J.M., Ramenghi, L., Fox, M.J., Cowan, F.M., Counsell, S.J., Edwards, A.D., 2014. Development of the optic radiations and visual function after premature birth. *Cortex* 56, 30–37.
- Habekost, T., Rostrup, E., 2007. Visual attention capacity after right hemisphere lesions. *Neuropsychologia* 45, 1474–1488.
- Habekost, T., Starrfelt, R., 2009. Visual attention capacity: a review of TVA-based patient studies. *Scand. J. Psychol.* 50, 23–32.
- Hagmann, P., Cammoun, L., Gigandet, X., Meuli, R., Honey, C.J., Wedeen, V.J., Sporns, O., 2008. Mapping the structural core of human cerebral cortex. *PLoS Biol.* 6 (7), e159.
- Hebb, D.O., 1949. *Organization of behavior*. Wiley, New York.
- Honey, C.J., Sporns, O., Cammoun, L., Gigandet, X., Thiran, J.P., Meuli, R., Hagmann, P., 2009. Predicting human resting-state functional connectivity from structural connectivity. *Proc. Natl. Acad. Sci. USA* 106, 2035–2040.
- Jones, D.K., Knosche, T.R., Turner, R., 2013. White matter integrity, fiber count, and other fallacies: the do's and don'ts of diffusion MRI. *NeuroImage* 73, 239–254.
- Karolis, V.R., Froudust-Walsh, S., Brittain, P.J., Kroll, J., Ball, G., Edwards, A.D., Dell'Acqua, F., Williams, S.C., Murray, R.M., Nosarti, C., 2016. Reinforcement of the brain's rich-club architecture following early neurodevelopmental disruption caused by very preterm birth. *Cereb. Cortex* 26 (3), 1322–1335.
- Komitova, M., Xenos, D., Salmaso, N., Tran, K.M., Brand, T., Schwarz, M.L., Ment, L., Vaccarino, F.M., 2013. Hypoxia-induced developmental delays of inhibitory interneurons are reversed by environmental enrichment in the postnatal mouse forebrain. *J. Neurosci.* 33, 13375–13387.
- Kraft, A., Dyrholm, M., Bundesen, C., Kyllingsbæk, S., Kathmann, N., Brandt, S.A., 2013. Visual attention capacity parameters covary with hemifield alignment. *Neuropsychologia* 51 (5), 876–885.
- Kraft, A., Dyrholm, M., Kehrer, S., Kaufmann, C., Bruening, J., Kathmann, N., Bundesen, C., Irlbacher, K., Brandt, S.A., 2015. TMS over the right precuneus reduces the bilateral field advantage in visual short term memory capacity. *Brain Stimul.* 8 (2), 216–223.
- Kringelbach, M., McIntosh, A., Ritter, P., Jirsa, V., Deco, G., 2015. The rediscovery of slowness: exploring the timing of cognition. *Trends Cogn. Sci. Elsevier {BV}*, 616–628.
- Kyllingsbæk, S., 2006. Modeling visual attention. *Behav. Res. Methods* 38, 123–133.
- Lindqvist, S., Skranes, J., Eikenes, L., Haraldseth, O., Vik, T., Brubakk, A.M., Vangberg, T.R., 2011. Visual function and white matter microstructure in very-low-birth-weight (VLBW) adolescents: a DTI study. *Vision. Res.* 51 (18), 2063–2070.
- Luck, S.J., Vogel, E.K., 1997. The capacity of visual working memory for features and conjunctions. *Nature* 390, 279–281.
- Magen, H., Emmanouil, T.A., McMains, S.A., Kastner, S., Treisman, A., 2009. Attentional demands predict short-term memory load response in posterior parietal cortex. *Neuropsychologia* 47 (8–9), 1790–1798.
- Meng, C., Bäuml, J.G., Daamen, M., Jaekel, J., Neitzel, J., Scheef, L., Busch, B., Baumann, N., Boecker, H., Zimmer, C., Bartmann, P., Wolke, D., Wohlschläger, A.M., Sorg, C., 2015. Extensive and interrelated subcortical white and gray matter alterations in preterm-born adults. *Brain Struct. Funct.* 221 (4), 2109–2121.
- Ment, L.R., Hirtz, D., Huppi, P.S., 2009. Imaging biomarkers of outcome in the developing preterm brain. *Lancet Neurol.* 8 (11), 1042–1055.
- Miller, S.P., Vigneron, D.B., Henry, R.G., Bohland, M.A., Ceppi-Cozzio, C., Hoffman, C., 2002. Serial quantitative diffusion tensor MRI of the premature brain: development in new-borns with and without injury. *J. Magn. Reson. Imaging* 16, 621–632.
- Mori, S., Wakana, S., Van Zijl, P.C.M., Nagae-Poetscher, L.M., 2005. *MRI Atlas of Human White Matter*. Elsevier, Amsterdam, The Netherlands.
- Mullen, K.M., Vohr, B.R., Katz, K.H., Schneider, K.C., Lacadie, C., Hampson, M., Makuch, R.W., Reiss, A.L., Constable, R.T., Ment, L.R., 2011. Preterm birth results in alterations in neural connectivity at age 16 years. *NeuroImage* 54 (4), 2563–2570.
- Nosarti, C., Rubia, K., Smith, A.B., Frearson, S., Williams, S.C., Rifkin, L., Murray, R.M., 2006. Altered functional neuroanatomy of response inhibition in adolescent males who were born very preterm. *Dev. Med. Child. Neurol.* 48, 265–271.
- Pandit, A.S., Ball, G., Edwards, A.D., Counsell, S.J., 2013. Diffusion magnetic resonance imaging in preterm brain injury. *Neuroradiology* 55 (Suppl 2), 65–95.
- Peterson, B.S., Vohr, B., Kane, M.J., Whalen, D.H., Schneider, K.C., Katz, K.H., Zhang, H., Duncan, C.C., Makuch, R., Gore, J.C., Ment, L.R., 2002. A functional magnetic resonance imaging study of language processing and its cognitive correlates in prematurely born children. *Pediatrics* 110, 1153–1162.
- Riegel, K., Orth, B., Wolke, D., Osterlund, K., 1995. *Die Entwicklung gefährdeter geborener Kinder bis zum 5 Lebensjahr*. Thieme, Stuttgart, (Germany).
- Roberts, R.E., Anderson, E.J., Husain, M., 2010. Expert cognitive control and individual differences associated with frontal and parietal white matter microstructure. *J. Neurosci.* 30, 17063–17067.
- Sereno, A.B., Kosslyn, S.M., 1991. Discrimination within and between hemifields: a new constraint on theories of attention. *Neuropsychologia* 29 (7), 659–675.
- Skranes, J., Vangberg, T.R., Kulseng, S., Indredavik, M.S., Evensen, K.A.I., Martinussen, M., Dale, A.M., Haraldseth, O., Brubakk, A.M., 2007. Clinical findings and white matter abnormalities seen on diffusion tensor imaging in adolescents with very low birth weight. *Brain* 130, 654–666.
- Smith, S.M., Nichols, T.E., 2009. Threshold-free cluster enhancement: addressing problems of smoothing, threshold dependence and localisation in cluster inference. *NeuroImage* 44, 83–98.
- Sperling, G., 1960. The information available in brief visual presentations. *Psychol. Monogr.: General. Appl.* 74, 1.
- Todd, J.J., Marois, R., 2004. Capacity limit of visual short-term memory in human posterior parietal cortex. *Nature* 428 (6984), 751–754.
- Tuch, D.S., Salat, D.H., Wisco, J.J., Zaleta, A.K., Hevelone, N.D., Rosas, H.D., 2005. Choice reaction time performance correlates with diffusion anisotropy in white matter pathways supporting visuospatial attention. *Proc. Natl. Acad. Sci. U S A* 102, 12212–12217.
- Unemoto, A., Drew, T., Ester, E.F., Awh, E., 2010. A bilateral field advantage for storage in visual working memory. *Cognition* 17 (1), 69–79.
- Vangberg, T.R., Skranes, J., Dale, A.M., Martinussen, M., Brubakk, A.M., Haraldseth, O., 2006. Changes in white matter diffusion anisotropy in adolescents born prematurely. *NeuroImage* 32, 1538–1548.
- Von Aster, M., Neubauer, A., Horn, R., 2006. *Wechsler Intelligenztest für Erwachsene (WIE). Deutschsprachige Bearbeitung und Adaptation des WAIS-III von David Wechsler*. Frank. Am. Main. (Ger.): Harcourt Test. Serv..
- Wolke, D., Meyer, R., 1999. Cognitive status, language attainment, and prereading skills of 6-year-old very preterm children and their peers: the Bavarian Longitudinal Study. *Dev. Med. Child. Neurol.* 41, 94–109.
- Xu, Y., Chun, M.M., 2006. Dissociable neural mechanisms supporting visual short-term memory for objects. *Nature* 440 (7080), 91–95.

## 4.7 SUPPLEMENTARY MATERIAL

In order to ensure that the posterior thalamic radiation ROI from the JHU-ICBM-DTI-81 white matter tract labels atlas that we used in our study was primarily a cortico-thalamic tract, we performed probabilistic tractography between the right occipital cortex and the right thalamus in native space for each of the subject. Since we found a significant association between vSTM storage capacity  $K$  and FA in the right posterior thalamic radiation and not in the left posterior thalamic radiation we did not perform probabilistic tractography in the left hemisphere. In more detail, we used the MNI 152 2-mm label atlas combined with the Harvard Oxford 25% 2-mm cortical atlas to create a mask of the right occipital cortex in standard space. We then transformed this ROI to individual structural space and then diffusion space using FSL FLIRT. Similarly, a mask of the right thalamus was created from the Oxford thalamic 25% 2-mm atlas.

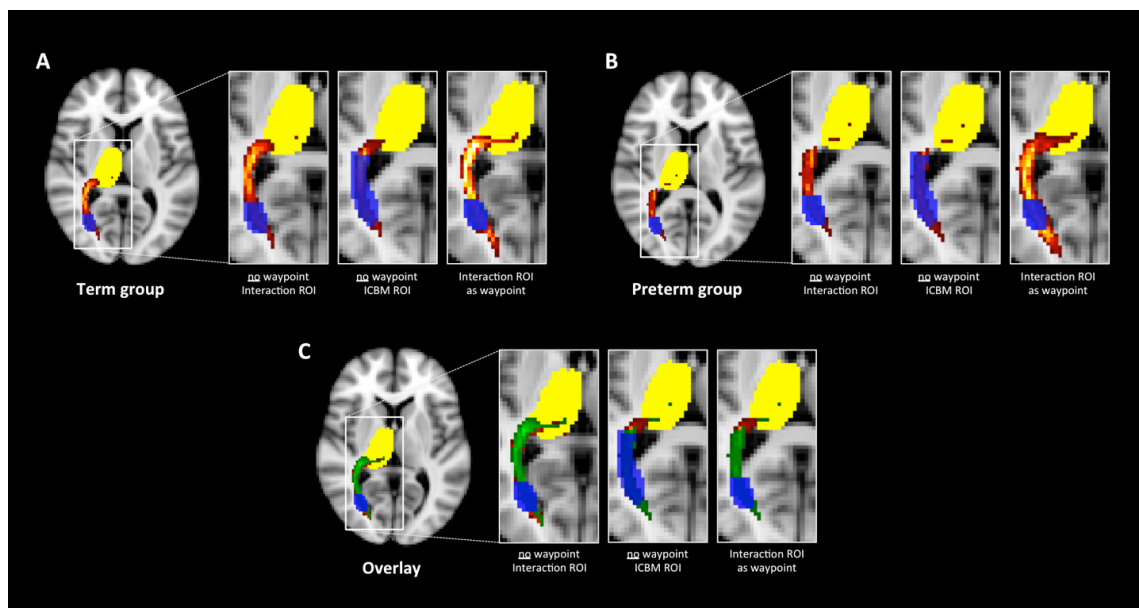


**Fig 1: Tractography between right occipital cortex and right thalamus in both term and preterm groups.** **A-B:** Axial and sagittal views representing the thresholded probabilistic path between right thalamus and right occipital cortex in the term group (**A**) and in the preterm group (**B**). The left and middle zoomed in windows show the paths obtained when seeding from right occipital cortex to right thalamus with no waypoint mask. The most right window represent the paths obtained when seeding from right occipital cortex to right thalamus using the significant cluster of voxels obtained from previous TBSS analysis as a waypoint mask. In the left and right windows, blue represent the significant TBSS interaction cluster, in the middle window, blue represents the JHU-ICBM-81-DTI white matter label atlas ROI of the right posterior thalamic radiation we used in our analysis. The overlay of both term and preterm paths is shown in **C**. Yellow represents the right thalamus, red represents the probabilistic path of the term group and green the probabilistic path of the preterm group. The three windows have similar legend as for A and B.

In order to ensure the ipsilateral specificity of the tracking, we created and used an exclusion mask for the opposite hemisphere, here a left hemisphere mask. We ran BedpostX for each subject followed by probtrackx seeding from the right occipital cortex to the right thalamus excluding the left hemisphere. In order to normalize the tracts, we divided the `fdt_paths` by the `waytotal` (total number of streamlines generated from the seed region that reaches the target region). In order to check whether our significant interaction cluster obtained by TBSS was located in cortico-thalamic tracts for all subjects, we transformed the `fdt_paths` back to standard space and created group averages for both the term- and preterm groups. We then overlapped our TBSS fill interaction cluster transformed into MNI 2-mm space with FSL FLIRT. As can be seen from figure 1, our cluster almost perfectly overlaps with the path. This is also the case for the whole ROI from the JHU-ICBM-DTI-81 white matter label atlas. In order to be even more accurate, we used the TBSS interaction cluster as a waypoint mask and tracked again from right occipital cortex to the right thalamus (fig 1, 3<sup>rd</sup> enhancing window from the left). As shown in figure 1, we can confirm that the tract we analyze with TBSS is primarily a cortico-thalamic tract.

In order to ensure that the FA images from the preterm group were as well aligned to the MNI template as the ones from the full-term group, we used the individual FA images previously aligned to the FMRIB58 FA standard space template and investigated the variance between groups. We thresholded each FA image to 0.2 in order to keep the main white matter tracts and binarized them to obtain a mask. Using matlab, we then calculated the variance of the FA mask for each group separately. For visualization, we used AMIRA (FEI). As shown in figure 2, the tracts corresponding to the posterior thalamic radiations and to the splenium of the corpus callosum have a variance close to zero within each group (figure 2A&C) and between groups (figure 2B). For better visualization, we then used only the significant (interaction) cluster found with TBSS (figure 2B,D,E,F&G). Moreover both term- and preterm-born subjects are well aligned to the FMRIB58 FA standard space template (figure 2D&G), and most of the mean FA skeleton mask shows a variance close to zero (Fig 2E&F).

Additionally, we calculated for each group how many voxels in each JHU-ICBM-DTI-81 atlas ROI we used had a variance above 0. We found that only 1.8% of the right posterior thalamic radiation voxels had a variance above 0 in the preterm group, and 1.3% in the term group. For the splenium of the corpus callosum, only 2.5% of the voxels had a variance above 0 in the preterm group, and 2.1% in the term group. We also calculated the global cumulative variance by summing up the variance of each voxel for both groups. We found that the global cumulative variance is only 6.8% larger in the preterm group:

$$\text{SumOfVariance(Preterm)} / \text{SumOfVariance(Term)} = 1.621\text{e}+05 / 1.518\text{e}+05 = 1.068$$

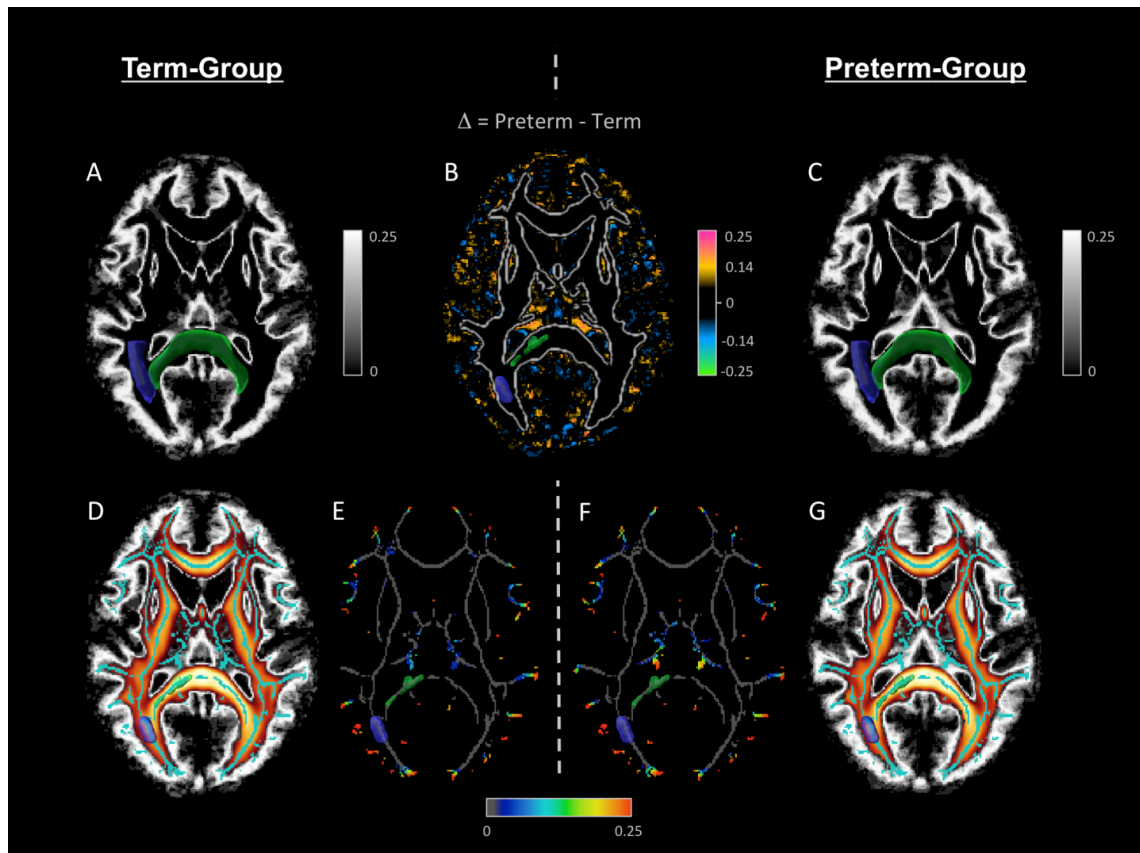


**Figure S2: Alignment term and preterm group FA maps to the FMRIB58 FA template. A & C :** Variance of the 0.2-thresholded individual FA-maps previously aligned to the FMRIB58 FA 1mm template for the Term-group (A) and Preterm-group (B) indicating the goodness of the alignment of the individual FA-maps (scale to the right indicating variance values). Blue represents the right posterior thalamic radiation and green the splenium of the corpus callosum. **B :** Difference of the Variance-maps calculated by  $\Delta = \text{variance}(\text{Preterm}) - \text{variance}(\text{Term})$ ; the ROIs are visualized in 3D using AMIRA in blue for posterior thalamic radiation (PTR) and green splenium corpus callosum; (scale to the right indicating orange/pink values for higher variance in the preterm group and blue/green values for higher variance in the Term group). **D & G :** Overlay of the TBSS-Skeleton (turquoise blue) on the MNI-FMRIB58 FA-Map (heatmap) overlaid by the FA Variance-Map of A and C. **E & F :** Variance of the skeleton voxels obtained as the product of the binarized skeleton with the Variance-map of A and C . Grey values indicate a variance of zero (scale shown below); the ROI's are visualized in 3D in blue for the PTR and green for the splenium.



---

# 5 GENERAL DISCUSSION

In this thesis, we investigated the relevance of the structural connectivity of posterior thalamus to visual cortices for vSTM capacity and the consequences of its alteration due to aging and premature birth.

## 5.1 KEY FINDINGS

### 5.1.1 FIRST STRUCTURAL EVIDENCE SUPPORTING THE NTVA ASSUMPTIONS OF A THALAMO-CORTICAL SYSTEM FOR VSTM PROCESSES

The aim of this thesis was to investigate the relevance of posterior thalamo-cortical tracts for vSTM capacity that is suggested by the NTVA model. Indeed, following a general idea from Hebb (1949), the NTVA assumes that sensory neurons coding for the representation of a selected object in the visual cortex are kept active once the sensory stimulation has disappeared via reciprocal connections to the corresponding parts of the vSTM map located in the TRN (Bundesen et al., 2005). In other words, feedback loops between visual cortices and the TRN constitute the vSTM system. However, no clear evidence for this assumption has been brought to light thus far. In order to test whether we can provide such evidence, we first used two distinct healthy young populations in which thalamo-cortical connections were analyzed with respect to their integrity or their connectivity. In our first study, we used probabilistic tractography between occipital cortices and posterior thalamus in healthy adults aged 20 to 53 years and found that vSTM capacity was significantly correlated with left PT-OC structural connectivity. When investigating this association in a more restricted age group using a sliding window approach, the second study brought the information that vSTM capacity was significantly associated with left PT-OC structural connectivity in young adults below 30 years of age. Interestingly, in our third study, we found that in healthy, full-term born, young adults at the age of 27 and born at term, vSTM capacity was associated with FA in a part of the right posterior thalamic radiation. These findings go beyond those of previous studies using the TVA framework, which found reduced vSTM capacity in patients with lesions to posterior tracts (Habekost and Rostrup 2007) and in a group of patients with thalamic stroke (Kraft et al., 2015). In particular, our findings suggest that specific connections, i.e., posterior thalamic connections to occipital cortices and their microstructure are relevant for vSTM capacity in healthy adults. Thus, our findings bring first structural evidence for the NTVA assumption of a posterior thalamo-cortical feedback loop system for vSTM processes (Bundesen et al., 2005). Our findings are also in agreement with those from Saalman and colleagues

(Saalman et al., 2012) who used neural recordings and DWI-derived tractography in macaques and found that the pulvinar synchronized the activity between cortical areas involved in attention allocation. They suggested that pulvino-cortical loops regulate the information transmitted between each cortical stage of visual processing and that, thus, internal processes, such as short term memory, rely heavily on these pulvino-cortical loops. Furthermore, our first study demonstrated that the association between left PT-OC structural connectivity and vSTM capacity was region and function specific. Indeed, no significant association with vSTM capacity was found when performing probabilistic tractography from motor cortices to posterior thalamus suggesting our finding was region specific. Similarly, no significant associations between left PT-OC structural connectivity and processing speed or perceptual threshold were found suggesting our finding was function specific. The absence of a significant association between visual processing speed and PT-OC structural connectivity in our first study is not very surprising, since a previous study from Espeseth and colleagues found that visual processing speed was significantly associated with FA in the superior longitudinal fasciculus and body and genu of the corpus callosum (Espeseth et al., 2014). Our findings of significant associations between vSTM capacity and the integrity and structural connectivity of posterior thalamus to occipital cortices were also strengthened by their independence from general cognitive abilities. Finally, the fact that these findings are consistent with each other across studies, although they were found in different populations assessed with different scanners, sequences and whole report paradigms strengthens their validity as first empirical, structural support for the NTVA model's assumption that recurrent loops between posterior thalamus and visual cortices subserve vSTM capacity.

In the first study, we not only analyzed attentional capacity parameters with a focus on vSTM capacity, but also attentional selection parameters, top down control and spatial bias. According to the NTVA, the computation of attentional weights of displayed visual objects at the end of the first wave of visual processing supposedly takes place in the pulvinar nucleus where the saliency map of objects is assumed to be located (Bundesen et al., 2005). As the pulvinar is supposed to send weighted information to higher-order visual areas, connections between posterior thalamic areas and the occipital cortex should be relevant for the efficiency of task-related weighting. Interestingly, we found a trend for a relationship between the individual level of top-down control  $\alpha$  and right PT-OC structural connectivity. This finding is in line with electrophysiological studies which suggested that the pulvinar nucleus plays an important role in selective attention (Desimone et al., 1990, Robinson and Petersen 1992, Olshausen et al., 1993, Shipp, 2003; Shipp, 2004, Saalman and Kastner 2011, Saalman 2012), and can be interpreted as empirical support for the NTVA assumption of a critical role of the pulvinar nucleus in task-related attentional weighting (Bundesen et al., 2005). This finding was also region- and function-specific since no significant association between top down control and the structural connectivity of posterior thalamus to motor cortices nor between right PT-OC structural connectivity and spatial bias was found.

---

Together our three studies bring first evidence for the relevance of posterior thalamo-cortical tracts for vSTM capacity and top down control as suggested by the NTVA.

### 5.1.2 THE ASSOCIATION BETWEEN vSTM CAPACITY AND POSTERIOR THALAMO-CORTICAL CONNECTIONS IS CHANGED WHEN THESE CONNECTIONS ARE ALTERED

In order to further validate the NTVA model, we explored the relevance of posterior thalamic connections to visual cortices for vSTM capacity in two populations known to exhibit posterior cortical and subcortical white matter damages: aging and premature birth. We investigated whether alterations of posterior thalamo-cortical connections might result in a change of association between vSTM capacity and such posterior thalamocortical tracts.

#### EXAMPLE OF HEALTHY AGING

Besides a decline in vSTM capacity, (Verhaegen et al., 1993; Gazzaley et al., 2005; Sander et al., 2011; McAvinue et al., 2012) it has been shown that aging leads to changes in white matter microstructure and connectivity such as changes in RD and AD in posterior thalamic areas (Kumar et al., 2013), and alterations in thalamo-cortical projections' volume (Hughes et al., 2012). Considering such structural alterations, our second study investigated whether the association between PT-OC structural connectivity and vSTM capacity remained the same throughout the lifespan or whether aging modified it. Using a regression model, we found a significant interaction effect between age and left PT-OC structural connectivity on vSTM capacity suggesting that the association between vSTM capacity and left PT-OC connection probability is modified by age. Such modifications of the association between vSTM capacity and a brain correlate with age had previously been reported (Wiegand et al., 2014a; Sander et al., 2011; Duarte et al., 2013). For example, Wiegand and colleagues, who used electroencephalography recordings, found a weaker association between vSTM capacity and contralateral delay activity (CDA) in older compared to younger adults (Wiegand et al., 2014a). Although the significant interaction effect between age and left PT-OC connection probability on vSTM capacity that we found suggested that aging affects this structure-function association, it did not provide information regarding the direction of change. In order to investigate the direction of this interaction, we examined the association between vSTM capacity and PT-OC connection probability as a pseudo-continuous function of age using a sliding window approach. This approach yielded intriguing findings: we found that in young individuals below 30 years of age, the association between left PT-OC and vSTM capacity was significantly negative before linearly inverting to a positive association around an age of 40. This association remained significantly positive above an age of 50. Interestingly, in our first study we found that the probability of connection between the left posterior

thalamus and the left occipital cortex was negatively associated with vSTM capacity in participants below the age of 55 years. Thus, our finding of a negative association between left PT-OC structural connectivity and vSTM capacity in young participants below the age of 30 years reproduce the finding from our first study. It would also suggest that the association between left PT-OC structural connectivity and vSTM capacity might not be negative for people below the age of 55 years in general but rather for people aged 30 and below. Due to the complex nature of the DWI signal and particularly the output of tractography, we could not interpret our first study's findings beyond the fact that vSTM capacity relied at least in part on PT-OC structural connectivity. Our finding of a continuum across aging in our second study brings additional meaning to the previously found negative association and suggests that there is a continuous age-related process influencing PT-OC connectivity so that the association with K is changed.

### EXAMPLE OF PRETERM BIRTH

In the third study we investigated whether vSTM capacity was distinctively associated with the integrity of cortico-thalamic and cortico-cortical tracts in preterm-born compared to full-term born young adults. We found that the association between vSTM capacity and FA in part of the posterior thalamic radiations significantly differed between groups. In young adults born at term, we found that the higher FA in part of the right posterior thalamic radiations, the higher the vSTM capacity. In contrast in young adults born prematurely, we found that vSTM capacity was significantly negatively associated with FA. These results suggest that the link between vSTM capacity and posterior thalamo-cortical connection is altered after preterm birth. This finding is in line with those of Karolis and colleagues (Karolis et al., 2016) and Meng and colleagues (Meng et al., 2015) who found altered cortico-thalamic loops and microstructure, respectively, in preterm born adults. We also found that vSTM capacity was positively associated with FA in part of the splenium of the corpus callosum in preterm born adults while no significant association was found in the full-term born group. Moreover, FA was reduced in the splenium of corpus callosum of preterm compared to full-term born adults. This discovery and the compensatory intrinsic functional connectivity findings in bilateral visual cortices found in preterm born adults with relatively preserved vSTM capacity (Finke et al., 2015) suggest that in preterm born adults a compensatory reorganization takes place so that the vSTM capacity system relies less on cortico-thalamic and more on cortico-cortical connections. This interpretation is in line with findings from Ball and colleagues (Ball and al., 2012; Ball et al., 2014) who found that reorganization of connectivity i.e. reduced cortico-thalamic and increased local cortico-cortical connectivity, takes place in infants following preterm birth. It is also in agreement with findings from Ceschin and colleagues (Ceschin et al., 2015) who suggested that the combination of thalamo-cortical and interhemispheric connectivity plays a role in the development of visual functions in preterm-born infants. Finally, our findings add evidence from a different cognitive modality to previous studies where adaptive plastic processes during a verbal paired associative task

were found. In this study, adults born very preterm exhibited a very different pattern of activation in learning and memory networks, which included the anterior cingulate cortex, caudate nucleus, thalamus and parahippocampal gyrus (Salvan et al., 2014).

Together, our second and third studies indicate that, when posterior thalamo-cortical connections are altered, the association with vSTM is also altered. Thus they add further evidence for the NTVA model of posterior thalamo-cortical connectivity being relevant for vSTM capacity.

### 5.1.3 THE ASSOCIATION BETWEEN VSTM CAPACITY AND THE MICROSTRUCTURE OF POSTERIOR THALAMO-CORTICAL CONNECTIONS IS COMPLEX

In the previous paragraph we discussed how the association between vSTM capacity and the structural connectivity of posterior thalamus to occipital cortices was changed when those tracts were altered. Such changes suggest an intricate association between PT-OC structural connectivity and vSTM capacity, which might reflect the complex relationship of PT-OC tracts microstructure to vSTM capacity. Indeed, in our second study, we found that the association between vSTM capacity and PT-OC structural connectivity was linearly inverting from negative to positive with increasing age. This continuum across aging suggested that there is a continuous process influencing PT-OC connectivity so that the association with  $K$  is changed. Considering this finding, the documented alterations of white matter properties during aging (Pfefferbaum et al., 2000, Hugenschmidt et al., 2008; Westlye et al., 2010) and previous studies suggesting that white matter microstructure mediates the impact of age on attention functions such as processing speed (Salami et al., 2012), we speculated that the inverse association between vSTM capacity and PT-OC structural connectivity was due to a change in white matter properties of PT-OC tracts. Although our results were not sufficient to determine the cause of this modified association, we investigated changes in white matter microstructure in an attempt to partly answer this hypothesis. As reported in previous studies (Hugenschmidt et al., 2008; Kumar et al., 2013) we found that FA was reduced and MD, RD and AD were increased in older compared to younger individuals. This suggested that aging impairs PT-OC tracts' microstructure. These changes with aging are consistent with post-mortem histological studies which have shown that in healthy aging, at the cellular level, axonal and myelin degeneration take place, along with other changes in the cellular environment, such as accumulation of cellular debris and formation of glial scars (Meier-Ruge et al., 1992; Aboitiz et al., 1996; Peters et al., 2002). For example, it has been shown that an increase in MD might likely be caused by a decrease in membrane density due to cell degeneration (Beaulieu 2002). Furthermore reduced FA might be interpreted as a decrease in the organization of white matter caused by various processes such as demyelination, axonal degradation or gliosis (Beaulieu 2002, Concha et al., 2006; Lebel et al., 2008; Assaf et al., 2008). The combination of decreased FA with increased MD, RD and AD is in line with findings from Burzynska and colleagues (Burzynska et al.,

2010) and implies a decrease in fiber organization which might be caused by axonal loss or gliosis (Beaulieu et al., 2002; Concha et al., 2006; Lebel et al., 2008 et Assaf et al., 2008).

Although the microstructure of PT-OC tracts was altered with aging, we found no significant changes of overall white matter volume. This is not surprising as it has been shown that white matter volume slightly increases until mid-adulthood (Van Buchem et al., 1999; Bartzokis et al., 2001), and according to some studies, even until the 6<sup>th</sup> decade of life (Westlye et al., 2010) before decreasing strongly from 65 years of age on (Westlye et al., 2010). One possible explanation for the differential pattern of reduced FA and unchanged white matter volume might be that the increase in white matter volume until mid-adulthood results from the increased complexity of myelinated fibers, with the presence of more crossing fibers. Indeed, more fibers crossing would reduce the FA value while increasing the volume (Tuch et al., 2005). A previous study that used magnetization transfer ratio has found a quadratic relationship between magnetic transfer ratio and age with a slight increase until the 40s and then a decrease (Van der Flier et al., 2002) also suggesting an increase in myelin content until mid-adulthood. Intriguingly, we found that the change of association between vSTM capacity and PT-OC structural connectivity from negative to positive took place around the age of 40 years. Thus, although we do not have the necessary results to make such hypothesis, we would speculate that changes in microstructural properties of the tracts connecting posterior thalamus to occipital cortices might mediate the effect of aging on vSTM capacity. The complex association between PT-OC tracts microstructure and vSTM capacity was also suggested by findings in our third study. Indeed, we found a negative association between vSTM capacity and FA in posterior thalamic tracts in preterm born adults. Although this finding of a negative association was surprising, it was not the first time that such association was reported since Tuch and colleagues (Tuch et al., 2005) also reported a negative and contra-intuitive association between choice reaction time and FA in the optic radiation and posterior thalamus. Thus, our finding of a negative association between FA in posterior thalamic radiations and vSTM capacity in preterm born adults could be explained - similarly to Tuch and colleagues (2005) - by the presence of crossing fibers, with the increase in FA of one fiber population leading to an overall decrease FA in the voxel (Tuch et al., 2003; Pierpaoli et al., 2001).

Our findings in aging and preterm birth suggest a complex relationship between white matter microstructure measures obtained from DTI and the underlying tissue organization, which also critically influences the association between white matter tracts such as PT-OC tracts and vSTM capacity.

#### 5.1.4 INTEGRATING OUR FINDINGS WITH CURRENT VIEWS

The thalamo-cortical NTVA model infers critical relevance of structural connectivity between posterior thalamus and dorsal cortical regions for vSTM capacity. The three studies of this thesis were the first experimental test of this assumption, and thus, provide the first empirical support of this

---

model. These findings do not suggest that tracts connecting posterior thalamus to occipital cortices are the only tracts subserving vSTM capacity. They simply suggest that they play a role in vSTM functions which has not been studied enough thus far. These findings also do not contradict previous studies that found fronto-parietal networks as being relevant for vSTM capacity (Courtney et al., 1998; Todd et Marois 2004; Xu and Chun 2006; Chechlacz et al., 2015) since we did not investigate fronto-parietal connections in this thesis. Moreover, it has been suggested that fronto-parietal areas might function as higher order structures for attention, for example to maintain attentional focus under distraction, rather than being the topographic maps of priority and visual short-term memory (Bundesen et al., 2005). As no distractors were present in the whole report tasks used to assess vSTM capacity, it is also possible that the fronto-parietal contribution to vSTM might be very low.

Finally, our findings that posterior thalamus and posterior thalamic connections are relevant for vSTM capacity fits with the current view of the thalamus shared by Sherman and Guillery, who, among others, suggest that the thalamus is not only a relay structure, but that it also coordinates cortico-cortical communication (Sherman et al., 2002; Guillery et al., 2002; Sherman and Guillery 2013; Schmid et al., 2012; Saalman et al., 2011). Indeed, a study by Saalman and colleagues, who used recordings and diffusion tractography in macaques performing a variant of the Eriksen flanker task, found that the pulvinar synchronized the activities between interconnected cortical areas related to attentional allocation and suggested that internal processes such as the maintenance of attention in expectation of a visual stimuli and short term memory relies on pulvino-cortical loops (Saalman et al., 2012). Overall, they hypothesized that a role for higher order thalamic nuclei such as the pulvinar might be the regulation of cortical synchrony to selectively route information across the cortex. Although our findings do not provide proof for such hypothesis, they suggest posterior thalamus (including the pulvinar) – visual cortex loops to subserve an important process, i.e., vSTM capacity.

## 5.2 LIMITATIONS

A first and general limitation of our studies is sample bias. Indeed, our first and second study participants were highly educated with most of the young participants attending university and the older participants being particularly highly functioning individuals with a rather high level of activity, education and high crystallized IQ. Thus, our findings might not be true for individuals with lower levels of education or IQ. Similarly, the preterm participants in our third study were composed of preterm born adults with relatively low neonatal complications at birth and high IQ. Thus, our findings cannot be generalized to other preterm born individuals with high neonatal complications. Such positive bias is not rare among preterm birth studies (Nosarti et al., 2007). It would thus be interesting to investigate the association between vSTM capacity and posterior thalamo-cortical connectivity in a group of adults born very preterm or with very low birth weight and a high number of neonatal complications.

Another limitation of our second study is the use of a cross-sectional sample. Unlike in longitudinal studies, we cannot generalize our findings to intra-individual changes across the lifespan (Salthouse et al., 2011).

It is also important to note that DWI is based on the diffusion of water molecules, which is less hindered along the axons than perpendicular to it (Beaulieu et al., 2002). Thus, local diffusion is dependent on local microstructure. However, one factor that can influence DTI metrics such as FA or MD is the partial volume effect. In brief, the signal obtained by DWI does not reflect the diffusion properties of brain tissue only, but also of free water (Pasternak et al., 2009). As free water is particularly present in the CSF, white matter voxels surrounding CSF are particularly sensitive to partial volume effect. Corrections for partial volume effect are not available to everyone making its use relatively rare. We thus did not use any respective correction and the reader should keep in mind that this effect might potentially influence our results (Vos et al., 2011). Finally, it is difficult to interpret our DTI-based results in terms of underlying microscopic changes since the number of streamlines generated by probabilistic tractography is not a direct measure of anatomical connectivity and their relationship to the underlying anatomy remains unclear (Jones, 2010; Jones et al., 2013; Jbabdi and Johansen-berg, 2011). Several factors can influence the number of streamlines such as the organization of myelin in regions bordering cortical grey matter (Reveley et al., 2015) fanning fibers or crossing fibers with less crossing fibers leading to increased connectivity values (Jbabdi and Johansen-Berg, 2011; Thomas et al., 2014; Reveley et al., 2015; Donahue et al., 2016). Crossing fibers are also a limitation of the tensor model and thus will affect FA, MD, RD and AD values as well.

## 5.3 FUTURE DIRECTIONS

As mentioned above, DTI-metrics such as FA and MD reflect the diffusivity of water molecules. However, how those measures actually relate to axonal density, fiber density or myelin remains quite unclear. New diffusion sequences allow for a more precise quantification of those properties. For example high angular resolution diffusion imaging (HARDI) measures the DW signal using a much larger number of diffusion weighted gradient directions than required for DTI, in order to capture the higher angular frequency features of the DW signal that are not adequately modelled by a single diffusion tensor (Tuch et al., 2002; Tournier et al. 2004). The use of more gradient directions allows for a more precise measure of the diffusion pattern of water molecules and thus of the brain tissue properties. However, more gradient directions also mean longer acquisition time and due to the multimodal nature of our studies it was not possible for us to use such sequences. Neurite orientation dispersion and density imaging (NODDI) is another diffusion MRI technique derived from HARDI and used to estimate the microstructural complexity of dendrites and axons in vivo (Zhang et al., 2011; Zhang et al., 2012). Such indices of neurites relate more directly to and provide more specific markers of brain tissue microstructure than the standard DTI-derived indices. With NODDI, the diffusion per voxel is modeled using a 3 compartment tissue model and an index of orientation dispersion is defined to characterize angular variation of neurites. This technique would be particularly interesting to use in studies of aging and preterm birth since neurite morphology is a key marker of brain development. Indeed it has been shown that an increase in the dispersion of neurite orientation distribution was associated with brain development (Conel, 1939) and aging, and a reduction in the dendritic density was linked with aging (Jacobs et al., 1997). Thus, it would be interesting to use such technique in combination with TVA-based assessment in order to understand which property of the PT-OC tracts is associated with vSTM capacity and how is it influenced by aging or preterm birth. Using such technique could help test our hypothesis of changes in white matter properties mediating the impact of age on vSTM capacity.

Finally, using a higher number of gradient directions and a multi compartment model also allows to measure fiber density, which has been shown to be more sensitive to neurodegenerative processes in amyotrophic lateral sclerosis (Stämpfli et al., 2018). We are currently aiming at using such measure to investigate the long-term alterations of white matter following premature birth and explore whether fiber density changes might be a better marker of preterm birth alterations than FA.

In this thesis, we investigated the structural underpinnings of vSTM capacity (namely posterior thalamo-cortical connectivity). However, in order to confirm our findings, it would be relevant to combine DTI-derived measures with functional measurements such as derived from functional MRI or Electroencephalography (EEG). As our second and third studies were part of a multimodal project that included fMRI, MPRAGE, FLAIR and EEG assessment, it would be interesting to correlate measures of white matter integrity and connectivity with intrinsic functional connectivity obtained from fMRI

data or with the amplitudes of ERPs derived from EEG recordings. For example, we could perform a functional connectivity analysis between thalamus and occipital cortices using the technique from Toulmin and colleagues (Toulmin et al., 2015) and use the voxels showing a significant blood-oxygen-level dependent signal difference between older and younger individuals as seed and target regions for tractography. We could then, for example, correlate tractography scores with vSTM capacity measurements.

Finally, considering the long term thalamocortical changes following premature birth and the reorganization of connectivity to subserve vSTM capacity, it would be interesting to assess the preterm born young adults again in older age and investigate whether the association between PT-OC structural connectivity and vSTM capacity also inverses from negative to positive at older age, to compare the findings with our second study.

## 5.4 CONCLUSION

In this thesis we investigated the relevance of posterior thalamo-cortical connections for vSTM capacity based on the NTVA model. Our studies brought first structural evidence of the NTVA thalamic model in a population of healthy young adults as well as in two populations with damage in posterior thalamo-cortical connectivity. Together they suggest that the posterior thalamus and its connections to visual cortices are relevant for vSTM capacity and should thus be considered part of the vSTM system in the same way as frontal and parietal regions.

---

## REFERENCES

- Aboitiz, F., Rodriguez, E., Olivares, R., Zaidel, E., 1996.** Age-related changes in fibre composition of the human corpus callosum: sex differences. *NeuroReport* 7, 1761–1764.
- Anderson, P., Doyle, L.W., 2003.** Neurobehavioral outcomes of school-age children born extremely low birth weight or very preterm in the 1990s. *J. Am. Med. Assoc.* 289 (24), 3264-3272.
- Andrews-Hanna, J.R., Snyder, A.Z., Vincent, J.L., Lustig, C., Head, D., Raichle, M.E., Buckner, R.L., 2007.** Disruption of large-scale brain systems in advanced aging. *Neuron.* 56, 924–935.
- Assaf, Y., Blumenfeld-Katzir, T., Yovel, Y., Basser, P.J., 2008.** AxCaliber: a method for measuring axon diameter distribution from diffusion MRI. *Magn. Reson Med.*, 59, 1347-1354.
- Atkinson, J., Braddick, O., 2007.** Visual and visuocognitive development in children born very prematurely. *Prog. Brain Res.* 164, 123-149.
- Atkinson, J., Braddick, O., 2012.** Visual attention in the first years: typical development and developmental disorders. *Dev Med Child Neurol.* 54, 589-595.
- Ball, G., Boardman, J.P., Rueckert, D., Aljabar, P., Arichi, T., Merchant, N., Gousias, I.S., Edwards, A.D., Counsell, S.J., 2012.** The effect of preterm birth on thalamic and cortical development. *Cereb. Cortex*, 22, 1016-1024.
- Ball, G., Boardman, J.P., Aljabar, P., Pandit, A., Arichi, T., Merchant, N., Rueckert, D., David Edwards, A., Counsell, S.J., 2013a.** The influence of preterm birth on the developing thalamocortical connectome. *Cortex J. Devot. Study Nerv. Syst. Behav.* 49, 1711–1721.
- Ball, G., Srinivasan, L., Aljabar, P., Counsell, S.J., Durighel, J., Hajnal, J.V., Rutherford, M.A., Edwards, A.D., 2013b.** Development of cortical microstructure in the preterm human brain. *Proc. Natl. Acad. Sci. USA* 110, 9541–9546.
- Ball, G., Aljabar, P., Zebari, S., Tusor, N., Arichi, T., Merchant, N., Robinson, E.C., Ogundipe, E., Rueckert, D., Edwards, A.D., Counsell, S.J., 2014.** Rich-club organization of the newborn human brain. *Proc. Natl. Acad. Sci. USA* 111(20), 7456–7461.
- Baron, I.S., Rey-Casserly, C., 2010.** Extremely Preterm Birth Outcome: A Review of Four Decades of Cognitive Research. *Neuropsychology Review* 20, 430-452.
- Bartzokis, G., Sultzer, D., Lu, P.H., Nuechterlein, K.H., Mintz, J., Cummings, J.L., 2004.** Heterogeneous age-related breakdown of white matter structural integrity: implications for cortical “disconnection” in aging and Alzheimer’s disease. *Neurobiol Aging*.25, 843–51.

- Barrick, T.R.,** Charlton, R.A., Clark, C.A., Markus, H.S., 2010. White matter structural decline in normal ageing: a prospective longitudinal study using tract-based spatial statistics. *Neuroimage*.51,565–577.
- Basser, P.J.,** Mattiello, J., LeBihan, D., 1994. MR diffusion tensor spectroscopy and imaging. *Biophys J*. 66, 259–267.
- Basser, P.J.,** Pierpaoli, C., 1996. Microstructural and physiological features of tissues elucidated by quantitative-diffusion-tensor MRI. *J. Magn. Reson. B*, 111(3), 209-219.
- Beaulieu, C.,** 2002.The basis of anisotropic water diffusion in the nervous system—a technical review. *NMR Biomed*. 15 (7–8),435–455.
- Behrens, T. E.,** Johansen-Berg, H., Woolrich, M. W., Smith, S. M., Wheeler-Kingshott, C. A., Boulby, P. A., Barker, G. J., Sillery, E. L., Sheehan, K., Ciccarelli, O., Thompson, A. J., Brady, J. M., Matthews, P. M., 2003. Non-invasive mapping of connections between human thalamus and cortex using diffusion imaging. *Nat Neurosci*, 6(7), 750-757.
- Behrens, T. E.,** Berg, H. J., Jbabdi, S., Rushworth, M. F., & Woolrich, M. W., 2007. Probabilistic diffusion tractography with multiple fibre orientations: What can we gain? *Neuroimage*, 34(1), 144-155.
- Bennett, I.J.,** Madden, D.J., Vaidya, C.J., Howard, D.V., Howard, J.H., 2010. Age-Related Differences in Multiple Measures of White Matter Integrity: A Diffusion Tensor Imaging Study of Healthy Aging. *Hum Brain Mapp*. 31(3), 378–390.
- Bennett, I.J.,** Madden, D.J., 2014. Disconnected aging: cerebral white matter integrity and age-related differences in cognition. *Neuroscience*, 276, 187-205.
- Bhagat, Y.A.,** Beaulieu, C.,2004. Diffusion anisotropy in subcortical white matter and cortical gray matter: changes with aging and the role of CSF-suppression. *J Magn Reson Imaging*. 20, 216–227.
- Blencowe H.,** Cousens S., Oestergaard M. Z., Chou D., Moller A.-B., Narwal R., Adler A., Garcia C. V., Rohde S., Say L. 2012. National, regional, and worldwide estimates of preterm birth rates in the year 2010 with time trends since 1990 for selected countries: a systematic analysis and implications. *The Lancet*, 379(9832), 2162–72.
- Borghesani, P.R.,** Madhyastha, T.M., Aylward, E.H., Reiter, M.A., Swarny, B.R., Warner Schaie, K., Willis, S.L., 2013.The association between higher order abilities, processing speed, and age are variably mediated by white matter integrity during typical aging. *Neuropsychologia*, 51, 1435–1444.

- Brickman**, A.M., Meier, I.B., Korgaonkar, M.S., Provenzano, F.A., Grieve, S.M., Siedlecki, K.L., Wasserman, B.T., Williams, L.M., Zimmerman, M.E., 2012. Testing the white matter retrogenesis hypothesis of cognitive aging. *Neurobiol Aging*, 33, 1699–1715.
- Broadbent**, D. E., 1971. *Decision and stress*. London: Academic Press.
- Bublak**, P., Redel, P., Finke, K., 2006. Spatial and non-spatial attention deficits in neurodegenerative diseases: assessment based on Bundesen's theory of visual attention (TVA). *Restor.Neurol.Neurosci.*, 24, 287–301.
- Bublak**, P., Redel, P., Sorg, C., Kurz, A., Förstl, H., Müller, H. J., Schneider, W. X., Finke, K., 2011. Staged decline of visual processing capacity in mild cognitive impairment and Alzheimer's disease. *Neurobiology of Aging*, 32(7), 1219–30.
- Bundesen**, C., 1990. A theory of visual attention. *Psychol. Rev.* 97, 523-547.
- Bundesen**, C., Habekost, T., Kyllingsbaek, S., 2005. A neural theory of visual attention: bridging cognition and neurophysiology. *Psychol. Rev.* 112, 291-328.
- Burgmans**, S., Gronenschild, E.H., Fandakova, Y., Shing, Y.L., van Boxtel, M.P., Vuurman, E.F., Uylings, H.B., Jolles, J., Raz N., 2011. Age differences in speed of processing are partially mediated by differences in axonal integrity. *Neuroimage*, 55, 1287-1297.
- Burzynska**, A.Z., Preuschhof, C., Backman, L., Nyberg, L., Li, S.C., Lindenberger, U., Heekeren, H.R., 2010. Age-related differences in white-matter microstructure: Region-specific patterns of diffusivity. *Neuroimage*. 49(3),2104-12.
- Ceschin**, R., Wisnowski, J.L., Paquette, L.B., Nelson, M.D., Blüml, S., Panigrahy, A., 2015. Developmental synergy between thalamic structure and interhemispheric connectivity in the visual system of preterm infants. *Neuroimage Clin.* 8, 462–472.
- Charlton**, R.A., Barrick, T.R., Markus, H.S., Morris, R.G., 2009. Theory of mind associations with other cognitive functions and brain imaging in normal aging. *Psychol Aging.*, 24, 338–348.
- Chechlacz**, M., Gillebert, C.R., Vangkilde, S.A., Petersen, A., Humphreys, G.W., 2015. Structural Variability within Frontoparietal Networks and Individual Differences in Attentional Functions: An Approach Using the Theory of Visual Attention. *J. Neurosci.* 35 (30), 10647-58.
- Concha**, L., Gross, D.W., Wheatley, B.M., Beaulieu, C., 2006. Diffusion tensor imaging of time-dependent axonal and myelin degradation after corpus callosotomy in epilepsy patients. *Neuroimage*. 32,1090–1099.

**Conel, J.L.**, 1939. Postnatal Development of the Human Cerebral Cortex: The Cortex of the Newborn. Vol. 1. Cambridge, MA: Harvard Univ. Press

**Counsell, S.J.**, Dyet, L.E., Larkman, D.J., Nunes, R.G., Boardman, J.P., Allsop, J.M., Fitzpatrick, J., Srinivasan, L., Cowan, F.M., Hajnal, J.V., Rutherford, M.A., Edwards, A.D., 2007. Thalamo-cortical connectivity in children born preterm mapped using probabilistic magnetic resonance tractography. *Neuroimage*, 33(8), 896-904.

**Courchesne, E.**, Chisum, H.J., Townsend, J., Cowles, A., Covington, J., Egaas, B., Harwood, M., Hinds, S., Press, G.A., 2000. Normal brain development and aging: quantitative analysis at in vivo MR imaging in healthy volunteers. *Radiology*. 216(3), 672–82.

**Courtney, S.M.**, Petit, L., Haxby, J.V., Ungerleider, L.G., 1998 The role of prefrontal cortex in working memory: examining the contents of consciousness. *Philos Trans R Soc Lond B Biol Sci.*, 353(1377), 1819-28. Review.

**Coxon, J.P.**, Van Impe, A., Wenderoth, N., Swinnen, S.P., 2012. Aging and inhibitory control of action: Cortico subthalamic connection strength predicts stopping performance. *J Neurosci.*, 32, 8401–8412.

**D'Onofrio, B.M.**, Class, Q.A., Rickert, M.E., Larsson, H., Langstrom, N., Lichtenstein, P., 2013. Preterm birth and mortality and morbidity: a population-based quasi-experimental study. *JAMA Psychiatry*, 70, 1231-1240.

**Dean, J.M.**, McClendon, E., Hansen, K., Azimi-Zonooz, A., Chen, K., Riddle, A., Gong, X., Sharifnia, E., Hagen, M., Ahmad, T., Leigland, L.A., Hohimer, A.R., Kroenke, C.D., Back, S.A., 2013. Prenatal cerebral ischemia disrupts MRI-defined cortical microstructure through disturbances in neuronal arborization *Science translational medicine* 5(168) 168ra7.

**Deng, W.**, 2010. Neurobiology of injury to the developing brain. *Nat Rev Neurol*. 6(6), 328-36.

**Desimone, R.**, Wessinger, M., Thomas, L., Schneider, W. 1990. Attentional control of visual perception: cortical and subcortical mechanisms. *Cold Spring Harb. Symp. Quant. Biol.*, 55, 963-971.

**Desimone, R., & Duncan, C.**, 1995. Neural mechanisms of selective visual attention. *Annu. Rev. Neurosci.* 18, 193-222.

**Donahue, C.J.**, Sotiropoulos, S.N., Jbabdi, S., Hernandez-Fernandez, M., Behrens, T.E., Dyrby, T., Coalson, T., Kennedy, H., Knoblauch, H., Van Essen, D.C., Glasser, M.F. 2016. Using Diffusion Tractography to Predict Cortical Connection Strength and Distance: A Quantitative Comparison with Tracers in the Monkey. *J. Neurosci.*, 36 (25), 6758-6770.

**Duarte, A.,** Hearons, P., Jiang, Y., Delvin, M.C., Newsome, R.N., Verhaeghen, P., 2013. Retrospective attention enhances visual working memory in the young but not the old: an ERP study. *Psychophysiology* 505, 465-476.

**Duncan, J.,** Bundesen, C., Olson, A., Humphreys, G., Chavda, S., Shibuya, H., 1999. Systematic analysis of deficits in visual attention. *Journal of Experimental Psychology: General*, 128, 450–478.

**Duncan J.,** Bundesen C., Olson A., Humphreys G., Ward R., Kyllingsbæk S., van Raamsdonk M., Rorden C., Chavda S., 2003. Attentional functions in dorsal and ventral simultanagnosia. *Cognitive Neuropsychology*, 20(8), 675–701.

**Dyrholm, M.,** Kyllingsbaek, S., Espeseth, T., Bundesen, C. 2011. Generalizing parametric models by introducing trial-by-trial parameter variability: The case of TVA. *Journal of Mathematical Psychology*, 55(6), 416-29.

**Espeseth, T.,** Vangkilde, S.A., Petersen, A., Dyrholm, M., Westlye, L.T., 2014. TVA-based assessment of attentional capacities-associations with age and indices of brain white matter microstructure. *Front. Psychol.* 5, 1177.

**Fama, R.,** Sullivan, E.V., 2015. Thalamic structures and associated cognitive functions: Relations with age and aging. *Neurosci Biobehav Rev.*, 54, 29–37.

**Fan, J.,** Mc Candliss, B.D., Sommer, T., Raz, A., Posner, M.I., 2002. Testing the efficiency and independence of attentional networks. *J. Cogn. Neurosci.* 14, 340–347.

**Finke, K.,** Bublak, P., Krummenacher, J., Kyllingsbæk, S., Müller, H. J., & Schneider, W. X. 2005. Usability of a theory of visual attention (TVA) for parameter-based measurement of attention I: Evidence from normal subjects. *Journal of the International Neuropsychological Society*, 11, 832-842.

**Finke, K.,** Bublak, P., Dose, M., Müller, H. J., Schneider, W. X., 2006. Parameter-based assessment of spatial and non-spatial attentional deficits in Huntington's disease. *Brain.* 129(5), 1137–51.

**Finke, K.,** Schneider, W. X., Redel, P., Dose, M., Kerkhoff, G., Müller, H. J., Bublak, P., 2007. The capacity of attention and simultaneous perception of objects: A group study of Huntington's disease patients. *Neuropsychologia*, 45(14), 3272-3284.

**Finke, K.,** Schwarzkopf, W., Müller, U., Frodl, T., Müller, H. J., Schneider, W. X., Engel, R. R., Riedel, M., Möller, H.-J., Hennig-Fast, K., 2011. Disentangling the adult attention-deficit hyperactivity disorder endophenotype: parametric measurement of attention. *Journal of Abnormal Psychology*, 120(4), 890.

**Finke, K.,** Neitzel, J., Bäuml, J.G., Redel, P., Müller, H.J., Meng, C., Jaekel, J., Daamen, M., Scheef, L., Busch, B., Baumann, N., Boecker, H., Bartmann, P., Habekost, T., Wolke, D., Wohlschläger, A.,

Sorg, C., 2015. Visual attention in preterm-born adults: specifically impaired attentional sub-mechanisms that link with altered intrinsic brain networks in a compensation-like mode. *NeuroImage* 107, 95-106.

**Gazzaley, A., Cooney, J.W., Rissman, J., D'Esposito, M., 2005.** Top-down suppression deficit underlies working memory impairment in normal aging. *Nat Neurosci.* 8,1298--1300.

**Ge, Y., Grossman, R.I., Babb, J.S., Rabin, M.L., Mannon, L.J., Kolson, D.L., 2002.** Age-related total gray matter and white matter changes in normal adult brain. Part I: volumetric MR imaging analysis. *AJNR Am J Neuroradiol.* 23(8),1327-33.

**de Groot, M., Ikram, M.A., Akoudad, S., Krestin, G.P., Hofman, A., van der Lugt, A., Niessen, W.J., Vernooij, M.W., 2015.** Tract-specific white matter degeneration in aging: the Rotterdam Study. *Alzheimers Dement.,* 11(3), 321-30.

**Guillery, R.W., Sherman, S.M., 2002.** Thalamic relay functions and their role in cortico-cortical communication: generalizations from the visual system. *Neuron,* 33(2),163-75. Review.

**Habekost, T., Bundesen, C., 2003.** Patient assessment based on a theory of visual attention (TVA): subtle deficits after a right frontal-subcortical lesion. *Neuropsychologia* 41, 1171–1188.

**Habekost, T., Rostrup, E., 2006.** Persisting asymmetries of vision after right side lesions. *Neuropsychologia* 44, 876–895.

**Habekost, T., Rostrup, E., 2007.** Visual attention capacity after right hemisphere lesions. *Neuropsychologia,* 45(7), 1474–88.

**Habekost, T., Petersen, A., Vangkilde, S., 2014.** Testing attention: comparing the ANT with TVA-based assessment. *Behav.Res.Methods,* 46, 81–94.

**Hagmann, P., Cammoun, L., Gigandet, X., Meuli, R., Honey, C.J., Wedeen, V.J., Sporns, O., 2008.** Mapping the structural core of human cerebral cortex. *PLoS Biol.* 6 (7), e159.

**Hebb, D. O., 1949.** Organization of behavior. New York: Wiley.

**Honey, C.J., Sporns, O., Cammoun, L., Gigandet, X., Thiran, J.P., Meuli, R., Hagmann, P., 2009.** Predicting human resting-state functional connectivity from structural connectivity. *Proc. Natl. Acad. Sci. USA* 106, 2035–2040.

**Hugenschmidt, C.E., Peiffer, A.M., Kraft, R.A., Casanova, R., Deibler, A.R., Burdette, J.H., Maldjian, J.A., Laurienti, P.J., 2008.** Relating imaging indices of white matter integrity and volume in healthy older adults. *Cereb Cortex,* 18, 433-442.

**Hughes, E.J., Bond, J., Svrckova, P., Makropoulos, A., Ball, G., Sharp, D.J., Edwards, A.D., Hajnal, J.V., Counsell, S.J.** 2012. Regional changes in thalamic shape and volume with increasing age. *NeuroImage*. 63,1134–1142.

**Jacobs, B., Driscoll, L., Schall, M.,** 1997. Life-span dendritic and spine changes in areas 10 and 18 of human cortex: a quantitative Golgi study. *J Comp. Neurol.*, 386, 661-680.

**Jacobs, H.I., Leritz, E.C., Williams, V.J., Van Boxtel, M.P., van der Elst, W., Jolles, J., Verhey, F.R., McGlinchey, R.E., Milberg, W.P., Salat, D.H.,** 2013. Association between white matter microstructure, executive functions and processing speed in older adults: The impact of vascular health. *Hum Brain Mapp.*, 34, 77–95.

**Jbabdi, S., & Johansen-Berg, H.,** 2011. Tractography: where do we go from here? *Brain Connect*, 1(3), 169-183.

**Jellison B.J., Field, A.S., Medow, J., Lazar, M., Salamat, MS., Alexander, A.L.,** 2004. Diffusion tensor imaging of cerebral white matter: a pictorial review of physics, fiber tract anatomy, and tumor imaging patterns. *AJNR Am J Neuroradiol.*, 25(3), 356-69.

**Jones, D.K.,** 2010. Challenges and limitations of quantifying connectivity in the human brain in vivo with diffusion MRI. *Imaging Med.*, 2, 341-355.

**Jones, D.K., Knosche, T.R., Turner, R.,** 2013. White matter integrity, fiber count, and other fallacies: the do's and don'ts of diffusion MRI. *Neuroimage*, 73, 239-54.

**Jost, K., Bryck, R. L., Vogel, E. K., & Mayr, U.,** 2011. Are Old Adults Just Like Low Working Memory Young Adults? Filtering Efficiency and Age Differences in Visual Working Memory. *Cerebral Cortex*, 21, 1147-1154.

**Karolis, V.R., Froudust-Walsh ,S., Brittain, P.J., Kroll, J., Ball, G., Edwards, A.D., Dell'Acqua, F., Williams, S.C., Murray, R.M., Nosarti, C.** 2016. Reinforcement of the Brain's Rich-Club Architecture Following Early Neurodevelopmental Disruption Caused by Very Preterm Birth. *Cerebral Cortex*, 26 (3), 1322-1335.

**Komitova, M., Xenos, D., Salmaso, N., Tran, K.M., Brand, T., Schwarz, M.L., Ment, L., Vaccarino, F.M.,** 2013. Hypoxia-induced developmental delays of inhibitory interneurons are reversed by environmental enrichment in the postnatal mouse forebrain. *J Neurosci* 33, 13375-13387.

**Kraft, A., Irlbacher ,K., Finke, K., Kaufmann, C., Kehrer, S., Liebermann, D., Bundesen, C., Brandt, S.A.,** 2015. Dissociable spatial and non-spatial attentional deficits after circumscribed thalamic stroke. *Cortex*, 64, 327–342.

- Kringelbach**, M., McIntosh, A., Ritter, P., Jirsa, V., Deco, G., 2015. The Rediscovery of Slowness: Exploring the Timing of Cognition. *Trends in Cognitive Sciences Elsevier* {BV} 616-628.
- Kumar**, R., Chavez, A.S., Macey, P.M., Woo, M.A., Harper, R.M., 2013. Brain axial and radial diffusivity changes with age and gender in healthy adults. *Brain Res.* 1512, 22-36.
- Kyllingsbæk**, S., 2006. Modeling visual attention. *Behavior. Research. Methods*, 38, 123–133.
- Le Bihan**, D., Breton, E., Lallemand, D., Aubin, M.L., Vignaud, J., Laval-Jeantet, M., 1988. Separation of diffusion and perfusion in intravoxel incoherent motion MR imaging. *Radiology*, 168(2), 497-505.
- Le Bihan**, D., 1990. Diffusion/perfusion MR imaging of the brain: from structure to function. *Radiology*, 177(2), 328-9.
- Lebel**, C., Walker, L., Leemans, A., Phillips, L., Beaulieu, C., 2008. Microstructural maturation of the human brain from childhood to adulthood. *Neuroimage*. 40(3),1044-55.
- Lockhart**, S.N., Mayda, A.B., Roach, A.E., Fletcher, E., Carmichael, O., Maillard, P., Schwarz, C.G., Yonelinas, A.P., Ranganath, C., Decarli, C., 2012. Episodic memory function is associated with multiple measures of white matter integrity in cognitive aging. *Front Hum Neurosci.*, 6:56.
- Luck**, S.J., Vogel, E.K., 1997. The capacity of visual working memory for features and conjunctions. *Nature*, 390, 279–281.
- Madden**, D.J., Spaniol, J., Costello, M.C., Bucur, B., White, L.E., Cabeza, R., Davis, S.W., Dennis, N.A., Provenzale, J.M., Huettel, S.A., 2009a. Cerebral white matter integrity mediates adult age differences in cognitive performance. *J Cogn Neurosci.*, 21, 289–302.
- Madden**, D.J., Bennett, I.J., Song, A.W., 2009b. Cerebral white matter integrity and cognitive aging: Contributions from diffusion tensor imaging. *Neuropsychol Rev.*, 19, 415–435.
- Madden**, D.J., Bennett, I.J., Burzynska, A., Potter, G.G., Chen, N.K., Song, A.W., 2012. Diffusion tensor imaging of cerebral white matter integrity in cognitive aging. *Biochim Biophys Acta*, 1822, 386–400.
- McAvinue**, L.P., Habekost, T., Johnson, K.A., Kyllingsbaek, S., Vangkilde, S., Bundesen, C., Robertson, I.H., 2012. Sustained attention, attentional selectivity, and attentional capacity across the lifespan. *Atten Percept Psychophys*, 74(8), 1570-82.
- Meier-Ruge**, W., Ulrich, J., Bruhlmann, M., Meier, E., 1992. Age-related white matter atrophy in the human brain. *Ann. N. Y. Acad. Sci.* 673, 260–269.

- Meng, C.**, Bäuml, J.G., Daamen, M., Jaekel, J., Neitzel, J., Scheef, L., Busch, B., Baumann, N., Boecker, H., Zimmer, C., Bartmann, P., Wolke, D., Wohlschläger, A.M., Sorg, C., 2015. Extensive and interrelated subcortical white and gray matter alterations in preterm-born adults. *Brain Struct Funct.*, 221 (4), 2109-21.
- Ment, L.R.**, Hirtz, D., Huppi, P.S., 2009. Imaging biomarkers of outcome in the developing preterm brain. *Lancet Neurology* 8 (11), 1042-1055.
- Mori, S.**, Crain, B.J., Chacko, V.P., van Zijl, P.C., 1999. Three-dimensional tracking of axonal projections in the brain by magnetic resonance imaging. *Ann. Neurol.*, 45(2), 265-269.
- Moseley, M.E.**, Cohen, Y., Kucharczyk, J., Mintorovitch, J., Asgari, H.S., Wendland, M.F., Tsuruda, J., Norman, D., 1990. Diffusion-weighted MR imaging of anisotropic water diffusion in cat central nervous system. *Radiology*, 176(2), 439-445.
- Nosarti, C.**, Giouroukou, E., Micali, N., Rifkin, L., Morris, R. G., Murray, R. M., 2007. Impaired executive functioning in young adults born very preterm. *Journal of the International Neuropsychological Society*, 13(04), 571–81.
- Olshausen, B.A.**, Anderson, C.H., Van Essen, D.C., 1993. A neurobiological model of visual attention and invariant pattern recognition based on dynamic routing of information. *J. Neurosci.*, 13, 4700-4719.
- Pasternak, O.**, Sochen, N., Gur, Y, Intrator, N., Assaf, Y., 2009. Free water elimination and mapping from diffusion MRI. *Magn. Res. Med.* 62(3), 717-30.
- Peters A.** 2002. The effects of normal aging on myelin and nerve fibers: a review. *Journal of Neurocytology*. 31, 581–593.
- Pfefferbaum, A.**, Sullivan, E.V., Hedehus, M., Lim, K.O., Adalsteinsson, E., Moseley, M., 2000. Age-related decline in brain white matter anisotropy measured with spatially corrected echo-planar diffusion tensor imaging. *Magn. Reson. Med.*, 44, 259-268.
- Pfefferbaum, A.**, Sullivan, E.V., 2003. Increased brain white matter diffusivity in normal adult aging: relationship to anisotropy and partial voluming. *Magn Reson Med.*, 49, 953–961.
- Pierpaoli, C.**, Basser, P.J., 1996. Toward a quantitative assessment of diffusion anisotropy. *Magn. Reson. Med.*, 36(6), 893-906.
- Pierpaoli, C.**, Barnett, A., Pajevic, S., Chen, R., Penix, L.R., Virta, A., Basser, P., 2001. Water diffusion changes in Wallerian degeneration and their dependence on white matter architecture. *Neuroimage*. 2001,6(1),1174-85.

**Raz, N., Lindenberger, U., Rodrigue, K.M., Kennedy, K.M., Head, D., Williamson, A., Dahle, C., Gerstorff, D., Acker, J.D., 2005.** Regional brain changes in aging healthy adults: general trends, individual differences and modifiers. *Cereb Cortex*, 15, 1676–89.

**Raz, N., Rodrigue, K.M., 2006.** Differential aging of the brain: patterns, cognitive correlates and modifiers. *Neurosci Biobehav Rev.* 30(6), 730–4.

**Redel, P., Bublak, P., Sorg, C., Kurz, A., Förstl, H., Müller, H. J., Schneider, W. X., Pernecky, R., Finke, K., 2012.** Deficits of spatial and task-related attentional selection in mild cognitive impairment and Alzheimer's disease. *Neurobiology of Aging.* 33(1), 195.

**Reveley, C., Seth, A.K., Pierpaoli, C., Silva, A.C., Yu, D., Saunders, R.C., Leopold, D.A., Ye, F.Q., 2015.** Superficial white matter fiber systems impede detection of long-range cortical connections in diffusion MR tractography. *Proc Natl Acad Sci U S A*, 112, 2820–2828.

**Reynolds, J.H., Chelazzi, L., Desimone, R., 1999.** Competitive mechanisms subserve attention in macaque areas V2 and V4. *J Neurosci.*, 19(5), 1736-53.

**Robinson, D.L., Petersen, S.E., 1992.** The pulvinar and visual salience. *Trends Neurosci.*, 15, 127-132.

**Saalman, Y.B., Kastner, S., 2011.** Cognitive and perceptual functions of the visual thalamus. *Neuron*, 71 , 209-223.

**Saalman, Y.B., Pinsk, M.A., Wang, L., Li X., Kastner S., 2012.** The pulvinar regulates information transmission between cortical areas based on attention demands. *Science*, 337, 753-756.

**Salami, A., Eriksson, J., Nilsson, L.G., Nyberg, L., 2012.** Age-related white matter microstructural differences partly mediate age-related decline in processing speed but not cognition. *Biochim Biophys Acta.*, 1822, 408–415.

**Salat, D.H., Chen, J.J., Van der Kouwe, A.J., Greve, D.N., Fischl, B., Rosas, H.D., 2011.** Hippocampal degeneration is associated with temporal and limbic gray matter/white matter tissue contrast in Alzheimer's disease. *Neuroimage.* 54(3),1795-802.

**Salmaso, N., Jablonska, B., Scafidi, J., Vaccarino, F.M., Gallo, V., 2014.** Neurobiology of premature brain injury. *Nat Neurosci.*, 17, 341-346.

**Salthouse, T.A., 2011.** Effects of age on time-dependent cognitive change. *Psychol Sci.* 22(5), 682-8.

**Salvan, P., Froudust Walsh, S., Allin, M.P., Walshe, M., Murray, R.M., Bhattacharyya, S., McGuire, P.K., Williams, S.C., Nosarti, C., 2014.** Road work on memory lane-Functional and structural alterations to the learning and memory circuit in adults born very preterm. *NeuroImage*, 102, 152–61

- Sander**, M.C., Werkle-Bergner, M., Lindenberger, U., 2011. Contralateral delay activity reveals life-span age differences in top-down modulation of working memory contents. *Cereb. Cortex*, 12, 2809-2819.
- Schmid**, M.C., Singer, W., Fries, P., 2012. Thalamic coordination of cortical communication. *Neuron*, 75(4), 551-2.
- Schulze**, E.T., Geary, E.K., Susmaras, T.M., Paliga, J.T., Maki, P.M., Little, D.M., 2011. Anatomical correlates of age-related working memory declines. *J Aging Res.*, 2011:606871.
- Schuz**, A.B.V., 2002. The human cortical white matter: quantitative aspects of cortico-cortical long-range connectivity. In: Shuey, A. & Miller, R., eds. *Cortical Areas: Unity and Diversity*. London: Taylor & Francis 377–384.
- Sexton** C.E., Mackay, C.E., Lonie, J.A., Bastin, M.E., Terriere, E., O'Carroll, R.E., Ebmeier, K.P., 2010. MRI correlates of episodic memory in Alzheimer's disease, mild cognitive impairment, and healthy aging. *Psychiatry Res.*, 184, 57–62.
- Sherman**, S.M., Guillery, R.W., 2002. The role of the thalamus in the flow of information to the cortex. *Philos Trans R Soc Lond B Biol Sci.* 357(1428), 1695-708. Review.
- Sherman**, S.M., Guillery, R.W., 2013. *Functional Connections of Cortical Areas: A New View from the Thalamus*. MIT Press, 1<sup>st</sup> edition.
- Shipp**, S., 2003. The functional logic of cortico-pulvinar connections. *Philos. Trans. R. Soc. Lond. B Biol. Sci.*, 358, 1605-1624.
- Shipp**, S., 2004. The brain circuitry of attention. *Trends Cogn. Sci.*, 8, 223-23.
- Shum**, D., Neulinger, K., O'Callaghan, M., Mohay, H., 2008. Attentional problems in children born very preterm or with extremely low birth weight at 7-9 years. *Arch Clin Neuropsychol.* 23, 103-112.
- Smith**, S.M., Jenkinson, M., Woolrich, M.W., Beckmann, C.F., Behrens, T.E., Johansen-Berg, H., Bannister, P.R., De Luca, M., Drobnjak, I., Flitney, D.E., Niazy, R.K., Saunders, J., Vickers, J., Zhang, Y., De Stefano, N., Brady, J.M., Matthews, P.M., 2004. Advances in functional and structural MR image analysis and implementation as FSL. *NeuroImage*, 23 Suppl 1, S208-219.
- Smith**, S.M., Jenkinson, M., Johansen-Berg, H., Rueckert, D., Nichols, T.E., Mackay, C.E., Watkins, K.E., Ciccarelli, O., Cader, M.Z., Matthews, P.M., Behrens, T.E.J., 2006. Tract-based spatial statistics: Voxelwise analysis of multi-subject diffusion data. *NeuroImage*, 31, 1487-1505.

**Sorg, C., Myers, N., Redel, P., Bublak, P., Riedl, V., Manoliu, A., Pernecky, R., Grimmer, T., Kurz, A., & Förstl, H., 2012.** Asymmetric loss of parietal activity causes spatial bias in prodromal and mild Alzheimer's disease. *Biological Psychiatry*. 71(9), 798–804.

**Starrfelt, R., Habekost T., Leff A. P., 2009.** Too little, too late: reduced visual span and speed characterize pure alexia. *Cerebral Cortex*, 19(12), 2880–90.

**Starrfelt, R., Habekost, T., Gerlach, C., 2010.** Visual processing in pure alexia: a case study. *Cortex*, 46, 242–255.

**Stämpfli, P., Sommer, S., Czell, D., Kozerke, S., Neuwirth, C., Weber, M., Sartoretti-Schefer, S., Seifritz, E., Gutzeit, A., Reischauer, C., 2018.** Investigation of Neurodegenerative Processes in Amyotrophic Lateral Sclerosis Using White Matter Fiber Density. *Clin Neuroradiol*. 2018 Feb 19. Epub

**Strang-Karlsson, S., Andersson, S., Paile-Hyvarinen, M., Darby, D., Hovi, P., Raikkonen, K., Pesonen, A.K., Heinonen, K., Jarvenpaa, A.L., Eriksson, J.G., Kajantie, E., 2010.** Slower reaction times and impaired learning in young adults with birth weight <1500 g. *Pediatrics*. 125, 74-82.

**Sullivan, E.V., Pfefferbaum, A., 2006.** Diffusion tensor imaging and aging. *Neurosci. Biobehav. Rev.*, 30, 749–761.

**Sullivan E.V., Rohlfing, T., Pfefferbaum, A., 2010a.** Quantitative fiber tracking of lateral and interhemispheric white matter systems in normal aging: relations to timed performance. *Neurobiol. Aging*. 31(3),464-81

**Teipel, S.J., Meindl, T., Wagner, M., Stieltjes, B., Reuter, S., Hauenstein, K.H., Filippi, M., Ernemann, U., Reiser, M.F., Hampel, H., 2010.** Longitudinal changes in fiber tract integrity in healthy aging and mild cognitive impairment: a DTI follow-up study. *J Alzheimers Dis*. 22,507–522.

**Thomas, C., Ye, F.Q., Irfanoglu, M.O., Modi, P., Saleem, K.S., Leopold, D.A., Pierpaoli, C., 2014.** Anatomical accuracy of brain connections derived from diffusion MRI tractography is inherently limited. *Proc Natl Acad Sci U S A*, 111,16574–16579.

**Todd, J.J., Marois, R., 2004.** Capacity limit of visual short-term memory in human posterior parietal cortex. *Nature* 428 (6984), 751–754.

**Toulmin, H., Beckmann, C.F., O’Muircheartaigh, J., Ball, G., Nongena, P., Makropoulos, A., Ederies, A., Counsell, S.J., Kennea, N., Arichi, T. Tusor, N., Rutherford, M.A., Azzopardi, D., Gonzalez-Cinca, N., Hajnal, J.V., Edwards, A.D. 2015.** Specialization and integration of functional thalamocortical connectivity in the human infant. *Proc. Natl. Acad. Sci.*, 112, 6485-6490.

- Tournier, J.D., Calamante, F., Gadian, D.G., Connelly, A., 2004.** Direct estimation of the fiber orientation density function from diffusion-weighted MRI data using spherical deconvolution. *NeuroImage*, 23, 1176-1185.
- Tuch, D.S., Reese, T.G., Wiegell, M.R., Makris, N., Belliveau, J.W., Wedeen, V.J., 2002.** High angular resolution diffusion imaging reveals intravoxel white matter fibre heterogeneity. *Magn. Reson. Med.* 48, 577–582.
- Tuch, D.S., Reese, T.G., Wiegell, M.R., Wedeen, V.J., 2003.** Diffusion MRI of complex neural architecture. *Neuron*. 40, 885–895.
- Tuch, D.S., Salat, D.H., Wisco, J.J., Zaleta, A.K., Hevelone, N.D., Rosas, H.D., 2005.** Choice reaction time performance correlates with diffusion anisotropy in white matter pathways supporting visuospatial attention. *Proc. Natl. Acad. Sci. U S A* 102, 12212–12217.
- Van der Flier, W., van den Heuvel, D., Weverling-Rijnsburger, A., Bollen, E., Westendorp, R., van Buchem, M., Middelkoop, H.A., 2002.** Magnetization transfer imaging in normal aging, mild cognitive impairment, and Alzheimer’s disease. *Ann Neurol*, 52, 62–7.
- Van de Weijer-Bergsma, E., Wijnroks, L., Jongmans, M.J., 2008.** Attention development in infants and preschool children born preterm: a review. *Infant Behav Dev.* 31, 333-351.
- Vernooij, M.W., de Groot, M., van der Lugt, A., Ikram, M.A., Krestin, G.P., Hofman, A., Niessen, W.J., Breteler, M.M., 2008.** White matter atrophy and lesion formation explain the loss of structural integrity of white matter in aging. *Neuroimage*, 43(3), 470-7.
- Verhaegen, P., Marcoen, A., Goossens, L., 1993.** Facts and fiction about memory aging: A quantitative integration of research findings. *Journal of Gerontology: Psychological Sciences*, 48,157-171.
- Vos, S.B., Jones, D.K., Viergever, M.A., Leemans, A., 2011.** Partial volume effect as a hidden covariate in DTI analyses. *Neuroimage*. 55(4), 1566-76.
- Walhovd, K.B., Westlye, L.T., Amlie, I., Espeseth, T., Reinvang, I., Raz, N., Agartz, I., Salat, D.H., Greve, D.N., Fischl, B., Dale, A.M., Fjell, A.M., 2011.** Consistent neuroanatomical age-related volume differences across multiple samples. *Neurobiol Aging*. 32(5),916-32.
- Westlye, L.T., Walhovd, K.B., Dale, A.M., Bjørnerud, A., Due-Tønnessen, P., Engvig, A., Grydeland, H., Tamnes, C.K., Østby, Y., Fjell, A.M., 2010.** Life-span changes of the human brain white matter: diffusion tensor imaging (DTI) and volumetry. *Cereb Cortex*, 20(9),2055-68.

**Wiegand, I., Töllner, T., Dyrholm, M., Müller, H. J., Bundesen, C., & Finke, K. (2014a).** Neural correlates of age-related decline and compensation in visual attention capacity. *Neurobiol. Aging*, 35, 2161–2173.

**Wiegand, I., Töllner, T., Habekost, T., Dyrholm, M., Müller, H. J., & Finke, K. (2014b).** Distinct neural markers of TVA-based visual processing speed and short-term storage capacity parameters. *Cereb. Cortex*, 24, 1967-1978.

**Wiegand, I., Lauritzen, M.J., Osler, M., Mortensen, E.L., Rostrup, E., Rask, L., Richard, N., Horwitz, A., Benedek, K., Vangkilde, S., Petersen, A., 2018.** EEG correlates of visual short-term memory in older age vary with adult lifespan cognitive development. *Neurobiol. Aging*, 62, 210-220.

**Wozniak, J.R., Lim, K.O., 2006.** Advances in white matter imaging: a review of in vivo magnetic resonance methodologies and their applicability to the study of development and aging. *Neurosci Biobehav Rev.* 2006, 30(6), 762-74.

**Xu, Y., Chun, M.M., 2006.** Dissociable neural mechanisms supporting visual short-term memory for objects. *Nature* 440 (7080), 91–95.

**Ystad, M., Hodneland, E., Adolfsdottir, S., Haasz, J., Lundervold, A.J., Eichele, T., Lundervold, A., 2011.** Corticostriatal connectivity and cognition in normal aging: A combined DTI and resting state fMRI study. *Neuroimage*, 55, 24–31.

**Zahr, N.M., Rohlfing, T., Pfefferbaum, A., Sullivan, E.V., 2009.** Problem solving, working memory, and motor correlates of association and commissural fiber bundles in normal aging: A quantitative fiber tracking study. *Neuroimage*. 44,1050–1062.

**Zhang, Y., Du, A.T., Hayasaka, S., Jahng, G.H., Hlavin, J., Zhan, W., Weiner, M.W., Schuff, N., 2010.** Patterns of age-related water diffusion changes in human brain by concordance and discordance analysis. *Neurobiol Aging*. 31(11),1991-2001.

**Zhang, H., Hubbard, P. L., Parker, G. J. M., Alexander, D. C., 2011.** Axon diameter mapping in the presence of orientation dispersion with diffusion MRI. *Neuroimage* 56, 1301–1315

**Zhang, H., Schneider, T., Wheeler-Kingshott, C. A., Alexander, D. C., 2012.** NODDI: practical in vivo neurite orientation dispersion and density imaging of the human brain. *Neuroimage* 61, 1000–1016.

---

# ACKNOWLEDGMENTS

First, I would like to thank specifically my supervisor **PD Dr. Kathrin Finke** for giving me the opportunity to take part in such an interesting project although I had no previous experience in the field of visual attention or DTI and to discover a new field. I also would like to thank her for her highly valuable input and comments all along my PhD and for letting me work independently. I would also like to thank particularly my second supervisor **PD Dr. Christian Sorg** for his regular supervision while giving me the freedom to develop my ideas; I am looking forward to our new projects. I am very thankful to both of them for their support, their enthusiasm and stimulating discussions. They taught me a lot and helped me grow as a researcher.

I would like to thank specifically **Prof. Dr. Hermann Müller** for co –selecting me to be part of the INDIREA project and for always giving very relevant and helpful inputs during our TAC meetings. I also would like to thank him and the department of Psychology from the LMU for funding me for 8 months after the Marie Curie grant finished.

A very special thank you to **Dr. Chun Meng** who has been an amazing mentor since the first day I started at the TUM-NIC. I would like to thank him for teaching me all the basics about DTI and giving me the proper tools to fly with my own wings. I also would like to thank him for his constant professionalism, happiness, friendship and for always being available to discuss about DTI-related issues even after he left the group.

I would also like to particularly thank my first mentor **Dr. Gregory Dal Bo** for being of great advice and for supporting me ever since he supervised me at McGill University six years ago. This first laboratory experience really gave me a taste for research. I would also like to thank him for sending me the application for this PhD position and encouraging me to apply, without him this thesis would not have seen the light of day.

I would especially like to thank my “work husband” **Natan Napiorkowski** and my “work wife” **Adriana Ruiz-Rizzo** for the great team work on the INDIREA project and for this unforgettable marriage experience. A special thank you to **Julia Neitzel** for her help with recruiting and scanning the participants and for accepting the charge of honorary member of the INDIREA family. Finally I would like to thank all of them for the amazing moments we spent together not only during the INDIREA or GSN workshops and retreats but especially outside of work. These moments have been essential to help me go through the tougher times of this PhD.

A special thank you to my amazing friends and colleagues, **Josef Bäuml** for sharing with me his expertise on preterm birth and his office, **Gabriel Castrillon**, **Tim Reess** and **Martin Gruber** for their help with programming, **Georgiana Rus** for the useful discussions about probabilistic

tractography, and together with **Judita Huber, Yue Ren, Siyi Chen, Xiyao Xie, Melanie Penning, Marleen Haupt Martina Postorino, Deniz Gürsel, Monica Emch, Katarzyna Kurcyus, Efsun Annac, Theresa Raiser, Nicoleta Rus, Henrike Bäuerlein, Mario Archila, Mihai Avram, Anselm Doll, Gasper Stukelj, Son Ta Dinh, Felix Brandl, Maria Berndt, Jens Göttler and Dennis Hedderich** for their constant friendship, support and all the great moments we shared. My time as a PhD student wouldn't have been as enjoyable without them.

A special thank you also to **Dr. Christine Preibisch** and **Stephan Kaczmarz** for showing us how to operate the scanner and for their help solving any problems originating from it.

I would like to especially thank my friends, **Gianluca Russo, Elisabetta Petrozziello and Giorgia Pollina**, for brightening our German courses and for welcoming me as an honorary member to their "Italian club".

A very special thank you also to **Francois Robert** and **Chloe Coudray** for making me feel at home and allowing me to express once in a while the values and pride dear to our country.

A big thank you to my great friend **Nina Nakayama** for her support and for proof-reading this thesis.

A huge thank you to **all the participants** for taking part in our studies and for their patience.

I would like to thank the Marie Curie ITN program from the European Union for financing this thesis and for the great opportunities they have given me to discover universities all over Europe. I also would like to thank all the people involved in the INDIREA network and particularly **Eleonora Fulcini** and **Iske Marshall**, for their amazing job as coordinators of the project.

I also would like to thank **Professor Claus Zimmer** from the Neuroradiology department of the Klinikum rechts der Isar for providing the MRI infrastructure and funds to finish writing this thesis.

A huge thank you to the GSN especially to **Birgit Reinbold, Julia Brenndörfer, Stephanie Bosse, Renate Herzog, Lena Bittl, Catherine Botheroyd and Raluca Goron** for all their help, wonderful administrative work and organization of amazing scientific and social events. Thank you also to the **GSN scientific Board** for financing me during 4 months after the Marie Curie grant finished.

Finally, I would like to thank from the bottom of my heart the most important people in my life who have been constantly providing me with their support:

Mein Liebling and **Dr. rer. nat. Felix Bäuerlein** not only for his love and support but also for all the scientific discussions we had which have helped me see my work from a different perspective and have led to a very successful collaboration on one manuscript. Very special thank you to his family as well for their support and for making me feel at home.

Un énorme merci à mes amis de très longue date Olivia de Courcel, Helene Patin, Celine Roustan, Alexandre et Juliette Bours, Anthony Binst, Dimitri Labat, Manon Raineri, Margaux Thierry, Pierre Van de Velde, Flavien Leclerc, Ariane Lemieux-Lepage, Salima Bouzaidi et familles de cœur, les familles De Courcel, Roustan, Bours et Patin pour leur amitié et leur soutien inconditionnels depuis 22 ans, je ne serais pas arrivée jusqu'ici sans eux.

Enfin, je voudrais terminer par adresser mes remerciements du fond du coeur a ma famille et plus particulierement a ma maman Patricia, la personne la plus forte et courageuse que je connaisse, pour son amour et soutien sans failles et pour avoir toujours cru en moi, même dans mes moments de doute les plus intenses. Sans elle, cette these n'aurait pas pu voir le jour.



## LIST OF PUBLICATIONS

1. **Menegaux A.**, Bäuerlein F.J.B., Vania A., Napiorkowski N., Neitzel J., Ruiz-Rizzo A., Müller H.J., Sorg C., Finke K. Aging modulates the association between vSTM capacity and the structural connectivity of posterior thalamus to occipital cortices (*in prep.*).
2. **Menegaux A.**, Napiorkowski N., Neitzel J., Ruiz-Rizzo A., Petersen A., Müller H.J., Sorg C., Finke K. Structural connectivity between posterior thalamus and occipital cortices underpins visual short-term memory capacity and attentional weighting in humans (Under review in *NeuroImage*).
3. Hedderich D., Bäuml J.G., Berndt M., **Menegaux A.**, Scheef L., Daamen M., Zimmer C., Boecker H., Bartmann P., Wolke D., Gaser C., Sorg C. Aberrant gyrification mediates the link between gestational age and adult IQ after premature birth (Under review in *Brain*).
4. Berndt M., Bäuml J.G., **Menegaux A.**, Meng C., Daamen M., Baumann N., Zimmer C., Boecker H., Bartmann P., Wolke D., Sorg C. Impaired structural connectivity between the pulvinar and dorsal attention network mediates the impact of premature birth on adult visual-spatial abilities (Under review in *Human Brain Mapping*).
5. Ruiz-Rizzo A.L., Sorg C., Napiorkowski N., Neitzel J., **Menegaux A.**, Müller H.J., Vangkilde S., Finke K. (2018). Decreased cingulo-opercular network functional connectivity mediates the impact of aging on visual processing speed. *Neurobiology of Aging* 73,50-60.
6. Vosberg D.\*, Zhang Y.\*, **Menegaux A.**, Chalupa A., Manitt C., Zehntner S., Eng C., DeDuck K., Allard D., Durand F., Dagher A., Benkelfat C., Srour M., Joobar R., Lepore F., Rouleau G., Théoret H., Bedell B., Flores C., Leyton M. (2018). Mesocorticolimbic Connectivity and Volumetric Alterations in DCC Mutation Carriers. *Journal of Neuroscience* 38(20),4655-4665.
7. **Menegaux, A.**, Meng, C., Neitzel, J., Bäuml, J. G., Müller, H.J., Bartmann, P. Wolke, D. Wohlschläger, A., Finke, K.\*, Sorg, C.\*. (2017). Impaired visual short-term memory capacity is distinctively associated with structural connectivity of the posterior thalamic radiation and the splenium of the corpus callosum in preterm-born adults. *NeuroImage* 150, 68-76.
8. Rocchetti J.\*, Isingrini E.\*, Dal Bo G.\*, Sagheby S., **Menegaux A.**, Tronche F., Levesque D., Moquin L., Gratton A., Tak Pan Wong T.P., Rubinstein M. and Giros B., 2015. Presynaptic D2 Dopamine Receptors Control Long-Term Depression and Memory Processes in the Temporal Hippocampus. *Biological Psychiatry* 77(6), 513-25.

\*These authors contributed equally



---

# CURRICULUM VITAE

**Aurore Menegaux**

Born on June 21st 1991

Andreestrasse 9, apt 413

80634 München

0176 72857384

[menegaux.aurore@gmail.com](mailto:menegaux.aurore@gmail.com)

## EDUCATION

**10/2014 to present: *PhD in systemic neurosciences***

Graduate School of Systemic Neurosciences, Ludwig-Maximilians-Universität München, Germany

**09/2011 –09/2013: *M.Sc. in Integrative Biology and Physiology***

Université Pierre et Marie Curie, Paris VI, in association with Ecole Normale Supérieure (ENS) de Paris, Paris, France

-Exchange semester at the Université de Montréal (Winter 2012), Montréal, Canada

**09/2010- 09/2011: *B.Sc. in Life Sciences***

Université Pierre et Marie Curie, Paris VI, Paris, France

**09/2008- 09/2010: *Preparatory classes in biology, chemistry, physics and earth sciences***

Lycée Thiers, Marseille, France

## PROFESSIONAL EXPERIENCE

**05/2018 to present: *Research Associate***

Department of Neuroradiology, Klinikum rechts der Isar, Technische Universität München, Germany

**04/2014- 04/2018: *Marie Curie early stage researcher***

Department of General and Experimental Psychology, Ludwig-Maximilians-Universität München, Germany

**02/2013 - 08/2013: *Research Assistant***

Douglas Mental Health University Institute, McGill University, Montréal, Canada

04/2012 – 08/2012: *Research Assistant*

Douglas Mental Health University Institute, McGill University, Montréal, Canada

### PUBLICATIONS

1. Hedderich D., Bäuml J.G., Berndt M., **Menegaux A.**, Scheef L., Daamen M., Zimmer C., Boecker H., Bartmann P., Wolke D., Gaser C., Sorg C. Aberrant gyrification mediates the link between gestational age and adult IQ after premature birth (Under review in *Brain*)
2. Berndt M., Bäuml J.G., **Menegaux A.**, Meng C., Daamen M., Baumann N., Zimmer C., Boecker H., Bartmann P., Wolke D., Sorg C. Impaired structural connectivity between the pulvinar and dorsal attention network mediates the impact of premature birth on adult visual-spatial abilities (Under review in *Human Brain Mapping*)
3. Ruiz-Rizzo A.L., Sorg C., Napiorkowski N., Neitzel J., **Menegaux A.**, Müller H.J., Vangkilde S., Finke K. Decreased cingulo-opercular network functional connectivity mediates the impact of aging on visual processing speed. *Neurobiology of Aging*, in press.
4. Vosberg D\*, Zhang Y\*, **Menegaux A.**, Chalupa A, Manitt C, Zehntner S, Eng C, DeDuck K, Allard D, Durand F, Dagher A, Benkelfat C, Srour M, Joobar R, Lepore F, Rouleau G, Théoret H, Bedell B, Flores C, Leyton M. (2018) Mesocorticolimbic Connectivity and Volumetric Alterations in DCC Mutation Carriers. *Journal of Neuroscience*, 38(20):4655-4665
5. **Menegaux, A.**, Meng, C., Neitzel, J., Bäuml, J. G., Müller, H.J., Bartmann, P. Wolke, D. Wohlschläger, A., Finke, K. \*, Sorg, C. \*, (2017). Impaired visual short-term memory capacity is distinctively associated with structural connectivity of the posterior thalamic radiation and the splenium of the corpus callosum in preterm-born adults. *NeuroImage* 150, 68-76.
6. Rocchetti J.\*, Isingrini E. \*, Dal Bo G. \*, Sagheby S., **Menegaux A.**, Tronche F., Levesque D., Moquin L., Gratton A., Tak Pan Wong T.P., Rubinstein M. and Giros B., 2015. Presynaptic D2 Dopamine Receptors Control Long-Term Depression and Memory Processes in the Temporal Hippocampus. *Biological Psychiatry* 77(6), 513-25.

### SCHOLARSHIPS

**09/2017 – 04/2018** : LMU Munich department of Psychology study scholarship

**05/2017 – 08/2017** : Graduate school of systemic neurosciences GSN-LMU study scholarship

**01/2012 – 04/2012** : Université Pierre and Marie Curie Mobility Scholarship

**04/2012 – 08/2012** : Region Ile de France Mobility scholarship

### SKILLS

Fluent in French and english, advanced knowledge of spanish, basic knowledge of german (A2), rudimentary knowledge of Chinese.

### ADDITIONAL WORK EXPERIENCE

**10/2013 - 02/2014: *Tutor in biology, maths and english***

Cours Ado, Grasse and Le Cannet, France

**07/2012 – 08/2012: *Public awareness / Fundraising agent***

Society for the Protection of Animals Canada, Montréal, Canada

**Summer 2009 and 2010: *Groom***

Equestrian Center La Gourmette, La Foux D'Allos, France



---

# EIDESSTATTLICHE VERSICHERUNG/AFFIDAVIT

Hiermit versichere ich an Eides statt, dass ich die vorliegende Dissertation “The relevance of posterior thalamo-cortical connectivity for visual short term memory capacity: Evidence from aging and premature birth” selbstständig angefertigt habe, mich außer der angegebenen keiner weiteren Hilfsmittel bedient und alle Erkenntnisse, die aus dem Schrifttum ganz oder annähernd übernommen sind, als solche kenntlich gemacht und nach ihrer Herkunft unter Bezeichnung der Fundstelle einzeln nachgewiesen habe.

I hereby confirm that the dissertation “The relevance of posterior thalamo-cortical connectivity for visual short term memory capacity: Evidence from aging and premature birth” is the result of my own work and that I have only used sources or materials listed and specified in the dissertation.

Munich, 31<sup>st</sup> of October 2018

Aurore Menegaux



# DECLARATION OF AUTHOR CONTRIBUTIONS

**Authors manuscript 1:** Aurore Menegaux , Natan Napiorkowski N, Julia Neitzel , Adriana L. Ruiz-Rizzo, Anders Petersen , Hermann J. Müller , Christian Sorg , Kathrin Finke

The author of this thesis is the first author of this manuscript. **A.M.**, K.F. and C.S. designed this study, **A.M.**, J.N. and A.R.R. acquired imaging data and N.N behavioral data, **A.M.** analyzed data and drafted the manuscript and. **A.M.**, A.P., H.J.M., K.F. and C.S. wrote and revised the manuscript before submission.

**Authors manuscript 2:** Aurore Menegaux, Felix J.B. Bäuerlein, Aliko Vania, Natan Napiorkowski , Julia Neitzel , Adriana L. Ruiz-Rizzo , Hermann J.,Müller , Christian Sorg , Kathrin Finke

The author of this thesis is the first author of this manuscript. **A.M.**, K.F. and C.S. designed this study, **A.M.**, J.N and A.R.R. acquired imaging data and N.N behavioral data, **A.M.** analyzed data with some help from A.V. supervised by **A.M.** as part of her bachelor thesis and with some tool provided by F.J.B.B., **A.M.** drafted the manuscript, **A.M.**, H.J.M., K.F. and C.S. wrote and revised the manuscript before submission.

**Authors manuscript 3:** Aurore Menegaux, Chun Meng, Julia Neitzel, Josef G. Bäuml , Hermann J.Müller, Peter Bartmann, Dieter Wolke, Afra M.Wohlschläger, Kathrin Finke, Christian Sorg

The author of this thesis is the first author of this manuscript. K.F. and C.S. designed this study, P.B. and D.W. recruited participants, J.G.B and C.M. acquired imaging data and J.N. behavioral data, **A.M.** analyzed the data under the supervision of C.M., **A.M.** drafted the manuscript and. **A.M.**, C.M., H.J.M., P.B., D.W., A.M.W., K.F. and C.S. wrote and revised the manuscript before submission.

Munich, 31st of October 2018

Aurore Menegaux      PD Dr. Kathrin Finke (1<sup>st</sup> supervisor)